UNIVERSIDADE DE SÃO PAULO

INSTITUTO DE QUÍMICA

Programa de Pós-Graduação em Ciências Biológicas (Bioquímica)

BRUNO CHAUSSE

Metabolic and Redox Effects of Intermittent Fasting

São Paulo

2015

BRUNO CHAUSSE

Metabolic and Redox Effects of Intermittent Fasting

Tese apresentada ao Instituto de Química da Universidade de São Paulo para a obtenção do título de Doutor em Ciências Biológicas (Bioquímica)

Orientadora: Alicia Juliana Kowaltowski

Coorientador: Licio Augusto Velloso

São Paulo

2015

Ficha Catalográfica
Elaborada pela Divisão de Biblioteca e
Documentação do Conjunto das Químicas da USP.

Chausse, Bruno
C499m Metabolic and redox effects of intermittent fasting / Bruno Chausse. -- São Paulo, 2015.
56p.

Tese (doutorado) - Instituto de Química da Universidade de São Paulo. Departamento de Bioquímica
Orientador: Kowaltowski, Alicia Juliana
Co-orientador: Velloso, Licio Augusto

1. Bioquímica I. T. II. Kowaltowski, Alicia Juliana, orientador. III. Velloso, Licio Augusto, co-orientador

574.192 CDD

Banca Examinadora de Tese de Doutorado

Candidato: Bruno Chausse

Orientadora: Alicia J. Kowaltowski

Membros:

1. _____

2. _____

3. _____

Com amor, para Ane e Olivia, Ricardo e Sara, Caio e Déborah

Agradecimento Especial

Este agradecimento especial é para a minha Orientadora, Alicia J. Kowaltowski, por seu comprometimento com a minha formação. Gostaria de agradecer por ter tido uma orientação tão próxima. Todas as dicas e até mesmo broncas foram fundamentais para o desenvolvimento deste trabalho e para a construção de um perfil profissional maduro. Nestes 5 anos de convívio pude aprender como fazer uma ciência objetiva, produtiva e relevante. Além disso, seu exemplo como professora e seu cuidado com cada aluno em particular me ajudou a definir o meu perfil como futuro docente. Outro importante exemplo foi o seu engajamento institucional, sempre conduzido com muita seriedade e comprometido com o crescimento e melhoria da nossa Universidade. Conviver com tudo isso me fez perceber que mais do que uma orientadora, você foi e sempre será a minha Mentora. Meu muito obrigado!

Agradecimentos

Ao meu Coorientador, Licio A. Velloso, por todas as contribuições ao trabalho e pelo aprendizado que a nossa convivência me proporcionou.

À Camille Caldeira, por todo o suporte técnico sem o qual esse trabalho não teria alcançado êxito e, principalmente, pela nossa amizade, caronas, placas de carro, roupas de bebê, brigas públicas, cantorias e tantas outras coisas que faziam do nosso laboratório o melhor ambiente de trabalho do qual já se ouviu falar!

À Fernada Cunha, por toda a sabedoria dos conselhos científicos e de vida e pela convivência de onde surgiu uma grande amizade com tons de irmandade e diversos sabores gastronômicos!

À Nanda, por sempre estar pronta a compartilhar todo seu conhecimento e sempre nos ajudar com nossos problemas experimentais e também pelo seu carinho, ouvido e alegria que faz da ciência algo bem mais humano!

À Talita, pelo auxílio nesta fase final do doc e na transição para o pós-doc e por toda amizade, conversas, HHs, risadas e talitadas que são inesquecíveis!

Ao Ignacio, pelos experimentos e discussões que me ajudaram a ampliar minha visão científica e também pela amizade e trocas culturais tão interessantes!

Ao Luis, pelo auxílio nas dificuldades experimentais com todo o seu conhecimento de tudo e por ser sempre tão prestativo em nos ajudar.

Ao Marcel, por me proporcionar a primeira experiência com orientação na qual aprendi muitas coisas, pelas discusões, experimentos e tudo que

envolveu o tempo que trabalhamos juntos. E, também pela nossa amizade, por poder ver o seu crescimento e por tantos momentos dignos de registro (só na memória)!

Aos ICs mais completos que já se viu na face da terra: Pâmela, Wilson, Júlia, Felipe e Sérgio; por sempre contribuirem com sua ciência e também com a sua vida.

A todos os colegas que passaram pelo laboratório e sempre contribuiram com a construção deste trabalho, seja por discussões e auxilios experiementais, seja pelo apoio e momentos de descontração: Nicole, Bruno Q, Ariel, Erich, Phillipe, Graciele, Thiré.

À Fernanda Cerqueira (Fezinha), por toda a sua contribuição na construção do que seria o meu projeto, pelas oportunidades e pela amizade sincera que pudemos desenvolver durante estes anos.

Ao Prof Demétrius Araújo e à Gláucia, por terem me apresentado o mundo da ciência e despertado o desejo de ser pesquisador em mim.

À Prof. Nadja e seu laboratório, pelas discussões e contribuições diversas durante todos esses anos.

Aos técnicos Doris e Edson, bem como aos funcionários do Biotério das Químicas, Silvânia Neves, Flávia M. Prates Ong, Renata Spalutto Fontes e Maria de Fátima de Souza, por todo o suporte indispensável para a elaboração deste trabalho.

Aos colegas da pós graduação, pelos momentos de estudo, discussões e colaborações.

Aos docentes do Instituto, pelo ensino e exemplo percibido na vida de cada um.

Aos nossos colaboradores, pelas contribuições experiementais na resolução de perguntas que não responderíamos sozinhos, principalmente à Carina e Gabi pela amizade e pela torca de conehcimento intensa!

À Universidade de São Paulo, por toda a infraestrutura e acolhimento durante todo o desenvolvimento deste trabalho.

Ao CNPq, CAPES, FAPESP, NAP e CEPID Redoxoma, pelo auxilio financeiro que possibilitou a realização deste trabalho.

Aos diversos amigos, pelo apoio e carinho que, mesmo sem compreender exatamente o que faço, foram fundamentais para a conclusão deste estudo.

Aos meus pais, Ricardo e Sara, que formaram o que sou e sempre estiveram presentes na minha vida, sem os quais eu não seria ninguém.

Aos meus irmãos, Caio e Déborah, que me ensinaram a divider, a viver em sociedade e também foram importantes todo este período.

À minha esposa, Ane, que me ensinou o que é amar e me acompanhou durante essa caminhada complexa me dando apoio e força para seguir em frente e que, juntamente com a nossa filha, Olivia, são o motivo da minha alegria e o bem mais precioso que possuo!

E, finalmente, à Deus, por me proporcionar todas as coisas!

Resumo

Chausse, B. – Estudo dos efeitos metabólicos e redox de dietas intermitentes. Tese de Doutorado, Instituto de Química, Universidade de São Paulo, São Paulo 2015.

As dietas intermitentes (IF) compreendem ciclos alternados de 24 horas de jejum e alimentação. Como os efeitos de IF sobre o balanço redox não são bem conhecidos, esse trabalho teve por objetivo avaliar os efeitos desta dieta sobre o estado redox de diferentes tecidos de ratos. Após um mês de tratamento, os fígados dos ratos em IF apresentaram um aumento de capacidade respiratória mitocondrial juntamente com níveis elevados de proteínas carboniladas. Verificou-se ainda um aumento em danos oxidativos no cérebro destes animais. IF promoveu significativa proteção contra danos oxidativos no coração, enquanto que não houve alterações no estado redox do músculo esquelético. Os efeitos metabólicos de IF também foram investigados com o intuito de compreender os mecanismos envolvidos com o menor peso e a hiperfagia promovidos por esta intervenção. Observou-se que o menor peso dos ratos submetidos à IF é consequência de um aumento em taxas metabólicas em dias de alimentação somado à oxidação lipídica aumentada durante o jejum. A hiperfagia, por sua vez, é consequencia de elevação nos níveis de neurotransmissores orexigênicos hipotalâmicos, mesmo quando estes animais estão alimentados. Os níveis do neutransmissor TRH também foram modulados por esta dieta, o que pode estar relacionado com as alterações de taxas metabólicas observadas no modelo. Concluímos, portanto,

que as dietas intermitentes promovem modificações funcionais no hipotálamo que estão associadas com diferenças no peso corpóreo e no apetite. Além disso, IF afeta o balanço redox de forma tecido específica, levando a um desbalanço oxidativo no fígado e no cérebro e à proteção contra danos oxidativos no coração.

Palavras-chave: Dietas Intermitentes, Metabolismo, Estresse Oxidativo

Abstract

Chausse, B. – Metabolic and Redox Effects of Intermittent Fasting. PhD Thesis - Instituto de Química, Universidade de São Paulo, São Paulo 2015.

Intermittent fasting (IF) is a dietary intervention that comprises 24 hour cycles alternating *ad libitum* feeding and fasting. We address here the effects of IF on redox state in different tissues, which are still poorly understood. After one month on the diet, IF rats livers presented increased mitochondrial respiratory capacity along with increased levels of protein carbonyls. Surprisingly, IF animals also presented an increase in oxidative damage in the brain. Conversely, IF promoted a substantial protection against oxidative damage in the heart. No difference in redox homeostasis was observed in the skeletal muscle. We also assessed metabolic effects of IF to uncover the mechanisms involved in the lower body mass and loss of feeding control in IF rats. As measured calorimetrically, IF animals presented high metabolic rates during feeding days and increased lipid oxidation on fasting days, which explains the lower body weight. IF-induced overeating was a consequence of increased expression of hypothalamic orexigenic neurotransmitters, even on feeding days. THR levels also were changed, in parallel with the feeding-dependent alterations on metabolic rates. Overall, we find that intermittent fasting promotes functional hypothalamic alterations associated with differences in body weight and appetite. In addition, IF affects redox balance in a tissue-specific manner, leading to redox imbalance in the liver and brain, as well as protection against oxidative damage in the heart.

Keywords: Intermittent Fasting, Metabolism, Oxidative Stress

Summary

1. Introduction

Aging is an irreversible process characterized by a time-dependent loss of cell function and integrity. The accumulation of cellular damage leads to the development of several diseases, including cancer, diabetes and neurodegenerative disorders. This progressive increase in dysfunction culminates in death [1]. The importance of the aging process in health maintenance and longevity has lead to the emergence of a complex field of research, which aims to understand cellular and molecular mechanisms underlying this process.

Advances in aging studies suggest specific cellular alterations are markers for aging progression in different species [1]. Genomic instability, or the time-dependent accumulation of genetic damage in the nuclear and mitochondrial genomes, is a commonly used aging marker [2]. Diverse aging-related diseases and syndromes are promoted by increases in DNA lesions, and the prevention of these modifications can delay aging [3-5]. In addition to genomic instability, telomere attrition and epigenetic alterations, such as histone modifications and DNA methylation, are genetic markers of aging [6-8].

Impaired protein homeostasis is other aging marker that is directly involved in the genesis of diseases such as Alzheimers and Parkinson´s [9]. Indeed, disturbing proteostasis experimentally leads to the development of several aging abnormalities. On the other hand, genetic manipulations that improve protein homeostasis prevent the development of these disorders [10]. Deficient clearance of senescent cells and stem cell exhaustion also contribute to accelerated aging since both processes decrease the capability of damaged

tissues to recover [11, 12]. Loss of tissue recovery capability increases the vulnerability towards age-related diseases such as anemia, osteoporosis and sarcopenia [1].

Aging is also marked by significant alterations in metabolic processes, including changes in intercellular communication [13, 14]. Increased inflammation and neuroendocrine dysfunction promote a rupture in the communication between hypothalamus and peripheral organs, deregulating nutrient sensing pathways [15, 16]. These defects in energetic status sensing are directly linked to the development of obesity, type II diabetes and related comorbidities [17].

Mitochondrial dysfunction also affects metabolic control during aging [18]. Age-related decreases in mitochondrial bioenergetics and biogenesis accelerate the aging process in mammals [19, 20] while lower respiratory chain efficiency and mutations in the mitochondrial genome exacerbate cell damage at advanced ages [1]. Furthermore, age-related mitochondrial dysfunction is accompainied by an increase in reactive oxygen species (ROS) production. Indeed, the onset of several age-related diseases involves redox imbalance [21]. At advanced ages, the levels of ROS production increase in parallel with cellular stress and damage increases. Although current evidence suggests that the primary effect of ROSunder most physiological conditions is the activation of compensatory homeostatic responses in aging, increased ROS production may exceed a threshold beyond the original homeostatic response and promote the age-associated oxidative damage [22]. Indeed, many protocols that delay aging attenuate age-related increases in oxidative damage [21].

Many distinct lines of evidence demonstrate that dietary restriction (DR) is effective in preventing the onset of age-related diseases [22]. DR comprises several types of food restriction and has been demonstrated to be effective in experimental models raging from yeast and *C. elegans* to more complex organisms such as rodents and primates [23, 24]. Examples of the beneficial effects of DR include the prevention of cancer, neurodegeneration, cardiovascular diseases and insulin resistance [25-28]. The variety of DR protocols in mammalian models makes data comparison between different studies difficult [29]. In this sense, the understanding of DR types and how each dietary protocol affects aging markers is important.

DR studies started in the early 20th century with the analysis of effects of dietary interventions on cancer progression as well as the consequences of early malnutrition on growth, reproduction and adult health [30, 31]. Early results indicated that DR delays maturation and increases animal longevity. In 1935, McCay et al. showed that calorie restriction (CR) without malnutrition increases the lifespan of rodents when compared to control animals, fed *ad libitum* (AL) [32]. Additional experiments from the same group suggested that the specific dietary intervention promoting longevity was the decrease in calorie ingestion [33]. After these initial findings, many studies were conducted to investigate CR effects on aging [34-37].

Over the years, diets distinct from CR were developed and used to investigate their effects on aging. Intermittent fasting (IF), for example, was first described in 1946 and found to slightly enhance animal lifespan [38]. More recent studies, however, have produced conflicting results regarding the effects of IF on animal longevity. Goodrick et al. observed an increase in the average

and maximum lifespans of IF animals, while Pearson et al. did not find any increment in animal longevity using this dietary intervention [39, 40].

IF is quite extensively used as an intervention equivalent to CR, despite the fact that these interventions present several other differences, in addition to their distinct effects on lifespan. Standard CR protocols involve a daily decrease in caloric intake ranging from 10% to 40% and a supplementation of micronutrients to avoid malnutrition. On the other hand, IF is an intervention in the frequency of feeding and comprises 24 hours cycles of fasting alternating with 24 hours of feeding [29, 41]. IF animals are able to gorge when food is available, and some groups report that overeating during feeding days can compensate for the food intake loss during fasting periods [28, 42]. Consequently, IF animals are not necessarily calorically-restricted.

CR protects against redox imbalance and prevents the onset of oxidative stress-related diseases [21]. Indeed, most studies find that CR promotes a decrease in oxidant production and a reduction in oxidative damage to biomolecules [41]. Long-term CR also avoids age-related insulin resistance, prevents the nitration of the insulin receptor and reduces oxidant release [28]. Conversely, the few exsisting studies investigating IF effects on redox status have observed small or even no alterations between IF and AL animals [21]. We find that long-term IF-treated rats display an increase in H_2O_2 release in the skeletal muscle and white adipose tissue, associated with marked insulin signaling impairment [28]. However, it is unclear if IF-induced insulin resistance occurs before or after oxidative imbalance. In addition, a description of IF effects on redox balance in different organs is lacking in the the literature. Here, we address the effects of short-term IF on oxidative imbalace in a tissue specific

manner to uncover how this change in feeding frequency alters redox state. This part of the study is presented in Chapter I.

As mentioned previously, IF does not always involve a decrease in caloric intake [42, 43]. Indeed, IF animals often present similar food intake to AL animals. Despite this potentially equal caloric uptake, IF animals present decreased body mass relative to AL animals, demonstrating that this diet promotes a reduction in energy conversion efficiency. This means that IF rats convert a smaller part of the energy contained in their food into body mass. The metabolic mechanisms involved in this change in feed efficiency are not well understood. Furthermore, the regulatory pathways involved in the gorging pattern these animals present also remain to be uncovered. Consequently, we also aimed to uncover the mechanisms involved in this lower energy conversion efficiency and overeating promoted by IF. This part of the study will be discussed in Chapter II.

2. Chapter I - Intermittent Fasting Results in Tissue-Specific Changes in Bioenergetics and Redox State

Bruno Chausse, Marcel A. Vieira-Lara, Angélica B. Sanchez, Marisa H. G. Medeiros, Alicia J. Kowaltowski*

Departamento de Bioquímica, Instituto de Química, Universidade de São Paulo, SP, Brazil

Reproduced from *PLoS One*. Accepted January 21th, 2015. Published March 6th, 2015.

PLOS | ONE

RESEARCH ARTICLE

Intermittent Fasting Results in Tissue-Specific Changes in Bioenergetics and Redox State

Bruno Chausse, Marcel A. Vieira-Lara, Angélica B. Sanchez, Marisa H. G. Medeiros, Alicia J. Kowaltowski*

Departamento de Bioquímica, Instituto de Química, Universidade de São Paulo, São Paulo, Brazil

* alicia@iq.usp.br

Citation: Chausse B, Vieira-Lara MA, Sanchez AB, Medeiros MHG, Kowaltowski AJ (2015) Intermittent Fasting Results in Tissue-Specific Changes in Bioenergetics and Redox State. PLoS ONE 10(3): e0120413. doi:10.1371/journal.pone.0120413

Academic Editor: Nuri Gueven, University of Tasmania, AUSTRALIA

Received: October 6, 2014

Accepted: January 21, 2015

Published: March 6, 2015

Data Availability Statement: All relevant data are within the paper and its Supporting Information files.

Funding: This work was supported by the Fundação de Amparo à Pesquisa do Estado de São Paulo (FAPESP), grant 10/51906, Instituto Nacional de Ciência e Tecnologia de Processos Redox em Biomedicina (INCT Redoxoma), Núcleo de Apoio à Pesquisa Redoxoma (NAP Redoxoma), Centro de Pesquisa, Inovação e Difusão de Processos Redox em Biomedicina (CEPID Redoxoma) grant 13/07937-8, and the John Simon Guggenheim Memorial Foundation. MAVL (grant 13/14203-0) is supported by an undergraduate fellowship from FAPESP. BC is

Abstract

Intermittent fasting (IF) is a dietary intervention often used as an alternative to caloric restriction (CR) and characterized by 24 hour cycles alternating *ad libitum* feeding and fasting. Although the consequences of CR are well studied, the effects of IF on redox status are not. Here, we address the effects of IF on redox state markers in different tissues in order to uncover how changes in feeding frequency alter redox balance in rats. IF rats displayed lower body mass due to decreased energy conversion efficiency. Livers in IF rats presented increased mitochondrial respiratory capacity and enhanced levels of protein carbonyls. Surprisingly, IF animals also presented an increase in oxidative damage in the brain that was not related to changes in mitochondrial bioenergetics. Conversely, IF promoted a substantial protection against oxidative damage in the heart. No difference in mitochondrial bioenergetics or redox homeostasis was observed in skeletal muscles of IF animals. Overall, IF affects redox balance in a tissue-specific manner, leading to redox imbalance in the liver and brain and protection against oxidative damage in the heart.

Introduction

Moderate reduction in *ad libitum* daily caloric intake without limiting essential and micronutrient access (caloric restriction, CR) is a well-established mechanism to promote longer lifespans and/or healthier aging in a wide range of organisms, including humans [1, 2]. The beneficial effects of CR diets are complex and widespread, but include the preservation over time of mitochondrial bioenergetic functions and redox balance (the difference between the production and removal of damaging oxidative species) [3, 4, 5].

The downside of CR is that it requires daily control of caloric intake, and is thus labor-intensive both for humans and to maintain in a laboratory animal setting. As an alternative to CR, some groups have proposed the use of intermittent fasting (IF), also referred to as intermittent feeding or every other day feeding [6, 7], in which *ad libitum* feeding periods are alternated with fasting, thus avoiding the strict daily control of caloric intake. In laboratory animals, this feeding protocol was first described by Carlson and Hoelzel, who observed a slight increment in rat life span [8]. Despite this early result suggesting a lifespan benefit similar to CR, subsequent studies have indicated that the enhancement in life expectancy promoted by IF, if

supported by a CNPq fellowship. The funders had no role in study design, data collection and analysis, decision to publish, or preparation of the manuscript.

Competing Interests: The authors have declared that no competing interests exist.

present, is certainly less robust [9, 10]. In humans, IF has been shown to reduce obesity and have positive effects on some pathologies [11, 12].

Despite some similarities such as promoting reduced body weight [13], substantial differences between CR and IF have been uncovered [5] and are, indeed, expected, since CR involves a daily reduction in food intake, while IF changes feeding frequency, and may not always result in a limitation of food ingestion [7, 14]. In fact, while CR enhances insulin sensitivity, we find that long-term IF results in insulin resistance [13]. We also find that long-term IF enhances tissue oxidant release and oxidative protein modifications in the skeletal muscle and adipose tissue [13], while long-term CR is mostly associated with the prevention of oxidative damage [4, 5]. Overall, IF effects on oxidative balance are not yet well determined. This study bridges this knowledge gap, and demonstrates that short-term IF affects redox balance in a tissue-selective manner.

Materials and Methods

Animals

Experiments were conducted in agreement with the NIH guidelines for the humane treatment of animals and were approved by the local Animal Care and Use Committee (Comissão de Ética em Cuidado e Uso Animal—Instituto de Química, USP) (Permit number: 21/2014). Male, 8-week-old Sprague Dawley rats were separated in two groups: one fed *ad libitum* (AL), and one with *ad libitum* access to food on alternating days (IF). The animals were lodged four individuals per cage in 12 hours light/dark cycles and given water *ad libitum*. Body mass was recorded before and after 1 month of the dietary intervention and cumulative food consumption over the treatment period was recorded for each cage. The average intake per animal was used to calculate feed conversion efficiency (average weight gain per cage × 100/average food intake per cage). Chow was alternately placed or removed at 5:00 pm for IF animals. After 1 month of the dietary intervention, AL and IF rats were euthanized by decapitation after 12 hours of overnight fasting.

Mitochondrial isolation

Mitochondrial isolation from different tissues was performed as described by Tahara et al., 2009 [15]. Briefly:

Liver mitochondria. The tissue was minced finely and washed with 4°C isolation buffer (250 mM sucrose, 10 mM Hepes, 1 mM EGTA, pH 7.2) and then homogenized with a 40 mL tissue grinder. The suspension was centrifuged at 600 g for 5 minutes and the resulting supernatant was centrifuged at 12,000 g for 5 minutes. The pellet was washed and resuspended in a minimal volume of the same buffer.

Brain mitochondria. The preparation used digitonin to release mitochondria from synaptosomes, resulting in a mixture of synaptosomal and nonsynaptosomal mitochondria. The brain was minced and washed with 125 mM sucrose, mannitol 250 mM, 10 mM Hepes, 10 mM EGTA, 0.01% BSA, pH 7.2 at 4°C. The homogenate was centrifuged at 2,000 g for 3 minutes and the supernatant transferred to a new tube and centrifuged at 12,000 g for 8 minutes. The resulting pellet was resuspended in a minimal volume of the isolation buffer devoid of EGTA.

Skeletal muscle mitochondria. Hind-limb muscles were dissected in isolation buffer (300 mM sucrose, 50 mM Hepes, 10 mM Tris, 1 mM EGTA, 0.2% BSA, pH 7.2) at 4°C to remove fatty and connective tissue. The tissue was processed with a Polytron homogenizer and then with a mechanized potter. The homogenate was centrifuged at 850 g for 5 minutes and the supernatant was centrifuged again at 10,000 g for 5 minutes. The pellet was resuspended

and centrifuged at 7,000 g for 5 minutes. The final mitochondrial pellet was prepared in a minimal volume of isolation buffer.

Heart mitochondria. Hearts were minced finely in isolation buffer (300 mM sucrose, 10 mM Hepes, 2 mM EGTA, pH 7.2) at 4°C, in the presence of 0.5 μM type I protease (bovine pancreas) to release mitochondria from the muscle fibers, and then washed in the same buffer in the presence of 1 mg/mL BSA. The suspension was homogenized in a 40 mL tissue grinder and centrifuged at 800 g for 5 minutes. The resulting supernatant was centrifuged at 9,500 g for 10 minutes and the mitochondrial pellet was resuspended in a minimal amount of isolation buffer.

Mitochondrial H_2O_2 release

Mitochondrial H_2O_2 release was measured in 0.125–0.500 mg protein/mL mitochondrial suspensions in experimental buffer (150 mM KCl, 10 mM Hepes, 2 mM KH_2PO_4, 0.1% BSA, pH 7.2) at 37°C, with continuous stirring in the presence of 25 μM Amplex Red and 0.5 U/mL horseradish peroxidase (HRP). Malate/glutamate, pyruvate/malate or succinate were used as substrates. Amplex Red is oxidized in the presence of extramitochondrial horseradish peroxidase bound to H_2O_2, generating resorufin, which can be detected with a fluorescence spectrophotometer operating at 563 nm excitation and 587 nm emission [16].

Mitochondrial O_2 consumption

O_2 consumption was monitored using a Clark-type electrode, coupled to a high-resolution Oroboros respirometry system [17] in 0.125–0.500 mg protein/mL mitochondrial suspensions under the same buffering conditions used in the H_2O_2 assay.

Citrate synthase activity

Tissues were homogenized with an electric potter in 50 mM phosphate buffer (pH, 7.5) at 4°C and centrifuged at 600 g for 10 minutes, in the presence of protease inhibitor (1:100). A mixture of 100 mM Tris-HCl, 100 μM Acetyl-CoA, 100 μM DTNB, 250 μM oxaloacetate and 0.1% Triton-X, pH 8.1, was incubated with homogenate supernatant at 30°C for 5 minutes. CoA-SH produced by the enzymatic reaction reduces the DTNB, which is followed by the increase in absorbance at 412 nm (extinction coefficient = 13.6 $mM^{-1} \cdot cm^{-1}$) (adapted from ref [18]).

Immunoblots

COX4 and NRF-1. Liver homogenates were prepared under the same conditions used for the citrate synthase assay and then diluted 4:1 in Laemmli buffer (100 mM Tris-HCl, 2% SDS, 10% glycerol and 0.1% bromophenol blue) for NRF-1 determinations. For COX4, homogenates were diluted in the same buffer, and heated at 100°C for 10 minutes. The proteins were separated by SDS-PAGE and transferred to nitrocellulose (COX4) or PVDF (NRF-1) membranes, which were then incubated with 5% BSA. Chemiluminescent detection was performed using primary anti-COX4 (1:1000), anti-NRF-1 (1:1000) antibodies and the respective secondary anti-mouse IgG (1:5000) and anti-rabbit IgG (1:5000) antibodies, both bound to peroxidase. The signals were quantified using ImageJ software and normalized by coloring the nitrocellulose and PVDF membranes with Ponceau and Coomassie Blue, respectively.

Carbonylated Proteins. Tissue homogenates were prepared under the same conditions as the citrate synthase assay. A derivatization of the sample was performed, adding equal volumes of 24% SDS and 40 mM 2,4-dinitrophenylhydrazine (DNPH, prepared in 10% trifluoroacetic acid). The mixture, incubated in the dark for 30 minutes, allows the reaction between the

DNPH and carbonyl groups in proteins. Samples were then treated with a neutralizing solution (1:3), of 2 M Tris, 30% glycerol and 19% 2-mercaptoethanol. The proteins were separated by SDS-PAGE and transferred to a PVDF membrane (adapted from ref. [19]).

Nitro-tyrosin (NO_2-Try) levels. Tissue homogenates were prepared under the same conditions as described for the citrate synthase assay. For dot blot experiments, 10 μL of homogenates containing 3 μg of protein were placed on nitrocellulose membranes. After they were dry, the membranes were blocked in a 4% BSA solution for one hour followed by an overnight incubation with primary anti-NO_2-Try (1:2000). After one hour incubation with the anti-rabbit IgG (1:10000) secondary antibody, NO_2-Try signals were identified using an Odyssey CLx system (LI-COR, Nebraska, USA). The signals were quantified using ImageJ software and normalized to protein levels by coloring the nitrocellulose membranes with Ponceau.

Antioxidant enzyme activities

Tissue homogenates were prepared as described for the citrate synthase assay. Glutathione peroxidase (GSH-Px) activity was measured as described in ref. [20]. A mixture of phosphate buffer, reduced glutathione (GSH), glutathione reductase (GR), EDTA, NADPH, NaN_3 and homogenate was used, and the reaction was initiated by the addition of H_2O_2. The decrease in the quantity of NADPH was followed by absorbance at 340 nm for 3 minutes. The glutathione reductase assay followed the protocol described in ref. [21]. GR catalyzes the reduction of GSSG to GSH in the presence of NADPH. The resulting GSH reacts with 5,5′-dithio-bis-2-nitrobenzoic acid (DTNB), producing 5-thio-2-nitrobenzoic acid (TNB), detected by absorbance at 412 nm. The catalase assay was adapted from ref. [22]. Homogenates were incubated in the same experimental buffer used in the H_2O_2 assay and the O_2 production rate was measured for 30 seconds after the addition of 200–800 μM H_2O_2 using a Clark-type electrode at 37°C with continuous stirring.

Glutathione levels

The concentrations of GSH and GSSG, as well as total glutathione, were determined using a colorimetric assay with DTNB, as described in ref. [23]. GSH reacts with DTNB producing TNB and GS-TNB, which is reduced back to GSH by GR. This process releases TNB, detected by absorbance at 412 nm.

Malondialdehyde (MDA) determination

Tissues were homogenized in TKM buffer (50 mM Tris-HCl, 25 mM KCl and 5 mM $MgCl_2$ and SDS 10%, pH 7,5). One milliliter of thio-barburic acid (TBA; 0.4% w/v in 133 mM HCl) and 150 uL butylated-hydroxytoluene (BHT; 0.2% w/v in 95% ethanol) were added to 1.2 mL of the homogenate. The mixture was heated to 90°C for 45 min, cooled on ice, and extracted with isobutanol. The isobutanolic phase was injected through a Shimadzu auto injector model SIL-20A (Shimadzu, Kyoto, Japan) in a Shimadzu HPLC system consisting of two pumps; LC-20AT connected to a Luna C18 (Phenomenex, Torrance, CA) reversed-phase column (250 mm x 4.6 mm i.d., particle size 10 μm). The flow rate of the isocratic eluent (5 mM potassium phosphate buffer, pH 7, with 23% methanol) was 1 mL/min. A RF-10A/XL fluorescence detector was set at an excitation wavelength of 515 nm and an emission wavelength of 553 nm. The data were processed using the Shimadzu LC Solution 1.25 software. Malonaldehyde-bisdiethylacetal was used to calibrate the fluorescence data, yielding a quantitative adduct of the malonaldehyde-TBA product. The data were expressed as pmol of MDA normalized by protein mass (adapted from [24]).

Statistical analysis

Data were analyzed using GraphPad Prism and Origin softwares. Figures are presented as average ± standard error and comparisons were performed using two-tailed Student t-tests. $p<0.05$ was considered significant.

Results

IF reduces body mass and energy conversion efficiency

IF diets have been extensively shown to reduce body mass [6, 7, 9]. Indeed, we observed that, after a month, IF rats presented lower body weights than AL control rats (Fig. 1A). The decrease in body weight was a reflection of two additive effects of the diet: a 14% reduction in food consumption (Fig. 1B) and a 40% decrease in energy conversion efficiency (Fig. 1C), or the amount of food ingested that results in weight gain. Similar decreases in energy conversion efficiency in IF have been reported previously and may be related to changes in hypothalamic energy metabolism control [25].

IF increases respiratory capacity in the liver, but not in other tissues

Restricted diets have been extensively shown to be related to changes in mitochondrial bioenergetics [2, 3, 26] which in turn are known to be determinant toward redox balance, since mitochondria are the most quantitatively relevant source of intracellular reactive oxygen species (ROS). We thus sought to determine if short-term IF lead to changes in mitochondrial bioenergetics in different tissues.

In Fig. 2, we measured isolated mitochondrial NADH-linked oxygen consumption rates using samples obtained from different tissues under two conditions: state 3, in which ADP is present, stimulating maximal ATP synthesis-linked respiration; and state 4, in which the ATP synthase inhibitor oligomycin is present, and respiration reflects the magnitude of the proton leak [27]. Interestingly, respiratory rates in both states were unchanged by IF in the brain (Fig. 2A), heart (Fig. 2B) and skeletal muscle (Fig. 2C). On the other hand, both ADP-stimulated and oligomycin-inhibited respiratory rates were increased in liver mitochondria isolated from IF animals (Fig. 2D). This increase in respiratory rate was accompanied by a slight increase in respiratory control ratios (the ratio between state 3 and state 4 oxygen consumption) in IF samples, indicating that it reflects an increment in electron transfer capacity and is not a consequence of increased proton leak.

In order to further investigate the effects of IF on liver mitochondrial bioenergetics, we determined respiratory rates using succinate (which feeds electrons into the respiratory chain through Complex II; Fig. 3A) and TMPD-ascorbate (which reduces cytochrome c and cytochrome c oxidase; Fig. 3B). Both substrates also supported higher oxygen consumption rates in samples from IF animals, indicating that the enhanced respiratory capacity involves the enhanced activity of terminal electron carriers. Indeed, tissue levels of mitochondrial complex IV (cytochrome oxidase, COX, Fig. 3C) were significantly enhanced in IF livers.

The activity of the mitochondrial electron transport chain is often linked to an overall increase in the biogenesis of all mitochondrial enzymes. To test if this was the case, we determined the levels of NRF-1, a transcription factor that activates key mitochondria biogenesis, promoting mitochondrial DNA transcription and replication. Interestingly, NRF-1 levels were unaltered by IF (Fig. 3C). Confirming that liver mitochondrial biogenesis as a whole was not induced by IF, we found that activity of citrate synthase, a citric acid cycle enzyme and mitochondrial mass marker was equal in both groups (Fig. 3D). Altogether, these data suggests that

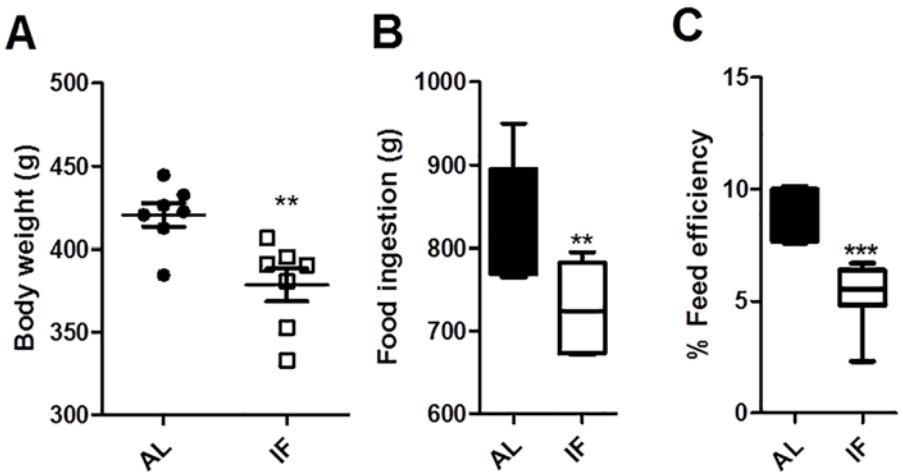

Fig 1. Intermittent fasting promotes lower body mass related to a mild reduction in caloric intake and lower energy conversion efficiency. (A) Average body weight per cage in (•) AL and (□) IF animals after one month of treatment. (B) Cumulative food intake over one month of treatment. (C) Energy conversion efficiency. Data represent averages ± SEM and were compared using *t* tests (n = 7 cages). ** $p<0.01$ vs AL. AL indicates *ad libitum* feeding, IF indicates intermittent fasting.

doi:10.1371/journal.pone.0120413.g001

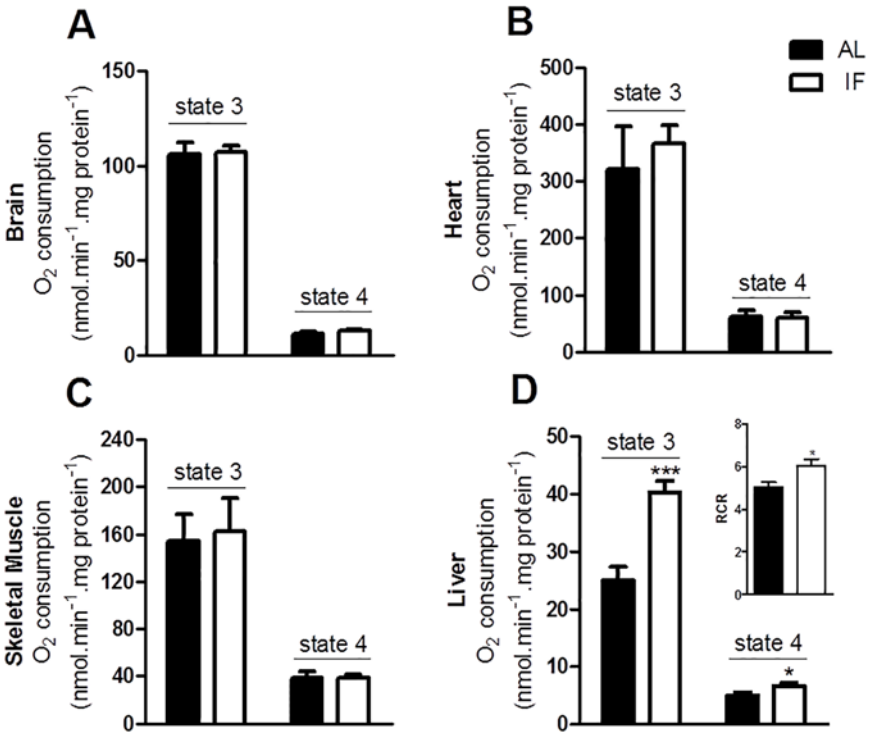

Fig 2. IF induces an increase in respiratory capacity in liver, without bioenergetic changes in other tissues. Oxygen consumption in isolated mitochondria from (A) brain, (B) heart, (C) skeletal muscle and (D) liver in the presence of 5 mM pyruvate plus 3 mM malate (A, B and D) or 2 mM glutamate plus 2 mM malate (C). State 3 was induced by the addition of 1 mM ADP and state 4 was achieved using 0.5 μg/mL oligomycin. The insert in Panel D represents respiratory control ratios (RCR), or state 3/state 4. Data represent averages ± SEM and were compared using *t* tests (n = 4–6 animals). * $p<0.05$ vs AL in the same respiratory state.

doi:10.1371/journal.pone.0120413.g002

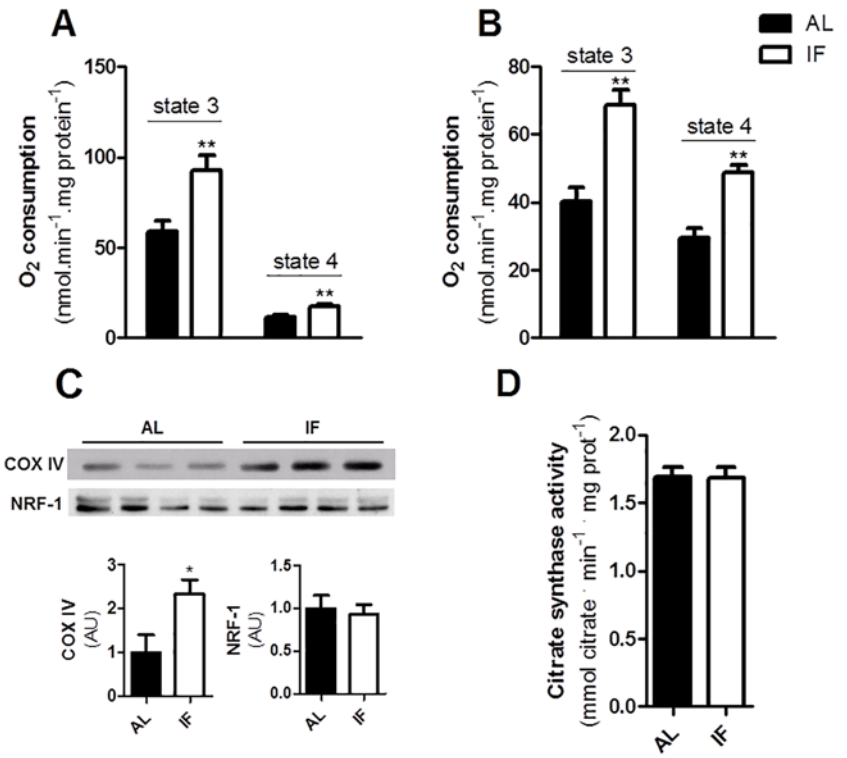

Fig 3. IF promotes enhanced electron transport capacity in the liver. Oxygen consumption in isolated mitochondria from livers in the presence of (A) 1 mM succinate plus 1 μM rotenone or (B) 200 μM TMPD plus 2 mM ascorbate. State 3 and state 4 were induced by ADP and oligomycin as described for Fig. 2. (C) COX-IV and NRF-1 levels measured as described in Materials and Methods. (D) Liver citrate synthase activity, determined as described in Materials and Methods. Data represent averages ± SEM and were compared using *t* tests (4–6 animals). * $p<0.05$, ** $p<0.01$ vs AL.

doi:10.1371/journal.pone.0120413.g003

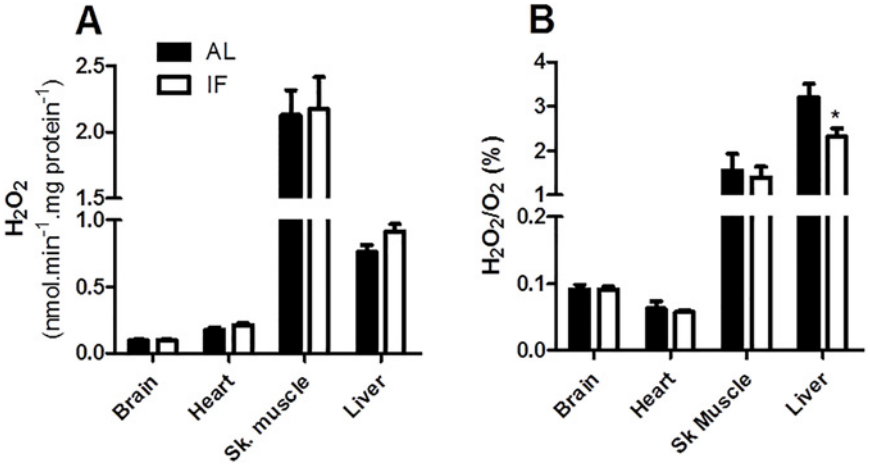

Fig 4. Reactive oxygen species production is not significantly altered by IF. (A) H_2O_2 release by isolated mitochondria in the presence of 1 mM ADP (state 3) and 5 mM pyruvate plus 3 mM malate (brain, heart and liver) or 2 mM glutamate plus 2 mM malate (skeletal muscle). (B) Ratio between H_2O_2 production and O_2 consumption by isolated mitochondria under the same conditions as panel A. Data represent averages ± SEM and were compared using *t* tests (n = 4–6 animals).

doi:10.1371/journal.pone.0120413.g004

IF induces an enrichment in respiratory chain proteins in liver mitochondria, without an overall increase in mitochondrial mass.

Mitochondrial reactive oxygen species release is unaltered by IF

In addition to determining changes in functional parameters, we measured the release of mitochondrial H_2O_2, a relatively stable and membrane-permeable ROS often used as a marker for oxidant production (Fig. 4) [28]. Interestingly, we found that IF did not significantly alter absolute H_2O_2 release in any tissue (Fig. 4A), although liver release was slightly increased ($p = 0.07$). IF decreased relative H_2O_2/O_2 release (Fig. 4B) in liver due to the enhanced O_2 consumption observed in Figs. 2 and 3, and no change in this ratio was observed in other tissues. Since changes in respiratory rates and mitochondrial coupling are often determinant toward mitochondrial oxidant generation, this result is compatible with our finding that IF does not alter mitochondrial bioenergetic parameters in brain, heart and skeletal muscle. Furthermore, the lack of changes in H_2O_2 in liver are compatible with the prior finding that oxidant release in this tissue is not strongly regulated by respiratory rates and coupling [15].

IF effects on antioxidants and oxidative damage are tissue-specific

Tissue redox status depends not only on the production of ROS but also on the levels and activities of antioxidant systems. We thus measured the activities of several key antioxidant enzymes in IF versus AL tissues (Table 1). The activity of glutathione peroxidase (GPx) [29], which uses glutathione (GSH) as an electron source to reduce and remove H_2O_2, was significantly decreased by IF in the skeletal muscle, and unchanged in all other tissues. Glutathione reductase, which restores GSH, was unchanged by this dietary intervention, in all tissues. Catalase, which also removes H_2O_2, was decreased by IF in the brain and unchanged in the other tissues. Overall, our data indicate that IF does not increase antioxidant enzyme activity and, if anything, promotes some tissue-specific decreases in oxidant buffering capacity.

We also determined the levels of different forms of glutathione, an intracellular reductant and redox state marker (Table 2). Levels of total glutathione (reduced plus oxidized), GSH, oxidized glutathione (GSSG) and GSH/GSSG ratios were mostly unchanged by IF, with a few exceptions: Livers of IF rats presented a significant increase in total glutathione and reduced GSH contents, which may be a consequence of a chronic exposure to a slightly increased oxidant generation (Fig. 4A). On the other hand, IF hearts presented lower levels of GSSG and, consequently, elevated GSH/GSSG ratios (Table 2), an indicative of a more reduced intracellular environment.

To determine the consequences of these tissue-specific modifications in antioxidant capacity, we measured the levels of protein carbonyls, MDA (a product of lipoperoxidation reactions) and nitro-tyrosine (NO_2-Tyr) as markers for biomolecule oxidative damage (Fig. 5). In keeping with the finding that IF hearts were in a more reduced state, as indicated by their GSSG levels (Table 2), we found that protein carbonyls and MDA levels were reduced by IF in this tissue (Fig. 5A and 5B). On the other hand, the brain presented enhanced protein carbonylation under IF, which may be a reflection of lower catalase activity. In the liver, a small decrease in the NO_2-Tyr signal and a robust increase in protein carbonylation levels was observed. The protein carbonylation effect may be a consequence of the slightly enchanced in oxidant generation in this tissue. There was no dietary-promoted difference in the measured oxidative damage markers in the skeletal muscle. Altogether, these data suggest that short-term IF affects redox balance in a tissue-specific manner, promoting protection against oxidative damage in the heart and leading to enhanced protein carbonylation in the brain and liver.

Table 1. Antioxidant enzyme activities.

		Brain	Heart	Muscle	Liver
Glutathione Peroxidase	**AL**	22.6 ± 1.30	119.9 ± 9.94	238.2 ± 13.13	168.5 ± 29.29
(mU· mg prot^{-1})	**IF**	21.2 ± 0.93	91.5 ± 8.52	195.0 ± 11.50*	174.8 ± 9.65
Glutathione Reductase	**AL**	5.21 ± 0.16	4.52 ± 0.34	12.80 ± 0.49	11.89 ± 0.26
(mU· mg prot^{-1})	**IF**	5.48 ± 0.09	4.04 ± 0.34	12.48 ± 0.55	12.02 ± 0.26
Catalase	**AL**	0.281 ± 0.02	0.933 ± 0.18	4.742 ± 0.36	0.841 ± 0.05
(μmol· mg prot^{-1}· min^{-1})	**IF**	0.229 ± 0.01*	0.850 ± 0.17	4.954 ± 0.39	0.738 ± 0.10

Values are means ± SEM and were compared using *t* tests (n = 4 animals).

* $p<0.05$ vs AL. AL indicates *ad libitum* feeding, IF indicates intermittent fasting.

doi:10.1371/journal.pone.0120413.t001

Discussion

Dietary interventions that reduce body weight relative to *ad libitum* food intake have received extensive attention due to their mostly positive effects on age-associated diseases [1, 2, 11]. Since aging is often accompanied by increased oxidative tissue damage and loss of mitochondrial activity, many studies involving CR have focused on the bioenergetic and redox effects of this diet [4, 30], mostly showing that it decreased oxidative damage [5]. On the other hand, IF is less studied, and sometimes even confused with CR in the literature [7], so its bioenergetic and redox effects are less clear. We thus sought to determine the redox and bioenergetic effects of IF and found that this diet affects these parameters in complex, tissue-specific manners.

Perhaps the most studied tissue relative to the effects of IF is the brain. Both IF and CR have been related to healthier brain aging by reducing oxidative damage [31–33]. Indeed, IF in aged animals partially restores the loss of some antioxidant enzymes, and decreases 8-hydroxy-deoxyguanosine DNA adducts accumulated over time [34, 35]. Thus, it was rather surprising to us to find that short-term IF in young animals leads to a significant increase in protein carbonyl signals in the brain of IF rats (Fig. 5), without measurable changes in mitochondrial function (Fig. 2), ROS release (Fig. 4), MDA or NO_2-Tyr (Fig. 5). This increased protein oxidative damage may be related to a small but significant decrease in brain catalase activity promoted by IF (Table 1). How this early increase in brain oxidative modifications relates to neurological protection in long-term IF models still remains to be uncovered, but the effects

Table 2. Glutathione levels.

		Brain	Heart	Muscle	Liver
Total Glutathione	**AL**	40.96 ± 3.06	21.24 ± 1.02	68.36 ± 8.19	11.37 ± 0.39
(nmol· mg protein^{-1})	**IF**	50.69 ± 2.81	22.63 ± 0.86	80.61 ± 14.57	15.30 ± 0.86*
GSH	**AL**	35.06 ± 3.42	14.57 ± 1.81	44.51 ± 8.76	9.00 ± 0.78
(nmol· mg protein^{-1})	**IF**	42.68 ± 2.45	19.44 ± 0.92	53.95 ± 13.36	12.70 ± 0.43*
GSSG	**AL**	3.62 ± 0.42	3.34 ± 0.42	11.92 ± 1.97	1.18 ± 0.20
(nmol· mg protein^{-1})	**IF**	4.64 ± 0.32	1.60 ± 0.15*	13.33 ± 1.08	1.30 ± 0.21
GSH/GSSG	**AL**	9.00 ± 0.34	4.68 ± 1.24	4.25 ± 1.38	8.36 ± 2.22
	IF	9.04 ± 0.29	12.45 ± 1.60*	4.03 ± 0.89	10.29 ± 1.62

Values are means ± SEM and were compared using *t* tests (n = 3–4 animals).

* $p<0.05$ vs AL. AL indicates *ad libitum* feeding, IF indicates intermittent fasting.

doi:10.1371/journal.pone.0120413.t002

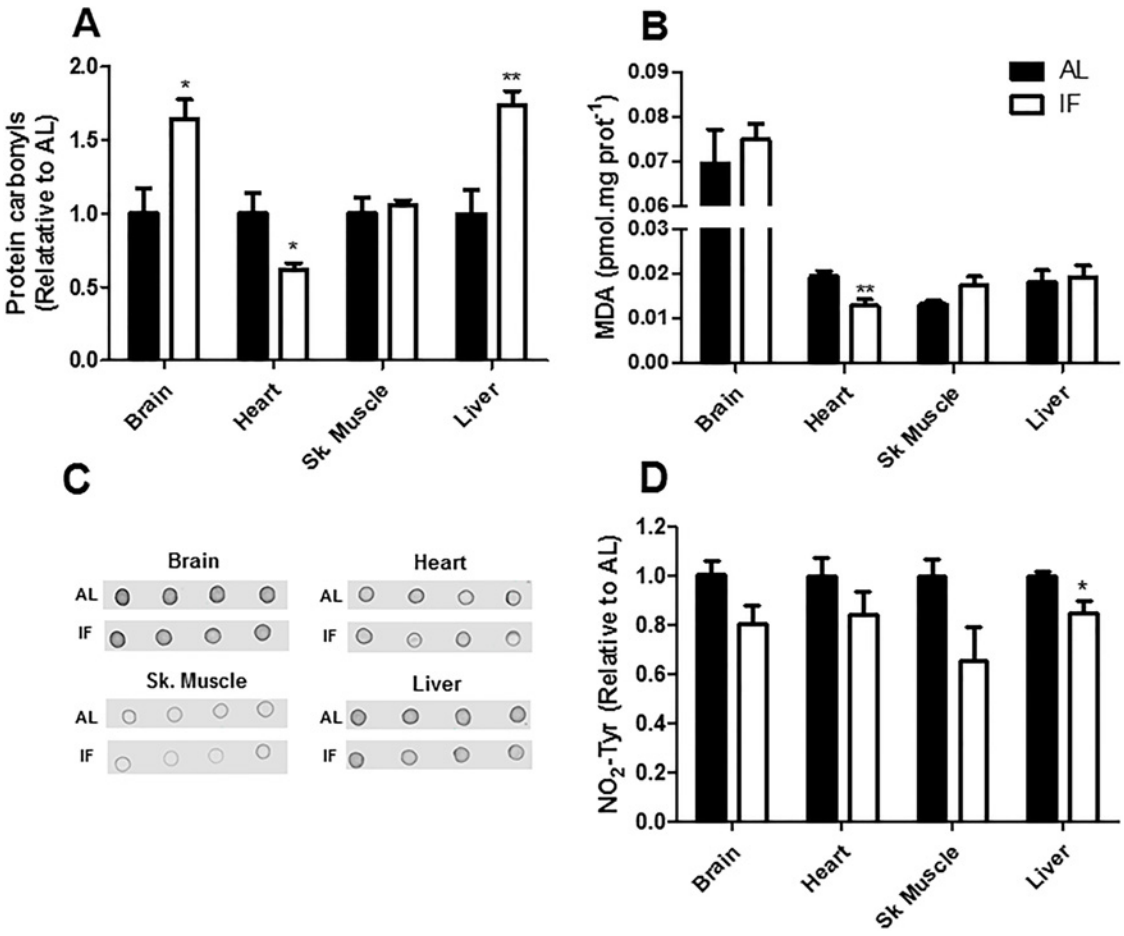

Fig 5. IF changes oxidative damage to biomolecules in a tissue-specific manner. (A) Carbonyl signals were quantified as described in Materials and Methods. (B) Malondaldehyde (MDA) levels were measured by HPLC as described in Materials and Methods. (C) Representative dot blots of NO_2-tyr signals. (D) Average densitometric results for the dot blots presented in C. Data represent averages ± SEM and were compared using *t* tests (n = 4–5 animals). * $p<0.05$, ** $p<0.01$ vs AL.

doi:10.1371/journal.pone.0120413.g005

are most probably unrelated, since other neuroprotective dietary interventions do not see increments in oxidative damage markers in the brain even in short-term studies [5].

IF and CR have also have been shown to protect the heart against ischemic injury [33, 36]. This protection has been attributed to activations in antioxidant defenses and stress response systems [35, 37]. In fact, long-term IF has been shown to improve antioxidant defenses and oxidative biomarker levels in the heart [34, 37, 38]. Here, we show that IF has an impact on heart redox state very early on, preventing the oxidation of glutathione (Table 2), protein carbonylation and MDA formation (Fig. 5).

Despite its central role in the control of energetic metabolism and aging, the skeletal muscle is still poorly studied regarding the effects of IF on redox state. Some long-term studies suggest that, unlike CR, IF may lead to a more oxidized state in this tissue, reducing antioxidant activity [39], increasing ROS production and oxidative protein modification [13]. Our short term study demonstrates that IF decreases glutathione peroxidase activity in the muscle (Table 1), although no changes are seen in glutathione redox state (Table 2) or oxidative damage markers (Fig. 5). Altogether, both our study and literature data suggest that IF does not prevent

oxidative damage in the skeletal muscle and may actually worsen the redox condition of this tissue relative to *ad libitum* diets.

The liver is expected to be largely impacted by a dietary intervention such as IF, which alternates fasting periods with significant overeating. However, the few existent studies reporting IF effects on oxidative balance in the liver did not observe changes in antioxidant defense systems or in DNA and lipid damage [35, 38, 40]. Indeed, the same is observed for CR, in which most work indicates that there is no change in redox balance in the liver [5]. This finding may reflect the fact that ROS generation in the liver is not overtly modified by changes in metabolic conditions or respiratory substrates [15]. In this study, we find that short-term IF is actually detrimental toward liver oxidative balance, as reflected by the enhanced levels of protein carbonylation (Fig. 5) and induction of glutathione synthesis (Table 2), which may be related to a slight increment in mitochondrial H_2O_2 release (Fig. 4A). Again, this indicates that not all restrictive dietary interventions with positive health-span effects produce immediate more favorable redox conditions in all organs.

Interestingly, short-term IF had very significant bioenergetic effects in the liver that were not observed in other organs: it increased respiratory capacity, irrespective of the substrate used (Figs. 2, 3), but did not enhance overall mitochondrial biogenesis (Fig. 3). In a mouse model of IF in which more significant limitation in food intake occurred, IF was also found to increase liver respiratory capacity, but this effect was accompanied by mitochondrial biogenesis [3]. The increased electron transport capacity of IF livers may be important to deal with the large fluctuations in metabolic demands in the liver under this dietary regimen, which alternates fasting periods (characterized by gluconeogenesis and β oxidation) with overeating (which promotes liver glycolysis and fatty acid synthesis).

Overall, our studies show that IF promotes complex and tissue-specific changes in mitochondrial bioenergetics and tissue redox state in a manner that is distinct from that observed in other restrictive dietary interventions. How these changes relate to both the desirable and deleterious long-term results of this dietary intervention, and how they relate to human responses to repeated fasting cycles, remains to be determined.

Supporting Information

S1 Dataset. Raw data.
(PDF)

Acknowledgments

The authors would like to gratefully acknowledge Camille C. Caldeira da Silva and Edson A. Gomes for their exceptional technical support and Silvania Nunes for expert animal husbandry and maintenance.

Author Contributions

Conceived and designed the experiments: BC MAVL ABS MHGM AJK. Performed the experiments: BC MAVL ABS. Analyzed the data: BC MAVL ABS MHGM AJK. Contributed reagents/materials/analysis tools: MHGM AJK. Wrote the paper: BC MAVL ABS MHGM AJK.

References

1. Redman LM, Ravussin E. Caloric restriction in humans: impact on physiological, psychological, and behavioral outcomes. Antioxid Redox Signal. 2011; 14: 275–287. doi: 10.1089/ars.2010.3253 PMID: 20518700

2. Speakman JR, Mitchell SE. Caloric restriction. Mol Aspects Med. 2011; 32: 159–221. doi: 10.1016/j.mam.2011.07.001 PMID: 21840335
3. Nisoli E, Tonello C, Cardile A, Cozzi V, Bracale R, Tedesco L, et al. Calorie restriction promotes mitochondrial biogenesis by inducing the expression of eNOS. Science. 2005; 310: 314–317. PMID: 16224023
4. Kowaltowski AJ. Caloric restriction and redox state: does this diet increase or decrease oxidant production? Redox Rep. 2011; 16: 237–241. doi: 10.1179/1351000211Y.0000000014 PMID: 22195991
5. Walsh ME, Shi Y, Van Remmen H. The effects of dietary restriction on oxidative stress in rodents. Free Radic Biol Med. 2014; 66: 88–99. doi: 10.1016/j.freeradbiomed.2013.05.037 PMID: 23743291
6. Anson RM, Jones B, de Cabo R. The diet restriction paradigm: a brief review of the effects of every-other-day feeding. Age (Dordr). 2005; 27: 17–25. doi: 10.1007/s11357-005-3286-2 PMID: 23598600
7. Cerqueira FM, Kowaltowski AJ. Commonly adopted caloric restriction protocols often involve malnutrition. Ageing Res Rev. 2010; 9: 424–430. doi: 10.1016/j.arr.2010.05.002 PMID: 20493280
8. Carlson AJ, Hoelzel F. Apparent prolongation of the life span of rats by intermittent fasting. J Nutr. 1946; 31: 363–375. PMID: 21021020
9. Goodrick CL, Ingram DK, Reynolds MA, Freeman JR, Cider N. Effects of intermittent feeding upon body weight and lifespan in inbred mice: interaction of genotype and age. Mech Ageing Dev. 1990; 55: 69–87. PMID: 2402168
10. Pearson KJ, Baur JA, Lewis KN, Peshkin L, Price NL, Labinskyy N et al. Resveratrol delays age-related deterioration and mimics transcriptional aspects of dietary restriction without extending lifespan. Cell Metab. 2008; 8: 157–168. doi: 10.1016/j.cmet.2008.06.011 PMID: 18599363
11. Martin B, Mattson MP, Maudsley S. Caloric restriction and intermittent fasting: two potential diets for successful brain aging. Ageing Res Rev. 2006; 5: 332–353. PMID: 16899414
12. Johnson JB, Summer W, Cutler RG, Martin B, Hyun DH, Dixit VDet al. Alternate day calorie restriction improves clinical findings and reduces markers of oxidative stress and inflammation in overweight adults with moderate asthma. Free Radic Biol Med. 2007; 42: 665–674. PMID: 17291990
13. Cerqueira FM, da Cunha FM, Caldeira da Silva CC, Chausse B, Romano RL, Garcia CC et al. Long-term intermittent feeding, but not caloric restriction, leads to redox imbalance, insulin receptor nitration, and glucose intolerance. Free Radic Biol Med. 2011; 51: 1454–1460. doi: 10.1016/j.freeradbiomed.2011.07.006 PMID: 21816219
14. Anson RM, Guo Z, de Cabo R, Lyun T, Rios M, Hagepanos A et al. Intermittent fasting dissociates beneficial effects of dietary restriction on glucose metabolism and neuronal resistance to injury from calorie intake. Proc Natl Acad Sci USA. 2003; 10: 6216–6220. PMID: 12724520
15. Tahara EB, Navarete FD, Kowaltowski AJ. Tissue-, substrate-, and site-specific characteristics of mitochondrial reactive oxygen species generation. Free Radic Biol Med. 2009; 46: 1283–1297. doi: 10.1016/j.freeradbiomed.2009.02.008 PMID: 19245829
16. Ferranti R, da Silva MM, Kowaltowski AJ. Mitochondrial ATP-sensitive K+ channel opening decreases reactive oxygen species generation. FEBS Lett. 2003; 536: 51–55. PMID: 12586337
17. Hütter E, Unterluggauer H, Garedew A, Jansen-Dürr P, Gnaiger E. High-resolution respirometry–a modern tool in aging research. Exp Gerontol. 2006; 41: 103–109. PMID: 16309877
18. Srere PA. Citrate synthase. Methods Enzymol. 1969; 13: 3–11.
19. Shacter E, Williams JA, Lim M, Levine RL. Differential susceptibility of plasma proteins to oxidative modification: examination by western blot immunoassay. Free Radic Biol Med. 1994; 17: 429–437. PMID: 7835749
20. Esworthy RS, Chu FF, Doroshow JH. Analysis of glutathione-related enzymes. In: Current Protocols in Toxicology. Wiley, 1999; Chapter 7.
21. Smith IK, Vierheller TL, Thorne CA. Assay of glutathione reductase in crude tissue homogenates using 5, 5′-dithiobis (2-nitrobenzoic acid). Anal Biochem. 1988; 175: 408–413. PMID: 3239770
22. Goldstein DB. A method for assay of catalase with the oxygen cathode. Anal Biochem. 1968; 24: 431–437. PMID: 5723299
23. Rahman I, Kode A, Biswas SK. Assay for quantitative determination of glutathione and glutathione disulfide levels using enzymatic recycling method. Nat Protoc. 2007; 1: 3159–3165.
24. Tatum VL, Ghangchit C, Chow CK. Measurement of malonaldehyde by high performance liquid chromatography with fluorescence detection. Lipids. 1990; 25: 226–229.
25. Chausse B, Solon C, Caldeira da Silva CC, Masselli Dos Reis IG, Manchado-Gobatto FB, et al. Intermittent fasting induces hypothalamic modifications resulting in low feeding efficiency, low body mass and overeating. Endocrinology. 2014; 155: 2456–2466. doi: 10.1210/en.2013-2057 PMID: 24797627

26. Caro P, Gómez J, López-Torres M, Sánchez I, Naudi A, Portero-Otín M, et al. Effect of every other day feeding on mitochondrial free radical production and oxidative stress in mouse liver. Rej Res. 2008; 11: 621–629. doi: 10.1089/rej.2008.0704 PMID: 18593280

27. Nicholls DG, Ferguson SJ. Bioenergetics 3. Academic Press: San Diego—CA, 2002; Chapter 5.

28. Cardoso AR, Chausse B, da Cunha FM, Luévano-Martínez LA, Marazzi TB, Pessoa PS et al. Mitochondrial compartmentalization of redox processes. Free Radic Biol Med. 2012; 52: 2201–2208. doi: 10.1016/j.freeradbiomed.2012.03.008 PMID: 22564526

29. Valko M, Leibfritz D, Moncol J, Cronin MT, Mazur M, Tesler J. Free radicals and antioxidants in normal physiological functions and human disease. Int J Biochem Cell Biol. 2007; 39: 44–84. PMID: 16978905

30. Cerqueira FM, Kowaltowski AJ. Mitochondrial metabolism in aging: effect of dietary interventions. Ageing Res Rev. 2012; 12: 22–28. doi: 10.1016/j.arr.2012.03.009 PMID: 22504406

31. Sanz A, Caro P, Ibañez J, Gómez J, Gredilla R, Barja G. Dietary restriction at old age lowers mitochondrial oxygen radical production and leak at complex I and oxidativeDNA damage in rat brain. J Bioenerg Biomembr. 2005; 37: 83–90. PMID: 15906153

32. Hyun DH, Emerson SS, Jo DG, Mattson MP, de Cabo R. Calorie restriction up-regulates the plasma membrane redox system in brain cells and suppresses oxidativestress during aging. Proc Natl Acad Sci USA. 2006; 103: 19908–19912. PMID: 17167053

33. Mattson MP, Wan R. () Beneficial effects of intermittent fasting and caloric restriction on the cardiovascular and cerebrovascular systems. J Nutr Biochem. 2005; 16: 129–137. PMID: 15741046

34. Wolf FI, Fasanella S, Tedesco B, Cavallini G, Donati A, Bergamini E et al. Peripheral lymphocyte 8-OHdG levels correlate with age-associated increase of tissue oxidative DNA damage in Sprague-Dawley rats. Protective effects of caloric restriction. Exp Gerontol. 2005; 40: 181–188. PMID: 15763395

35. Sharma S, Singh R, Kaur M, Kaur G. Late-onset dietary restriction compensates for age-related increase in oxidative stress and alterations of HSP 70 and synapsin 1 protein levels in male Wistar rats. Biogerontology. 2010; 11: 197–209. doi: 10.1007/s10522-009-9240-4 PMID: 19609710

36. Chandrasekar B, Nelson JF, Colston JT, Freeman GL. Calorie restriction attenuates inflammatory responses to myocardial ischemia-reperfusion injury. Am J Physiol Heart Circ Physiol. 2001; 280: 2094–2102.

37. Castello L, Froio T, Maina M, Cavallini G, Biasi F, Leonarduzzi G et al. Alternate-day fasting protects the rat heart against age-induced inflammation and fibrosis by inhibiting oxidative damage and NF-kB activation. Free Radic Biol Med. 2010; 48: 47–54. doi: 10.1016/j.freeradbiomed.2009.10.003 PMID: 19818847

38. Kaneko T, Tahara S, Matsuo M. Retarding effect of dietary restriction on the accumulation of 8-hydroxy-2′-deoxyguanosine in organs of Fischer 344 rats during aging. Free Radic Biol Med. 1997; 23: 76–81. PMID: 9165299

39. Radák Z, Takahashi R, Kumiyama A, Nakamoto H, Ohno H, Ookawara T et al. Effect of aging and late onset dietary restriction on antioxidant enzymes and proteasome activities, and protein carbonylation of rat skeletal muscle and tendon. Exp Gerontol. 2002; 37: 1423–1430. PMID: 12559411

40. Armeni T, Pieri C, Marra M, Saccucci F, Principato G. Studies on the life prolonging effect of food restriction: glutathione levels and glyoxalase enzymes in rat liver. Mech Ageing Dev. 1998; 101: 101–110. PMID: 9593316

3. Chapter II - Intermittent Fasting Induces Hypothalamic Modifications Resulting in Low Feeding Efficiency, Low Body Mass and Overeating

Bruno Chausse[1], Carina Solon[2], Camille C. Caldeira da Silva[1], Ivan G. Masselli dos Reis[3], Fúlvia B. Manchado-Gobatto[3], Claudio A. Gobatto[3], Licio A. Velloso[2] and Alicia J. Kowaltowski[1]

[1]Departamento de Bioquímica, Instituto de Química, Universidade de São Paulo, Brazil; [2]Faculdade de Ciências Médicas, Universidade Estadual de Campinas, Brazil; [3]Faculdade de Ciências Aplicadas, Universidade Estadual de Campinas, Brazil

Reproduced from *Endocrinology*. Accepted April 29th, 2014. Published online May 5th, 20

Intermittent Fasting Induces Hypothalamic Modifications Resulting in Low Feeding Efficiency, Low Body Mass and Overeating

Bruno Chausse, Carina Solon, Camille C. Caldeira da Silva, Ivan G. Masselli dos Reis, Fúlvia B. Manchado-Gobatto, Claudio A. Gobatto, Licio A. Velloso, and Alicia J. Kowaltowski

Departamento de Bioquímica (B.C., C.C.C., A.J.K.), Instituto de Química, Universidade de São Paulo, 05508-000 Brazil; Faculdade de Ciências Médicas (C.S., L.A.V.), Universidade Estadual de Campinas, 13083-970 Brazil; Faculdade de Ciências Aplicadas (I.G.M., F.B.M-G., C.A.G.), Universidade Estadual de Campinas, 13084-350 Brazil

Intermittent fasting (IF) is an often-used intervention to decrease body mass. In male Sprague-Dawley rats, 24 hour cycles of IF result in light caloric restriction, reduced body mass gain, and significant decreases in the efficiency of energy conversion. Here, we study the metabolic effects of IF in order to uncover mechanisms involved in this lower energy conversion efficiency. After 3 weeks, IF animals displayed overeating during fed periods and lower body mass, accompanied by alterations in energy-related tissue mass. The lower efficiency of energy use was not due to uncoupling of muscle mitochondria. Enhanced lipid oxidation was observed during fasting days, whereas fed days were accompanied by higher metabolic rates. Furthermore, an increased expression of orexigenic neurotransmitters AGRP and NPY in the hypothalamus of IF animals was found, even on feeding days, which could explain the overeating pattern. Together, these effects provide a mechanistic explanation for the lower efficiency of energy conversion observed. Overall, we find that IF promotes changes in hypothalamic function that explain differences in body mass and caloric intake. **(*Endocrinology* 155: 2456–2466, 2014)**

Intermittent fasting (IF), also referred to as intermittent feeding or every other day feeding, is a dietary intervention for laboratory animals that involves fasting and feeding cycles, usually of 24 hours each (1). This feeding protocol results in weight loss and is thus often adopted as an alternative to caloric restriction (1), despite contradictory evidence regarding its effect on lifespan (2, 3). IF has also been suggested as a measure to enhance laboratory animal healthspan, decreasing obesity and metabolic disorders associated with aging (4). Indeed, several groups have demonstrated that IF affects stress resistance, energy metabolism, and signaling pathways associated with enhanced healthspan (5–8).

Although many metabolic effects of IF have been studied, little attention has been given to the fact that, despite their reduced body mass, IF animals often show similar overall caloric intake to ad libitum-fed animals (1, 9). This result indicates a lower energy conversion efficiency in IF which remains to be mechanistically explained, and may reflect changes in peripheral and/or central regulation of energy metabolism.

Peripheral tissues control body mass by promoting changes in energy expenditure. Energy can be effectively dissipated by adaptive thermogenesis promoted by mitochondrial uncoupling (10), or an enhanced proton leak across the inner mitochondrial membrane, leading to lower ATP synthesis and loss of a larger fraction of the energy released from electron transport as heat (11). Indeed, skeletal muscle, heart, and brown adipose tissues are sources of energy expenditure due to mitochondrial uncoupling (12–16).

ISSN Print 0013-7227 ISSN Online 1945-7170
Printed in U.S.A.

Received November 15, 2013. Accepted April 29, 2014.
First Published Online May 5, 2014

Abbreviations: AGRP, agouti-related peptide; CRH, corticotropin-releasing hormone; IF, intermittent fasting; MCH, melanin-concentrating hormone; NPY, neuropeptide Y; POMC, proopiomelanocortin; RER, respiratory exchange ratios; SM, skeletal muscle; TRH, thyrotropin-releasing hormone; UCP, uncoupling protein.

In the central nervous system, feeding behavior and body mass are primarily controlled by neurons within the arcuate nucleus in the hypothalamus (reviewed in Reference 17). A subpopulation of orexigenic neurons stimulates appetite and energy conservation, whereas anorexigenic neurons suppress appetite and increase energy dissipation (18). Both populations are sensitive to leptin, a hormone that is secreted by adipocytes in a manner correlated with increases in adipose mass (19). Leptin inhibits orexigenic pathways and induces anorexigenic signaling (20), maintaining body mass homeostasis. Thus, changes in leptin levels or resistance to leptin signaling are involved in obesity and related metabolic abnormalities (21, 22).

Here, we study changes in mitochondrial and hypothalamic function in order to uncover the mechanisms leading to overeating and to lower feed conversion efficiency in IF animals. Our results explain the lower feed efficiency, and also uncover alterations in hypothalamic signaling responsible for the gorging feeding pattern.

Materials and Methods

Animals and tissue collection

All experiments were conducted in agreement with the National Institutes of Health guidelines for humane treatment of animals and were reviewed and approved by the local Animal Care and Use Committee. Male, 8-week-old Sprague-Dawley rats were separated into two groups: AL, fed ad libitum; and IF, which had ad libitum access to food on alternating days. The animals were lodged four individuals per cage, in 12 hours light/dark cycles, and given water ad libitum. A standard AIN-93 M diet produced by Rhoster was used in the study. Body mass and food consumption were recorded daily. Cumulative food consumption over the treatment period was recorded for each cage and the average intake per animal was used to calculate feed conversion efficiency [(average weight gain per cage/average food intake per cage) × (100)]. Fecal mass was quantified during 24-hour periods in metabolic cages, and data are presented as 48-hour profiles, to include both fasting and feeding periods. Fecal cholesterol ester and triglyceride content was measured by thin layer chromatography as previously described in reference 23. Chow was alternately placed or removed at 5:00 pm for IF animals. After 3 weeks of dietary intervention, the AL and IF rats were euthanized by decapitation after 12 hours of overnight fasting or feeding (as indicated for each experiment). Diazepam 5 mg/ml (Compaz), Xylazine 2% (Syntec), and Ketamine 50 mg/ml (Cristalia) were used as anesthetics in experiments that measured in vivo leptin responses. Livers, epididymal, and visceral (retroperitoneal plus mesenteric) adipose tissues, soleus and planataris muscles were dissected and weighed. Serum was also collected. Total hind limb skeletal muscle (SM) was pooled and homogenized.

Biochemical determinations

Serum leptin and ghrelin levels were measured by ELISA (Millipore) in animals fasted for 12 hours (Table 1) or fed animals (data not shown) following the manufacturer's instructions. Serum, liver, and SM triglycerides were determined using a commercial colorimetric kit (Doles). A glucose analyzer (Accu-Check Performa) was used to determine fasting glucose levels.

Indirect calorimetry

O_2 consumption, CO_2 release, and respiratory exchange ratios (RER) were measured in fed and fasted animals using an indirect open circuit calorimeter (MM-100, CWE, Inc), as indicated by the manufacturer.

Spontaneous activity

Spontaneous activity of rats was assessed using a gravimetric method adapted from Biesiadecki et al (24). Briefly, IF and AL cages (4 animals per cage) were maintained on a top-loading electronic scale (Lider Balanças, model PLA 30 kgf) with an amplified force register (MK Controle e Instrumentação, model MKTC-05) and coupled to a signal acquisition module (National Instruments, model USB 6008). Signals were captured using LABVIEW Signal Express software, at 30 Hertz (Hz). Before the beginning of the experiments, individual calibration slopes were determined for each register system using known weights. Spontaneous activity was determined by the sum of differences of weight between two registers, in modular values (Equation 1).

$$AE(gf) = \sum |x2 - x1|, |x3 - x2|, \ldots, |(xn+1) - xn|$$

Modular values were used, since upward movements registered negative values whereas downward movements registered positive values. Data analysis were performed during 23 hours (12 hours of dark and 11 hours of light). Since animal handling (weighing and feed control) were conducted between 5:00 and 6:00 pm, this time period was excluded from the analysis.

Table 1. Biochemical and Physiological Parameters in AL and IF Animals

	AL	IF	Fasted IF	Fed IF
Fasting glucose (mg · dL^{-1})	108.2 ± 2.8	103.2 ± 4.8		
Fasting ghrelin (ng · dL^{-1})	1.76 ± 0.26	1.64 ± 0.16		
48 h feces output (g)	23.99 ± 2.19	23.68 ± 0.87		
Triglycerides				
Serum (mg · dL^{-1})	0.977 ± 0.032		0.930 ± 0.036	1.098 ± 0.018[a,b]
Liver (mg · dL^{-1} · mg prot^{-1})	1.303 ± 0.170		0.963 ± 0.054	2.048 ± 0.360
SM (mg · dL^{-1} · mg prot^{-1})	5.593 ± 0.580		5.535 ± 0.530	5.850 ± 0.530
Temperature (°C)	37.44 ± 0.05		37.23 ± 0.09	37.74 ± 0.11[a]

Values are means ± SEM (n = 18 for glucose measurements, n = 8–16 for temperatures and ghrelin measurements and n = 4 for all others measurements). [a], $P < .05$ verus AL; [b], $P < .05$ vs fasted IF.

Effect of leptin on food intake

For this assay, rats were food deprived for 12 hours (6:00 am to 6:00 pm) after a feeding period, and, at 6:00 pm, were treated with a single intraperitonial dose of PBS (100 μL) or leptin (100 μL, 10^{-6} M). Food ingestion was determined every 2 hours over the next 12 hours (adapted from Yamada et al, Reference 25). Data plotted were for the first 4 hours following the injection, which we found was the period of most noticeable leptin action. A similar experiment was conducted with animals injected at 8:00 am, with comparable results (not shown).

Intact SM fiber preparation and respiration

Soleus muscles were separated from connective tissues and manually teased into small myofiber bundles under a magnifying glass. These bundles were shredded to maximize the surface area. All processing was conducted over ice. Respiratory measurements were performed using an Oroboros high-resolution respirometry system (26) in experimental buffer containing 2.68 mM KCl, 1.47 mM KH_2PO_4, 136.89 mM NaCl, 81 mM Na_2HPO_4, and 10 mM glucose at 37°C.

Citrate synthase activity

SM samples were homogenized using an electric potter in buffer containing 300 mM sucrose, 50 mM HEPES, 10 mM Tris, 1 mM EGTA, and 0.2% BSA, pH 7.2, HCl. Tissues lysates were centrifuged (850 *g*, 5 minutes, at 4°C), and the resulting supernatants were collected. A reaction mixture of 20 mM Tris-HCl pH 8.0, 0.42 mM acetyl-coenzyme A, 0.1 mM DTNB [5,5-dithiobis(2-nitrobenzoic acid)] and 20 mg of total protein was incubated at 37°C for 5 minutes. The reaction was initiated by the addition of 0.5 mM oxaloacetate. The reduction of DTNB by citrate synthase was measured spectrophotometrically for 3 minutes at 412 nm (extinction coefficient = 13.6 $mM^{-1} \cdot cm^{-1}$; adapted from 27). Activities are expressed as μmol citrate $\cdot$ min^{-1} $\cdot$ mg $protein^{-1}$.

Isolation of skeletal muscle mitochondria

SM mitochondria were isolated from fasted rat hind limbs as described in reference 28. Hind limb muscles were dissected over iced 10 mM Na EDTA-supplemented PBS to remove fatty acids and connective tissues and then washed and finely minced in 300 mM sucrose, 50 mM HEPES, 10 mM Tris, 1 mM EGTA, and 0.2% BSA (pH 7.2, HCl), at 4°C. The tissue was processed for 2 seconds with a Polytron homogenizer and then transferred to a mechanized potter and homogenized. The suspension was centrifuged at 850 *g* for 3 minutes, and the supernatant was centrifuged again at 10000 *g* for 5 minutes. The pellet was resuspended and centrifuged at 7000 *g* for 3 minutes. The final mitochondrial pellet was resuspended in a minimal volume of isolation buffer. Protein quantification was conducted using the Bradford method.

Isolated mitochondrial respiration

SM mitochondrial respiration was followed using a Oroboros high-resolution respirometry system (26). O_2 consumption was monitored using 0.125 mg/mL of isolated mitochondrial suspensions of fasted animals in experimental buffer containing 150 mM KCl, 10 mM HEPES, 2 mM KH_2PO_4, 2 mM $MgCl_2$, 2 mM EGTA, 1 mM malate, 1 mM glutamate, and 1% BSA, pH 7.2, at 37°C. State 3 respiration (in the presence of active oxidative phosphorylation) was induced by the addition of 1 mM ADP, and state 4 respiration (in the absence of oxidative phosphorylation) was promoted by adding 1 μg/mL oligomycin, an ATP synthase inhibitor.

Immunoblotting

For experiments that measured leptin responses, the abdominal cavities of anesthetized rats were opened and the animals received an injection of leptin (100 μL, 10^{-6} M) or PBS (100 μL) through the vena cava. After 30 minutes, the hypothalamus was excised and immediately homogenized in solubilization buffer (1% Triton X-100, 100 mM Tris-HCl, pH 7.4, 100 mM sodium pyrophosphate, 100 mM sodium fluoride, 10 mM EDTA, 10 mM sodium orthovanadate, 2.0 mM phenylmethylsulfonylfluoride, and 0.1 mg aprotinin/mL) at 4°C with a Polytron PTA 20S homogenizer (model PT 10/35; Brinkmann Instruments). Insoluble material was removed by centrifugation for 15 minutes at 9000 *g*. The protein concentration of the supernatants was determined by the Bradford method. In immunoblot experiments, 0.05–0.20 mg of protein extracts were separated by SDS-PAGE, transferred to nitrocellulose membranes, and blotted with phospho-JAK-2 (P-JAK-2) (sc16566-R, rabbit polyclonal, Santa Cruz Biotechnology) and phospho-STAT-3 (P-STAT-3) (sc8059, mouse monoclonal, Santa Cruz Biotechnology) antibodies. Specific bands were detected by chemiluminescence and data were normalized to β-actin.

qRT-PCR

The expression of neuropeptide Y (NPY), agouti-related peptide (AGRP), thyrotropin-releasing hormone (TRH), corticotropin-releasing hormone (CRH), orexin, proopiomelanocortin (POMC), and melanin-concentrating hormone (MCH) were measured in hypothalamus samples obtained from fed and fasted AL and IF rats. Although whole hypothalamus samples were used, it should be noted that these neurotransmitters are produced primarily in the arcuate nucleus (NPY, AGRP, and POMC) or in second order neurons localized in adjacent hypothalamic nuclei (MCH, TRH, orexin, and CRH). Intron-skipping primers were obtained from Applied Biosystems. The following primers were used in the experiment: POMC Rn: 00595020-m1e M m:00435874-m1; NPY Rn: 0056168-m1e Mm:00445771-m1; AgRP Rn: 01431703-g1e Mm:00475829-m1; MCH Rn: 00561766-g1e Mm:01242886-g1; CRH Rn: 01462137-m1e Mm:01293920-s1; orexin Rn00565995-m1; TRH Rn: 00564880-m1e Mm:01182425-g1. Glyceraldehyde-3-phosphate dehydrogenase primers were used as a control. There was no statistical difference in average Ct for GAPDH from AL and IF animals in the same dietary state (fasting: 25.69 $\pm$ 0.2709 and 25.04 $\pm$ 0.4608 to AL and IF rats, respectively) (feeding: 20.97 $\pm$ 0.5528 for AL animals and 20.13 $\pm$ 0.3556 for IF animals). Real-time RT-PCR analysis of gene expression was performed in an ABI Prism 7700 sequence detection system (Applied Biosystems). The optimal concentration of cDNA and primers, as well as the maximum amplification efficiency, was obtained through a five-point, 2-fold dilution curve analysis for each gene. Each PCR contained 3.0 ng of reverse transcribed RNA, 200 nM of each specific primer, TaqMan (Applied Biosystems), and ribonuclease-free water to a final volume of 20 μL. Real-time data were analyzed using the Sequence Detector System 1.7 from Applied Biosystems (29).

Statistical analysis

Data were analyzed using GraphPad Prism and Origin Software. Figures represent averages ± SEM and were compared using *t* tests or ANOVA, as described in figure legends. Two-tailed *P* values under .05 were considered significant.

Results

Intermittent fasting promotes gorging feeding patterns and low feed conversion efficiency

Eight-week-old Sprague Dawley rats were either fed AL or maintained on an IF diet, which alternates 24-hour feeding and 24-hour fasting periods, over three weeks. IF animals presented significant daily fluctuations of approximately 10% of their total weight (Figure 1A), as well as significantly lower body mass gains over 3 weeks compared to AL animals.

The 3-week weight gain was 22.50 ± 3.05 g for IF animals and 50.39 ± 2.70 g for AL rats (n = 24, $P < .05$ as assessed by repeated measures of fed animals at the last time point vs the same group before the dietary intervention). During the treatment, IF animals gorged when offered food, and ate approximately 53% of their daily food consumption within the first 2 hours after food offering (Figure 1B). Interestingly, IF rats presented slightly lower cumulative food ingestion over the treatment (Figure 1C), representing a 20% restriction of energy intake. In addition to this moderate decrease in caloric intake, IF animals displayed much lower feed conversion efficiency when compared to AL (Figure 1D), indicating that this diet changes not only food intake but also has an impact on energy metabolism. Fecal output mass was similar between the groups (Table 1) whereas cholesterol esters and triglyceride content in feces was 15% higher in IF animals (data not shown), indicating that IF may reduce absorption, which may be a factor in the lower feed conversion efficiency. However, since this change is mild, we hypothesized that changes in metabolic efficiency could also be involved in the decreased energy use observed in IF rats.

In order to identify reasons for the difference in energy efficiency observed, we measured the mass of metabolically-relevant tissues. We found a decrease in liver mass from IF animals during fasting days (Figure 2A), which is probably a consequence of the utilization of hepatic glycogen and lipids as energetic sources. Indeed, the levels of hepatic triglycerides in IF-fed rats were 212.6% of that in IF-fasted animals ($P = .0512$; Table 1). SM tissue mass was also affected by IF; soleus (Figure 2B) and plantaris (Figure 2C) muscle weight were reduced, even when SM mass was normalized to whole body mass (AL - 0.0566 ± 0.0012%, IF - 0.0522 ± 0.0006% for soleus; AL - 0.1459 ± 0.0032%, IF - 0.1303 ± 0.0023% for plantaris), indicating a condition of sarcopenia induced by IF. In addition, epididymal adipose tissue mass was significantly reduced in IF rats during both feeding and fasting phases (although this difference was not significant when normalized to body weight), whereas the visceral adipose reservoir was not (Figure 2, D and E).

IF does not alter SM mitochondrial mass or function

The loss of SM mass and lower feed conversion efficiency promoted by IF may be due to central and/or peripheral changes in energy metabolism, which alter the use of lipids vs carbohydrates and the amount of useful energy extracted from these substrates. We initially investigated if peripheral changes in energy conversion occur in IF by quantifying and verifying the coupling of SM mitochondria in IF animals. We found (Figure 3A) that intact SM fibers present equal O_2 consumption rates in IF and AL animals, suggesting that mitochondrial mass and coupling are unaltered. Indeed, the content of mitochondria was determined by measuring SM citrate synthase activity, a marker for mitochondrial mass, and found to be equal in both AL and IF (Figure 3B). Next, we determined mitochondrial respiration and coupling, which can affect the quantity of ATP produced from a given substrate (reviewed in Reference 30). Mitochondria were isolated from SM and their oxygen consumption rates were measured under conditions in which ATP was being synthesized and respiration is maximized (state 3 respiration, in the presence of added ADP; Figure 3C) and also in the absence of ATP

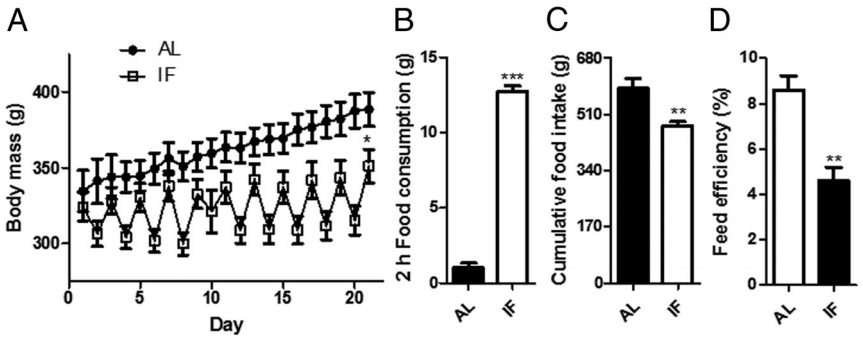

Figure 1. Intermittent fasting promotes overeating, lower feed conversion efficiency and reduced body mass. A, Body mass variations over time in AL (●) and IF (■) animals (n = 8). B, Cumulative food intake during the first two hours of refeeding (n = 7–10). C, Cumulative food intake (n = 6) and (D) feed conversion efficiency over three weeks of treatment (n = 6). Data represent averages ± SEM and were compared using *t* tests. *, $P < .05$; **, $P < .01$; ***, $P < .001$ vs AL. AL indicates ad libitum feeding, IF indicates intermittent fasting.

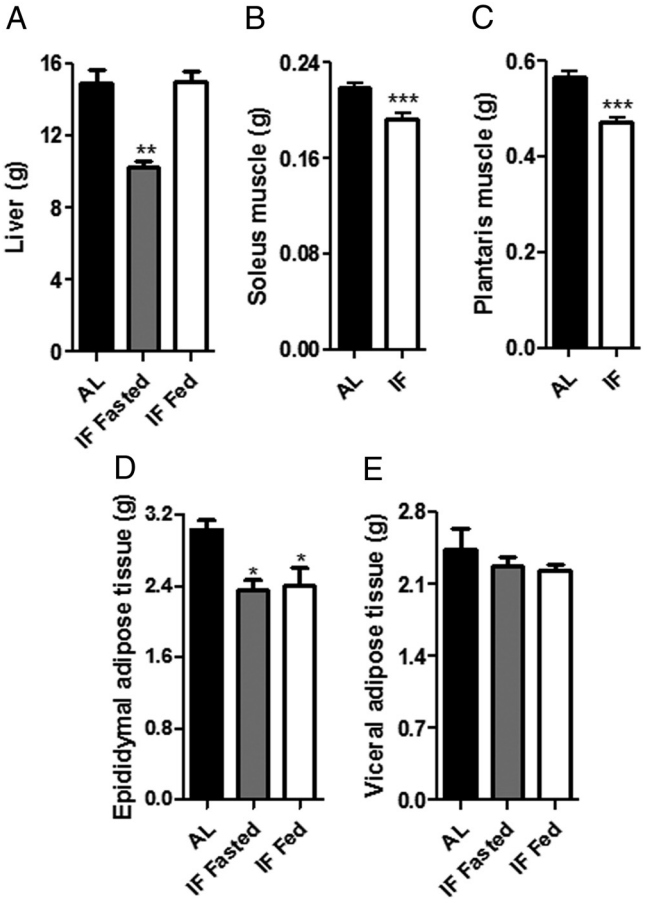

Figure 2. IF differentially affects energy-related tissues mass. A, Liver mass (n = 4). Soleus (B) and plantaris (C) muscle mass of fasted animals (n = 16). D, Epididymal adipose tissue mass (n = 8). E, Visceral (retroperitoneal plus mesenteric) adipose tissue mass (n = 4). Data represent averages ± SEM and were compared using *t* tests (Panels B and C) and 1-way ANOVA followed by Bonferroni post test (Panels A, D, and E). *, $P < .05$; **, $P < .01$; ***, $P < .001$, vs AL. AL indicates ad libitum feeding, IF indicates intermittent fasting.

synthesis (state 4, in the presence of the ATP synthase inhibitor oligomycin). These results were similar when BSA, which inhibits uncoupling proteins, was omitted from the experimental media, and when experiments were conducted in fed animals (results not shown). A lack of difference in state 4 respiratory rates indicates that mitochondrial coupling is equal in both experimental groups, and eliminates a role for changes in SM mitochondrial coupling as the mechanism responsible for the lower energy conversion efficiency and sarcopenia observed in IF animals. A different use of lipids as the SM energy source during fasting or feeding periods is also not the cause for decreased SM mass, because triglyceride levels were the same (Table 1).

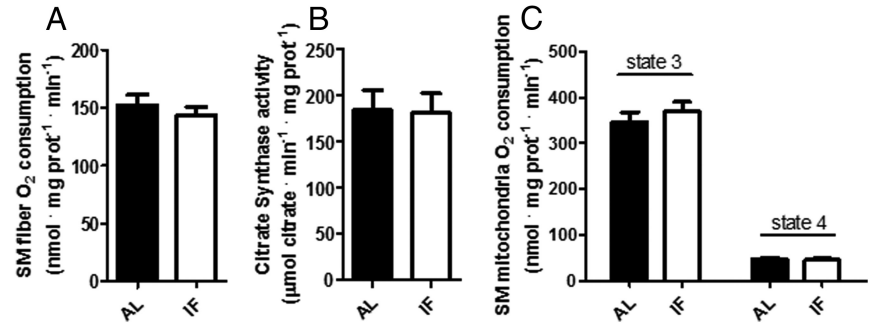

Figure 3. IF does not alter mitochondrial mass or coupling. A, SM fiber respiratory rates were measured as described in Materials and Methods (n = 14); B, Skeletal muscle citrate synthase activity, determined as described in Materials and Methods (n = 8); C, Isolated SM mitochondrial respiration in state 3 (phosphorylating), induced by 1 mM ADP, and in state 4 (nonphosphorylating), induced by 1 µg/mL oligomycin, was measured as described in Materials and Methods (n = 14–16). All measurements were made using fasted animals. AL indicates ad libitum feeding, IF indicates intermittent fasting.

Spontaneous motor activity is decreased by IF

Alterations in energy conversion efficiency observed in IF animals could be a consequence of changes in activity levels. Therefore, we measured the spontaneous activity of both groups. Surprisingly, we found that, overall, IF rats present lower activity levels than control animals (Table 2). Although there was no significant difference in spontaneous activity between the groups during light periods, during dark periods IF animals presented decreased activity when fasted. These data indicate that alterations in spontaneous activity cannot explain the difference in feed efficiency observed.

IF promotes higher metabolic rates on feeding days and enhanced lipid oxidation on fasting days

Because no differences in isolated mitochondrial energy conversion efficiency or spontaneous movement were observed, changes in whole animal energy conversion are probably attributable to central alterations in the control of energy metabolism. In order to investigate this possibility, we conducted whole animal indirect calorimetry experiments, measuring O_2 consumption and CO_2 production (Figure 4). We found that IF animals presented higher O_2 consumption and CO_2 emission on fed days (Figure 4, A and B, open bars), which is indicative of higher rates of oxidative catabolic metabolism. In addition to high respiratory rates, IF animals also presented elevated body temperatures (Table 1), further indicating enhanced metabolic rates on feeding days.

On fasting days (Figure 4, gray bars), IF animals presented similar O_2 consumption rates to AL rats (Figure 4A), but with lower CO_2 release (Figure 4B). As a result, the RER (CO_2 produced per O_2 consumed; Figure 4C) was lower. This indicates a preferential oxidation of

Table 2. Spontaneous Activity (kgf · 10^{-3}) of AL and IF Animals During Dark (12 Hours) and Light (11 Hours) Periods, Evaluated in Collective Cages (4 Rats Per Cage)

Group	Period	
	Night (6:00 pm–6:00 am)	Day (6:00 am–5:00 pm)
AL	3420.0 ± 267.8	1137.5 ± 118.2
Fasted IF	1741.4 ± 239.5[a,b]	854.1 ± 159.3
Fed IF	2758.2 ± 577.4	1036.8 ± 216.0

Values are means ± SEM (n = 4–8 cycles). [a], $P < .05$ verus AL; [b], $P < .05$ vs fed IF, both during the night period.

lipids during the IF fasting period, because lipids are more highly reduced and require larger proportions of O_2 to be catabolized (31, 32). The result is compatible with our data showing a loss of liver mass tissue during IF fasting days (Figure 2A) and the alterations in triglyceride contents in both serum and liver (Table 1). Altogether, this data indicates that lower body weight in IF is a consequence of elevated basal metabolic rates during feeding days associated with increased lipid oxidation during fasting days.

IF, but not AL animals, are leptin-sensitive

We investigated next the effects of IF on the control of appetite and energy metabolism at the hypothalamic level, in order to uncover possible mechanisms responsible for the changes in metabolic rates. Leptin signaling was tested first, since it regulates both appetite and energy expenditure (20). After fasting for 12 hours, food intake was measured in AL and IF animals, with or without leptin injections. Interestingly, AL animals showed no response to leptin (Figure 5A), ingesting equal amounts of food. This is a surprising result because 3-month old rats are young and not expected to present significant metabolic impairments that animals maintained on AL diets develop over time, including characteristics of the metabolic syndrome (obesity, insulin resistance, and hyperleptinemia at advanced ages) (8, 33–36, 56). The surprising results indicating AL animals were leptin-resistant were supported by measurements of hypothalamic P-JAK-2 (Figure 5B) and P-STAT-3 (Figure 5C) that are induced by leptin: no significant changes were observed in AL animals treated with this hormone, confirming they display apparent hypothalamic leptin resistance. Increased levels of leptin in the serum of AL animals (Figure 5D) are also compatible with a condition of leptin resistance, whereas fasting levels were found to be equal between both groups (results not shown). On the other hand, IF animals did respond to leptin with decreased food intake (Figure 5A) and increased P-JAK-2 and P-STAT-3 after feeding (Figure 5, B and C, respectively), indicating that this restricted diet preserves leptin signaling over time, as observed in other restrictive dietary interventions (36). Indeed, the decreased level of serum leptin observed in IF animals (Figure 5D) is in agreement with literature data linking low levels of this hormone with adequate responses to their signaling (36, 56). Interestingly, in the absence of exogenous leptin, 4-hour food intake in IF rats was noticeably higher than in AL-fed animals (Figure 5A). Since both groups were submitted to the same time interval of fasting prior to this experiment, this result suggests IF affects the central control of appetite over time, increasing hunger, as also indicated by the gorging feeding pattern observed in Figure 1B.

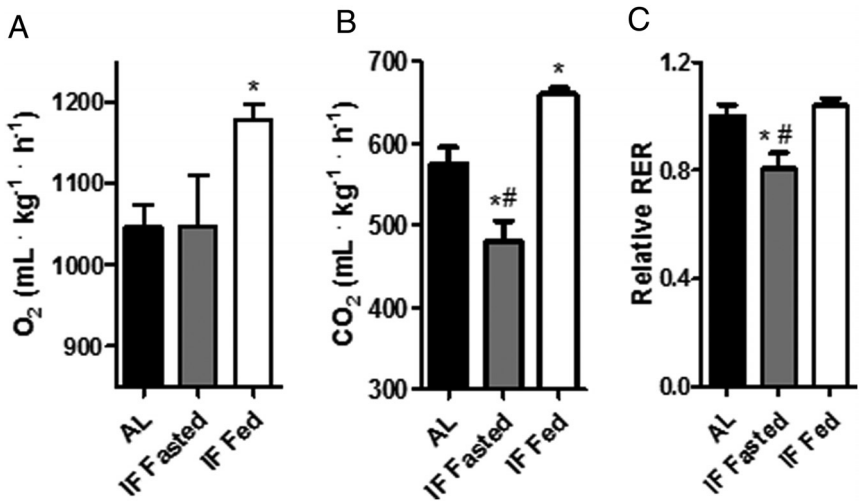

Figure 4. IF promotes higher metabolic rates on feeding days and enhanced lipid oxidation on fasting days. Twenty-four hours O_2 consumption (A) and CO_2 production (B) production were measured as described in Materials and Methods. C, Respiratory exchange ratios (RER; CO_2/O_2) were calculated from the data in Panels A and B. Data were normalized to AL respiratory rates (n = 4–6). Data represent averages ± SEM and were compared using 1-way ANOVA followed by Bonferroni post test *, $P < .05$ vs AL; #, $P < .05$ vs Fed IF. AL indicates ad libitum feeding, IF indicates intermittent fasting.

IF increases orexigenic neurotransmitters and decreases TRH expression

Our results studying leptin effects indicated that IF animals present preserved leptin responses, and that leptin signaling is not responsible for the gorging feeding pattern of these animals. In order to gain insight into the mechanism responsible for enhanced appetite in IF animals, we measured mRNA levels of hypothalamic neurotransmitters involved in appetite and metabolic regulation. mRNA levels of CRH, which is anorexigenic (reviewed in Reference 37), were unchanged by IF (Figure 6, A and B, fasted and fed levels, respec-

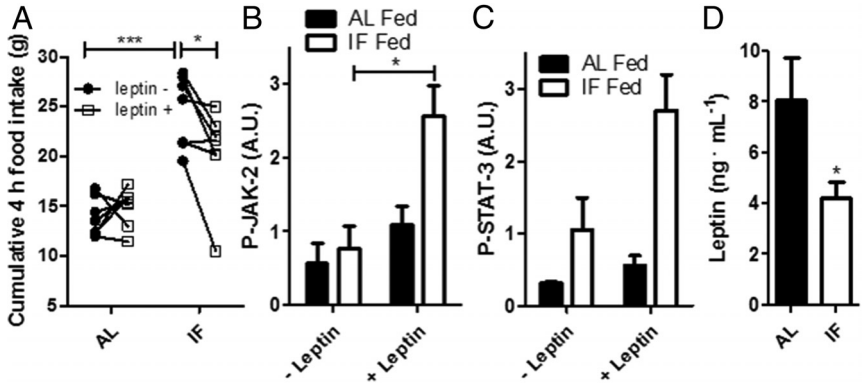

Figure 5. IF, but not AL animals, are leptin-sensitive. A, Spontaneous food intake over 4 hours was measured after 12 hours fasting in AL or IF animals injected with leptin (□) or PBS (●) (n = 7). Lines connect data collected from the same animal. P-JAK-2 (B) and P-STAT-3 (C) levels were measured as described in Materials and Methods (n = 4). D, Serum leptin levels in fed AL and IF animals (n = 8). *, $P < .05$ vs Fed IF. Data represent averages ± SEM and were compared using *t* tests (paired, for panel A). *, $P < .05$; ***, $P < .001$. AL indicates ad libitum feeding, IF indicates intermittent fasting.

tively), as were levels of orexigenic MCH (reviewed in Reference 38) and anorexigenic POMC (reviewed in Reference 38). On the other hand, IF animals presented increased expression of orexigenic neurotransmitters AGRP (reviewed in Reference 38) and NPY (reviewed in Reference 38), even on feeding days. The expression of orexin, an orexigenic neurotransmitter produced in lateral hypothalamus, was higher in fasted IF animals. This result is in line with the leptin-sensitive overeating displayed by IF animals. Overeating was not related to increased ghrelin release, since the levels of this hormone was similar both in fasted animals on each diet (Table 1) and when fed (results not shown).

Furthermore, mRNA levels of TRH were decreased in fasted IF animals (Figure 6A), but returned to control levels on feeding days (Figure 6B). Since TRH controls the levels of circulating thyroid hormones and thermogenesis, this modification may be related to the observed increase in feeding metabolic rates for IF animals (Figure 4). Overall, the changes in hypothalamic function promoted by IF explain both the overeating patterns displayed by these animals and, possibly, the lower energy conversion efficiency resulting in lower weight gain.

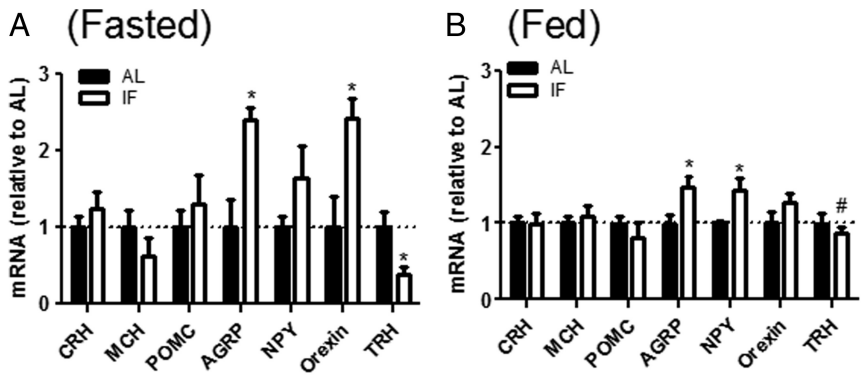

Figure 6. IF increases orexigenic neurotransmitters and decreases TRH. Relative quantities of hypothalamic neurotransmitter mRNAs were measured as described in Materials and Methods on fasting (A) and feeding (B) days (n = 4–8). Data represent averages ± SEM and were compared using *t* tests. *, $P < .05$ vs AL levels of the same neurotransmitter; # ,< .05 vs TRH in fasted IF. AL indicates ad libitum feeding, IF indicates intermittent fasting.

Discussion

The effect of dietary interventions on animal health has attracted increasing attention since it is widely recognized that restricted diets can have positive effects on aging parameters in laboratory animals. In this sense, many effects of IF have been uncovered, mainly pertaining to metabolic and stress responses associated with aging (reviewed in Reference 9).

While the long-term effects of IF are certainly interesting, a consistent finding even with short-term IF is that animals overeat when offered food, often ingesting the same amount of food as AL animals, but maintaining lower body mass (1, 40, 41). Indeed, our data in Figure 1 demonstrate that IF animals have a lower weight gain, and also ingest approximately 20% less food. In addition to the decreased food consumption, other alterations must be related to IF animals' lower body mass, because this dietary intervention promotes a highly significant decrease in energy conversion efficiency. This report was designed to uncover mechanisms responsible for the decreased use of substrate energy in IF animals, and, in the process of doing so, also uncovered mechanisms underlying the gorging feeding pattern.

Previous studies have shown that changes in energy expenditure in IF are not associated with increased ambulatory activity (42, 43). Indeed, we observed that IF animals overall move less than control animals (Table 2), and spontaneous activity cannot explain the differences in energy expenditure. Despite a reduction in overall movement, IF animals presented an increment in basal metabolic rates (Figure 4) on fed days, which is suggestive of higher thermogenesis (because less energy is conserved in these animals and is not used for locomotion, it must be dis-

sipated as heat). Indeed, we found that hypothalamic levels of TRH significantly rose in IF animals during feeding days relative to fasting days (Figure 6). This thermogenic neurotransmitter stimulates the production of thyroid-stimulating hormone and, consequently, increases energy expenditure and contributes toward lower body mass gains (reviewed in Reference 44), a result compatible with higher body temperatures measured in IF animals. Our results thus suggest that IF is capable of stimulating TRH neurons, resulting in global modifications of metabolic rates and reduced feed conversion efficiency, although this mechanism remains to be further investigated.

Reduced efficiency of energy conversion is also related in many experimental models to changes in muscular energy use, mainly by decreasing the coupling of SM mitochondria, resulting in lower generation of ATP and higher heat release (14, 15). In this sense, some groups observed that decreased mitochondrial coupling due to uncoupling protein (UCP) 3 expression is involved in the regulation of energy expenditure in SM (45, 46). Other studies find that changes in UCP3 levels do not necessarily modify mitochondrial coupling in this tissue (47, 48). The existence of UCP1-expressing brown adipocytes within the SM promoting enhanced thermogenesis has been observed in some animal models (49). Other studies (5) have suggested that the control of mitochondrial biogenesis and content may be responsible for changes in energy conversion efficiency observed with dietary interventions. As a result, we quantified markers of mitochondrial activity, mass and coupling (Figure 3). An extensive collection of results showed no difference in AL vs IF animals, indicating that direct changes in mitochondrial metabolism are not responsible for the enhanced energy expenditure observed. These data also indicate that differences in mitochondrial physiology are not related to decreased SM mass of IF animals. Since there were no differences in lipid content in SM (Table 1), sarcopenia could be a consequence of alterations in protein metabolism in this tissue. Indeed, during severe fasting, proteins are largely utilized as a fuel source. In addition, dietary interventions and aging usually induce alterations in muscle protein metabolism, including activating the ubiquitin proteasome system activity and altering protein turnover (50, 51, 52).

Since IF does not alter mitochondrial coupling, it seems plausible to suggest that IF animals have reduced efficiency of energy usage due to changes in metabolic patterns promoted by the intermittent availability of substrates. In most animal models, fasting involves an energy conservation strategy in which metabolic rates are decreased and lipids are used as the energy source for most organs. This is accompanied by increased blood flow to the white adipose tissue, higher triglyceride hydrolysis, and increased circulating levels of fatty acids (53–55). Indeed, large changes in energy metabolism were observed in IF animals on fed vs fasting days (Figure 4). On fasting days, IF animals present enhanced lipid oxidation, as indicated by the low RER, resulting in decreased liver mass (Figure 2A) and reduced serum and liver triglyceride content (Table 1). On the other hand, feeding days in IF animals resulted in higher O_2 consumption and CO_2 production rates relative to AL, indicative of higher metabolic rates. The RER was equal to AL fed animals, indicating that the proportion of carbohydrate metabolized was equal. This, associated with the high food ingestion, weight fluctuations observed (Figure 1), and fluctuations in liver mass (Figure 2) and content (Table 1) suggest that IF animals produce fat from carbohydrate on feeding days, and consume the lipid stored while fasting, resulting in higher overall metabolic conversions and, as a result, energy expenditure.

Although explaining for the low energy conversion efficiency observed in IF, these results do not explain another striking characteristic of IF animals: the gorging feeding pattern (Figure 1B). Because leptin acts on the arcuate nucleus of the hypothalamus, promoting anorexigenic pathways that induce satiety and increase energy expenditure (reviewed in Reference 38), we tested the responsiveness of both groups to leptin (Figure 5). Our experiments measuring food intake show that IF animals are leptin-sensitive and, therefore, their overeating behavior is not a consequence of impairments in leptin control of appetite. Surprisingly, in spite of their young age, AL rats

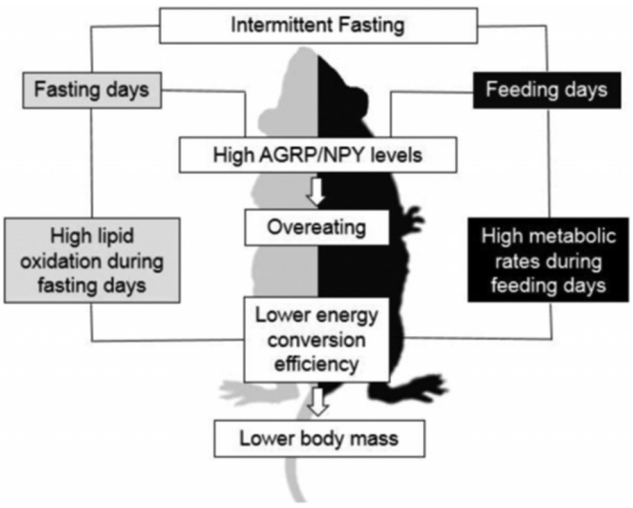

Figure 7. Proposed mechanisms underlying lower energy conversion efficiency and overeating in IF. Intermittently fasted animals present higher AGRP and NPY levels both when fed and fasted, leading to overeating when food is available. High levels of lipid oxidation on fasting days, associated with higher catabolic rates during feeding days, promote lower energy conversion efficiency leading to lower body mass in IF.

presented leptin resistance. This is line with the idea that standard AL rodents are overfed and sedentary, displaying several age-related metabolic abnormalities prevented by dietary restriction protocols (36, 56). Nevertheless, the premature unresponsiveness of AL animals to leptin stimulus is surprising. Indeed, in the development of obesity, the hypothalamus is often first site for the development of metabolic abnormalities (57). Perhaps the modifications we find in our animals are an early stage of changes leading to the obese, insulin-resistant, phenotype observed at more advanced ages. Additional experiments are necessary to better address this premature effect of AL diets on leptin responsiveness.

Recent studies have demonstrated that the structural organization of the blood-hypothalamus barrier is altered by fasting cycles, improving access of orexigenic factors to the arcuate nucleus (58), an effect that may be present in our model but was not explored here. Furthermore, the expression of the orexigenic neurotransmitter NPY has been shown to be altered by high-fat diets (59) and stress (60). We found here that IF animals presented elevated expression of NPY and AGRP, even when fed (Figure 5), and increased orexin expression during fasting, a result that mechanistically explains the overeating observed. This adds another characteristic to the regulation of the release of these neurotransmitters: feeding periodicity. In addition, we found that food consumption in IF animals was elevated even when they were submitted to fasting times comparable to AL animals (Figure 5). Indeed, it is known that the effect of peripheral signals affecting hunger can persist for hours after hormonal removal (61). These changes in signaling in our model are unrelated to circulating ghrelin levels (Table 1), but may involve differences in blood-hypothalamus barrier permeability (58). Irrespective of the specific mechanism, these data demonstrate that IF promotes longer-term changes in hunger regulation at the hypothalamic level. In keeping with this finding, IF rats presented low plasmatic leptin levels, a result in line with previous studies (42), which, again, indicates a predominance of orexigenic signaling. It is known that specific neuronal populations can be resistant to leptin, whereas others maintain their sensitivity (22, 62, 63), an effect which may explain the changes in anorexigenic (TRH) and orexigenic (NPY and AGRP) neurotransmitters when IF animals are fed (Figure 6).

Overall, our work provides a mechanistic explanation for the decrease in energy conversion efficiency promoted by IF by demonstrating that this dietary intervention alters metabolic rates and hypothalamic signaling, increasing orexigenesis (summarized in Figure 7). This results in a gorging feeding pattern as well as enhanced lipid oxidation when fasting and elevated basal metabolic rates during feeding, with overall lower gains in body mass. Relating these results to human physiology would be highly speculative, because the metabolic rates, dietary and housing conditions are vastly different. However, we believe, based on this data, that it is of high interest to evaluate in further studies if intermittent feeding patterns alter metabolic rates and hunger responses in humans.

Acknowledgments

The authors gratefully acknowledge the outstanding technical support of Camille C. Caldeira-da-Silva, Edson A. Gomes, and Doris D. Araújo, as well as excellent animal care from the animal facilities crew lead by Silvania Neves and experimental help from Dr Luis Alberto Luevano-Martinez.

Address all correspondence and requests for reprints to: Prof. Alicia J. Kowaltowski, MD, PhD, Universidade de São Paulo - Departamentod e Bioquímica, Av. Prof. Lineu Prestes, 748, São Paulo, SP, Brazil 05508-000. E-mail: alicia@iq.usp.br.

This work was supported by Fundação de Amparo à Pesquisa no Estado de São Paulo (FAPESP), Conselho Nacional de Desenvolvimento Científico e Tecnológico (CNPq), Instituto Nacional de Ciência e Tecnologia de Processos Redox em Biomedicina, Núcleo de Apoio à Pesquisa de Processos Redox em Biomedicina, and Centro de Pesquisa, Inovação e Difusão de Processos Redox em Biomedicina. B.C. and C.S. are doctoral students supported by CNPq and FAPESP fellowships.

Disclosure Summary: The authors have nothing to disclose.

References

1. **Cerqueira FM, Kowaltowski AJ.** Commonly adopted caloric restriction protocols often involve malnutrition. *Ageing Res Rev*. 2010;7:552–560.
2. **Carlson AJ, Hoelzel F.** Apparent prolongation of the life span of rats by intermittent fasting. *J Nutr*. 1946;31:363–375.
3. **Pearson KJ, Baur JA, Lewis KN, et al.** Resveratrol delays age-related deterioration and mimics transcriptional aspects of dietary restriction without extending life span. *Cell Metab*. 2008;8:157–168.
4. **Wan R, Camandola S, Mattson MP.** Intermittent food deprivation improves cardiovascular and neuroendocrine responses to stress in rats. *J Nutr*. 2003;133:1921–1929.
5. **Nisoli E, Tonello C, Cardile A, et al.** Calorie restriction promotes mitochondrial biogenesis by inducing the expression of eNOS. *Science*. 2005;301:314–317.
6. **Halagappa VK, Guo Z, Pearson M, et al.** Intermittent fasting and caloric restriction ameliorate age-related behavioral deficits in the triple-transgenic mouse model of Alzheimer's disease. *Neurobiol Dis*. 2007;26:212–220.
7. **Caro P, Gómez J, López-Torres M, et al.** Effect of every other day feeding on mitochondrial free radical production and oxidative stress in mouse liver. *Rejuvenation Res*. 2008;11:621–629.
8. **Cerqueira FM, Cunha FM, Caldeira da Silva CC, et al.** Long-term intermittent feeding, but not caloric restriction, leads to redox imbalance, insulin receptor nitration and glucose intolerance. *Free Radic Biol Med*. 2011;51:1454–1460.
9. **Anson RM, Jones B, de Cabo R.** The diet restriction paradigm: a

brief review of the effects of every-other-day feeding. *Age (Dordr)*. 2005;27:17–25.
10. **Lowell BB, Spiegelman BM.** Towards a molecular understanding of adaptive thermogenesis. *Nature*. 2000;404:652–660.
11. **Brand MD, Brindle KM, Buckingham JA, Harper JA, Rolfe DFS, Stuart JA.** The significance and mechanism of mitochondrial proton conductance. *Int J Obes Relat Metab Disord*. 1999;23:S4–S11.
12. **Minokoshi Y, Kim YB, Peroni OD, Fryer LG, Müller C, Carling D, Kahn BB.** Leptin stimulates fatty-acid oxidation by activating AMP-activated protein kinase. *Nature*. 2002;415:339–343.
13. **Cannon B, Nedergaard J.** Brown Adipose Tissue: Function and Physiological Significance. *Physiol Rev*. 2004;84:277–359.
14. **Singh A, Wirtiz M, Parker N, et al.** Leptin-mediated changes in hepatic mitochondrial metabolism, structure, and protein levels. *PNAS*. 2009;106:13100–13105.
15. **Henry BA, Andrews ZB, Rao A, Clarke IJ.** Central leptin activates mitochondrial function and increases heat production in skeletal muscle. *Endocrinology*. 2011;152:2609–2618.
16. **Whittle AJ, López M, Vidal-Puig A.** Using brown adipose tissue to treat obesity – the central issue. *Trends Mol Med*. 2011;17:405–411.
17. **Friedman JM.** Leptin and the regulation of body weight. *Keio J Med*. 2010;60:1–9.
18. **Hahn TM, Breininger JF, Baskin DG, Schwartz MW.** Coexpression of Agrp and NPY in fasting-activated hypothalamic neurons. *Nat Neurosci*. 1998;1:271–272.
19. **Zhang Y, Proenca R, Maffei M, Barone M, Leopold L, Friedman JM.** Positional clone of mouse obese gene and its human homologue. *Nature*. 1994;372:425–432.
20. **Baskin DG, Hahn TM, Schwartz MW.** Leptin sensitive neurons in the hypothalamus. *Horm Metab Res*. 1999;31:345–350.
21. **Velloso LA, Schwartz MW.** Altered hypothalamic function in diet-induced obesity. *Int J Obes*. 2011;35:1455–1465.
22. **Könner C, Brüning JC.** Selective insulin and leptin resistance in metabolic disorders. *Cell Metab*. 2012;16:144–152.
23. **Cartwright, IJ.** 1993 Separation and analysis of phospholipids by thin layer chromatography. In: Graham JM, Higgins JA, eds. Methods molecular biology. Biomembrane protocols. Vol. 19. Totowa: Humana Press Inc; 153–167.
24. **Biesiadecki BJ, Brand PH, Koch LG, Britton SL.** A gravimetric method for the measurement of total spontaneous activity in rats. *Proc Soc Exp Biol Med*. 1999;222:65–69.
25. **Yamada T, Katagiri H, Ishigaki Y, et al.** Signals from intra-abdominal fat modulate insulin and leptin sensitivity through different mechanisms: neuronal involvement in food-intake regulation. *Cell Metab*. 2006;3:223–229.
26. **Hütter E, Unterluggauer H, Garedew A, Jansen-Dürr P, Gnaiger E.** High-resolution respirometry–a modern tool in aging research. *Exp Gerontol*. 2006;41:103–109.
27. **Srere PA.** Citrate synthase. *Methods Enzymol*. 1969;13:3–11.
28. **Tahara EB, Navarete FD, Kowaltowski AJ.** Tissue-, substrate-, and site-specific characteristics of mitochondrial reactive oxygen species generation. *Free Radic Biol Med*. 2009;46:1283–1297.
29. **Bertelli DF, Araujo EP, Cesquini M, et al.** Phosphoinositide-specific inositol polyphosphate 5-phosphatase IV inhibits inositide trisphosphate accumulation in hypothalamus and regulates food intake and body weight. *Endocrinology*. 2006;147:5385–5399.
30. **Jastroch M, Divakaruni AS, Mookerjee S, Treberg JR, Brand MD.** Mitochondrial proton and electron leaks. *Essays Biochem*. 2010;47:53–67.
31. **Livesey G, Elia M.** Estimation of energy expenditure, net carbohydrate utilization, and net fat oxidation and synthesis by indirect calorimetry: evaluation of errors with special reference to the detailed composition of fuels. *Am J Clin Nutri*. 1988;47:608–628.
32. **Even PC, Mokhtarian A, Pele A.** Practical aspects of indirect calorimetry in laboratory. *Neurosci Biobehav Rev*. 1994;18:435–447.
33. **Weindruch R.** The retardation of aging by caloric restriction: Studies in rodents and primates. *Toxicol Pathol*. 1996;24:742–745.
34. **Barzilai N, Banerjee S, Hawkins M, Chen W, Rossetti L.** Caloric restriction reverses hepatic insulin resistance in aging rats by decreasing visceral fat. *J Clin Invest*. 1998;101:1353–1361.
35. **Friedman JM, Halaas JL.** Leptin and the regulation of body weight in mammals. *Nature*. 1998;395:763–770.
36. **Fernández-Galaz C, Fernández-Agulló T, Pérez C, et al.** Long-term food restriction prevents ageing-associated central leptin resistance in wistar rats. *Diabetologia*. 2002;45:997–1003.
37. **Rothwell NJ.** Central effects of CRF on metabolism and energy balance. *Neurosci Biobehav Rev*. 1990;14:263–271.
38. **Barsh GS, Schwartz MW.** Genetic approaches to studying energy balance: perception and integration. *Nat Rev Genet*. 2002;3:589–600.
39. **Parker JA, Bloom SR.** Hypothalamic neuropeptides and the regulation of appetite. *Neuropharmacology*. 2012;63:18–30.
40. **Anson RM, Guo Z, de Cabo R, et al.** Intermittent fasting dissociates beneficial effects of dietary restriction on glucose metabolism and neuronal resistance to injury from calorie intake. *Proc Natl Acad Sci USA*. 2003;100:6216–6220.
41. **Hipkiss AR.** Dietary restriction, glycolysis, hormesis and ageing. *Biogerontology*. 2007;8:221–224.
42. **Martin B, Pearson M, Kebejian L, et al.** Sex-dependent metabolic, neuroendocrine, and cognitive responses to dietary energy restriction and excess. *Endocrinology*. 2007;148:4318–4333.
43. **Yamamoto Y, Tanahashi T, Kawai T, et al.** Changes in behavior and gene expression induced by caloric restriction in C57BL/6 mice. *Physiol Genomics*. 2009;39:227–235.
44. **Lechan RM, Fakete C.** The TRH neuron: a hypothalamic integrator of energy metabolism. *Prog Brain Res*. 2006;153:209–235.
45. **Harper ME, Dent R, Monemdjou S, et al.** Decreased mitochondrial proton leak and reduced expression of uncoupling protein 3 in skeletal muscle of obese diet-resistant women. *Diabetes*. 2002;51:2459–2466.
46. **Choi CS, Fillmore JJ, Kim JK, et al.** Overexpression of uncoupling protein 3 in skeletal muscle protects against fat-induced insulin resistance. *J Clin Invest*. 2007;117:1995–2003.
47. **Cadenas S, Buckingham JA, Samec S, et al.** UCP2 and UCP3 rise in starved rat skeletal muscle but mitochondrial proton conductance is unchanged. *FEBS Lett*. 1999;462:257–260.
48. **Shabalina IG, Hoeks J, Kramarova TV, Schrauwen P, Cannon B, Nedergaard J.** Cold tolerance of UCP1-ablated mice: a skeletal muscle mitochondria switch toward lipid oxidation with marked UCP3 up-regulation not associated with increased basal, fatty acid or ROS-induced uncoupling or enhanced GDP effects. *Biochim Biophys Acta*. 2010;1797:968–980.
49. **Almind K, Manieri M, Sivitz WI, Cinti S, Kahn CR.** Ectopic brown adipose tissue in muscle provides a mechanism for differences in risk of metabolic syndrome in mice. *Proc Natl Acad Sci USA*. 2007;104:2366–2371.
50. **Zhang F, Paterson AJ, Huang P, Wang K, Kudlow JE.** Metabolic control of proteasome function. *Physiology*. 2007;22:373–379.
51. **Altun M, Besche HC, Overkleeft HS, et al.** Muscle wasting in aged, sarcopenic rats is associated with enhanced activity of the ubiquitin proteasome pathway. *J Biol Chem*. 2010;285:39597–39608.
52. **Tomaru U, Takahashi S, Ishizu A, et al.** Decreased proteasomal activity causes age-related phenotypes and promotes the development of metabolic abnormalities. *Am J Pathol*. 2012;180:963–972.
53. **Swy M, Do F.** Starvation-induced changes in metabolic rate, blood flow, and regional energy expenditure in rats. *Can J Physiol Pharmacol*. 1986;64:1252–1258.
54. **Sugden MC, Holness MJ, Palmer TN.** Fuel selection and carbon flux during the starved-to-fed transition. *Biochem J*. 1989;263:313–323.
55. **Cahill GF.** Fuel metabolism in starvation. *Annu Rev Nutr*. 2006;26:1–22.
56. **Martin B, Jia S, Maudsleyb S, Mattson MP.** "Control" laboratory

rodents are metabolically morbid: Why it matters. *Proc Natl Acad Sci USA*. 2010;107:6127–6133.
57. **Prada PO, Zecchin HG, Gasparetti AL, et al.** Western diet modulates insulin signaling, c-Jun N-terminal kinase activity, and insulin receptor substrate-1ser307 phosphorylation in a tissue-specific fashion. *Endocrinology*. 2005;146:1576–1587.
58. **Langlet F, Levin BE, Luquet S, et al.** Tanycytic VEGF-A boosts blood-hypothalamus barrier plasticity and access of metabolic signals to the arcuate nucleus in response to fasting. *Cell Metab*. 2013; 17:607–617.
59. **la Fleur SE, Ji H, Manalo SL, Friedman MI, Dallman MF.** The hepatic vagus mediates fat-induced inhibition of diabetic hyperphagia. *Diabetes*. 2003;52:2321–2330.
60. **Kuo LE, Kitlinska JB, Tilan JU, et al.** Neuropeptide Y acts directly in the periphery on fat tissue and mediates stress-induced obesity and metabolic syndrome. *Nat Med*. 2007;13:803–811.
61. **Yang Y, Atasoy D, Su HH, Sternson SM.** Hunger states switch a flip-flop memory circuit via a synaptic AMPK-dependent positive feedback loop. *Cell*. 2011;146:992–1003.
62. **Correia MLG, Haynes WG, Rahmouni K, Morgan DA, Sivitz WI, Mark AL.** The concept of selective leptin resistance: Evidence from agouti yellow obese mice. *Diabetes*. 2002;51:439–442.
63. **Mark AL, Correia MLG, Rahmounia K, Haynesa WG.** Selective leptin resistance: a new concept in leptin physiology with cardiovascular implications. *J Hypertens*. 2002;20:1245–1250.

4. Conclusions

- IF affects redox status in a tissue-specific manner in rats.
- IF promotes redox imbalance in the liver and brain and protects against oxidative damage in the heart.
- IF treatment results in lower body mass, overeating and decrased energy conversion efficiency.
- Decreased body mass is the consequence of an increase in metabolic rates on feeding days in addition to enhanced lipid oxidation during fasting periods.
- IF leads to an increase in the expression of orexigenic neurotransmitters in the hypothalamus, even on feeding days, which could explain the overeating pattern.
- IF promotes the modulation of TRH levels in IF rats during fasting days, a finding that could be related to the observed alterations in metabolic rates.

5. References

1. López-Otín C, Blasco MA, Partridge L, Serrano M, Kroemer G The hallmarks of aging. Cell. 2013; 153: 1194-1217.

2. Moskalev AA, Shaposhnikov MV, Plyusnina EN, Zhavoronkov A, Budovsky A, Yanai H, Fraifeld VE The role of DNA damage and repair in aging through the prism of Koch-like criteria. Ageing Res Rev. 2013; 12: 661-684.

3. Burtner CR, Kennedy BK Progeria syndromes and ageing: what is the connection? Nat Rev Mol Cell Biol. 2010; 11: 567-578.

4. Baker DJ, Dawlaty MM, Wijshake T, Jeganathan KB, Malureanu L, van Ree JH, Crespo-Diaz R, Reyes S, Seaburg L, Shapiro V, Behfar A, Terzic A, van de Sluis B, van Deursen JM Increased expression of BubR1 protects against aneuploidy and cancer and extends healthy lifespan. Nat Cell Biol. 2013; 15: 96-102.

5. Hoeijmakers JH DNA damage, aging, and cancer. N Engl J Med. 2009; 361: 1475-1485.

6. Blackburn EH, Greider CW, Szostak JW Telomeres and telomerase: the path from maize, Tetrahymena and yeast to human cancer and aging. Nat Med. 2006; 12: 1133-1138.

7. Blasco MA Telomere length, stem cells and aging. Nat Chem Biol. 2007; 3: 640-649.

8. Fraga MF, Esteller M Epigenetics and aging: the targets and the marks. Trends Genet. 2007; 23: 413-418.

9. Powers ET, Morimoto RI, Dillin A, Kelly JW, Balch WE Biological and chemical approaches to diseases of proteostasis deficiency. Annu Rev Biochem. 2009; 78: 959-991.

10. Zhang C, Cuervo AM Restoration of chaperone-mediated autophagy in aging liver improves cellular maintenance and hepatic function. Nat Med. 2008; 14: 959-965.

11. Collado M, Blasco MA, Serrano M Cellular senescence in cancer and aging. Cell. 2007; 130: 223-233.

12. Rossi DJ, Jamieson CH, Weissman IL Stems cells and the pathways to aging and cancer. Cell. 2008; 132: 681-696.

13. Laplante M, Sabatini DM mTOR signaling in growth control and disease. Cell. 2012; 149: 274-293.

14. Russell SJ, Kahn CR Endocrine regulation of ageing. Nat Rev Mol Cell Biol. 2007; 8: 681-691.

15. Zhang G, Li J, Purkayastha S, Tang Y, Zhang H, Yin Y, Li B, Liu G, Cai D Hypothalamic programming of systemic ageing involving IKK-b, NF-kB and GnRH. Nature. 2013; 497: 211-216.

16. Salminen A, Kaarniranta K, Kauppinen A Inflammaging: disturbed interplay between autophagy and inflammasomes. Aging (Albany NY) 2012; 4: 166-175.

17. Velloso LA, Schwartz MW Altered hypothalamic function in diet-induced obesity. Int J Obes (Lond). 2011; 35: 1455-1465.

18. Cerqueira FM, Kowaltowski AJ Mitochondrial metabolism in aging: effect of dietary interventions. Ageing Res Rev. 2013; 12: 22-28.

19. Sahin E, DePinho RA Axis of ageing: telomeres, p53 and mitochondria. Nat Rev Mol Cell Biol. 2012; 13: 397-404.

20. Kujoth GC, Hiona A, Pugh TD, Someya S, Panzer K, Wohlgemuth SE, Hofer T, Seo AY, Sullivan R, Jobling WA Mitochondrial DNA mutations, oxidative stress, and apoptosis in mammalian aging. Science. 2005; 309: 481-484.

21. Walsh ME, Shi Y, Van Remmen H The effects of dietary restriction on oxidative stress in rodents. Free Radic Biol Med. 2014; 66: 88-99.

22. Hekimi S, Lapointe J, Wen Y Taking a ‘‘good’’ look at free radicals in the aging process. Trends Cell Biol. 2011; 21: 569-576.

23. Colman RJ, Anderson RM, Johnson SC, Kastman EK, Kosmatka KJ, Beasley TM, Allison DB, Cruzen C, Simmons HA, Kemnitz JW, Weindruch R Caloric restriction delays disease onset and mortality in rhesus monkeys. Science. 2009; 325: 201-204.

24. Fontana L, Partridge L, Longo VD Extending healthy life span—from yeast to humans. Science 2010; 328: 321-326.

25. Keenan K, Soper K, Smith P, Ballam G, Clark R Diet overfeeding and moderate dietary restriction in control Sprague-Dawley rats: I. effects on spontaneous neoplasms. Toxicol Pathol. 1995; 23: 269-286.

26. Halagappa V, Guo Z, Pearson M, Matsuoka Y, Cutler R, LaFerla F, Mattson M Intermittent fasting and caloric restriction ameliorate agerelated behavioral deficits in the triple-transgenic mouse model of Alzheimer's disease. Neurobiol Dis. 2007; 26: 212-220.

27. Mattson M, Wan R Beneficial effects of intermittent fasting and caloric restriction on the cardiovascular and cerebrovascular systems. J Nutr Biochem. 2005; 16: 129-137.

28. Cerqueira FM, Cunha FM, Caldeira da Silva CC, Chausse B, Romano RL, Garcia CCM, Colepicolo P, Medeiros MHG, Kowaltowski AJ Long-term intermittent feeding, but not caloric restriction, leads to redox imbalance, insulin receptor nitration and glucose intolerance. Free Radic Biol Med. 2011; 51: 1454-1460.

29. Cerqueira FM, Kowaltowski AJ Commonly adopted caloric restriction protocols often involve malnutrition. Ageing Res Rev. 2010; 7: 552-560.

30. Rous F The influence of diet on transplant and spontaneous tumors. J Exp Med. 1914; 20: 433-451.

31. Osborne TB, Mendel LB, Ferry ER The resumption of growth after long continued failure to grow. J Biol Chem. 1915; 23: 439-454.

32. McCay CM, Crowell MF, Maynard LA The effect of retarded growth upon the length of life and upon the ultimate body size. J Nutr. 1935; 10: 63-79.

33. McCay CM, Maynard, LA, Sperling G, Barnes LL Retarded growth, lifespan, ultimate body size, and age changes in the albino rat after feeding diets restricted in calories. J Nutr. 1939; 18: 1-13.

34. Masoro EJ, Yu BP, Bertrand H Action of food restriction in delaying the aging processes. Proc Natl Acad Sci USA. 1982; 79: 4239-4241.

35. Weindruch R, Walford RL Dietary restriction in mice beginning at 1 year of age: effect on life-span and spontaneous cancer incidence. Science. 1982; 215: 1415-1418.

36. Sohal RS, Weindruch R Oxidative Stress, Caloric Restriction, and Aging Science. 1996; 273(5271): 59-63.

37. Froy O, Miskin R Effect of feeding regimens on circadian rhythms: implications for aging and longevity. Aging. 2010; 2: 7-27.

38. Carlson AJ, Hoelzel F Apparent prolongation of the life span of rats by intermittent fasting. J Nutr. 1946; 31: 363-375.

39. Goodrick CL, Ingram DK, Reynolds MA, Freeman JR, Cider N Effects of intermittent feeding upon body weight and life span in inbred mice: Interaction of genotype and age. Mech Ageing Dev. 1990; 55: 69-87.

40. Pearson KJ, Baur JA, Lewis KN, Peshkin L, Price NL, Labinskyy N, Swindell WR, Kamara D, Minor RK, Perez E, Jamielson HA, Zhang Y, Dunn SR, Sharma K, Pleshko N, Woollett LA, Csiszar A, Ikeno Y, Le Counter D, Elliott PJ, Becker KG, Navas P, Ingram DK, Wolf NS, Ungvari D, Sinclair DA, de Cabo R Resveratrol delays age-related deterioration and mimics transcriptional aspects of dietary restriction without extending lifespan. Cell Metab. 2008; 8: 157-168.

41. Speakman JR, Mitchell SE Caloric restriction. Mol Aspects Med. 2011; 32: 159-221.

42. Anson RM, Jones B, de Cabo R The diet restriction paradigm: a brief review of the effects of every-other-day feeding. Age. 2005; 27: 17-25.

43. Anson RM, Guo Z, de Cabo R, Lyun T, Rios M, Hagepanos A, Ingram DK, Lane MA, Mattson MP Intermittent fasting dissociates beneficial effects of dietary restriction on glucose metabolism and neuronal resistance to injury from calorie intake. Proc Natl Acad Sci USA. 2003; 10: 6216-6220.

Attachments

Curriculum Vitae

Bruno Chausse
PhD student
Instituto de Química
Universidade de São Paulo - Brazil

Work Adress: Departamento de Bioquímica, Instituto de Química, Universidade de São Paulo, Av. Prof. Lineu Prestes, 748, bloco 10 sup., sala 1059, 05508-000, São Paulo, SP, Brazil.
Tel: +55 11 3091 8556
Email: brunochausse@gmail.com

1. Formal Education

2010 - present PhD in Biochemistry, Instituto de Química, Universidade de São Paulo, Brazil

2006 - 2010 Bachelor's in Biology, Universidade Federal da Paraíba, Brazil

2. Complementary Education

2011 Redox Processes in Biomedicine School (40 h) Society for Free Radical Biology and Medicine.

2010 Short Term Course in Medicinal Plants (3 h) V Reunião Regional da FeSBE, Brazil.

2009 Short Term Course in *In Silico* Analysis of the Genome, Proteome and Transcriptome. (75 h) Faculdade de Ciências - Universidade do Porto, Portugal.

2008 - 2009 Academic Exchange Program. (600 h) Universidade do Porto, Portugal.

2008 Short Term Course in General Toxicology. (75 h) Faculdade de Ciências - Universidade do Porto, Portugal.

2008 III Biochemistry Summer Course. (80 h). Instituto de Química – USP, Brazil.

3. Undergraduate Research Activities

08/2007 - 07/2008 Citotoxic Analysis of Natural and/or Bioactive Compounds on Cell Cultures. Advisor: Demetrius Antônio Machado de Araújo. Departamento de Biologia Molecular/Universidade Federal da Paraíba, Brazil. Financial Support: CNPq

09/2009 - 07/2010 Evaluation of the Cytotoxic Activity of Carvacrol on Normal and Tumoral Cells. Advisor: Demétrius Antônio Machado de Araújo. Departamento de Biologia Molecular/Universidade Federal da Paraíba, Brazil. Financial Support: CNPq

4. Honors

2013 Instituto de Química-USP Travel Award for the Keystone Symposium C6 - Neuronal Control of Appetite, Metabolism and Weight, Instituto de Química - USP.

2013 Cone-Sul Symposium Travel Award and Oral Presentation, SBBq Annual Meeting, Brazil.

2011 Travel Award - I São Paulo Advanced School on Redox Processes in Biomedicine, South American Group of the Society for Free Radicals Biology and Medicine.

2010 Honors for the poster Evaluation of the cytotoxic activity of carvacrol on cell line HL-60 and MCF-7. V Reunião Regional da FeSBE.

2008 Bolsas Luso-Brasileiras, Academic Exchange, Universidade do Porto, Santander Universidades.

6. Bibliographic Production

Articles published in Scientific Journals

1. Chausse, Bruno; Vieira-Lara, Marcel A.; Sanchez, Angélica B., Medeiros, Marisa H.G.; Kowaltowski, Alicia J. Intermittent Fasting Results in Tissue-Specific Changes in Bioenergetics and Redox State. Plos One, accepted (in press), 2015.

2. Chausse, Bruno; Solon, Carina; Caldeira da Silva, Camille C.; Masselli Dos Reis, Ivan G.; Manchado-Gobatto, Fúlvia B.; Gobatto, Claudio A.; Velloso, Licio A.; Kowaltowski, Alicia J. Intermittent Fasting Induces Hypothalamic Modifications Resulting in Low Feeding Efficiency, Low Body Mass and Overeating. Endocrinology (Philadelphia), v. 155, p. 2013-2057, 2014.

3. Cardoso, Ariel R.*; **Chausse, Bruno***; da Cunha, Fernanda M.*; Luévano-Martínez, Luis A.*; Marazzi, Thire B.M.*; Pessoa, Phillipe S.*; Queliconi, Bruno B.*; Kowaltowski, Alicia J. Mitochondrial Compartimentalization of Redox Processes. Free Radical Biology & Medicine, v. 52, p. 2201-2208, 2012.
***Authors contributed equally – Alphabetical order**.

4. Cerqueira, Fernanda M.; da Cunha, Fernanda M.; Caldeira da Silva, Camille C.; **Chausse, Bruno**; Romano, Renato L.; Garcia, Camila C.M.; Colepicolo, Pio; Medeiros, Marisa H.G.; Kowaltowski, Alicia J. Long-term Intermittent Feeding, but not Caloric Restriction, Leads to Redox Imbalance, Insulin Receptor Nitration, and Glucose Intolerance. Free Radical Biology & Medicine, v. 51, p. 1454-1460, 2011.

Submited articles

1. Forni, Maria F.; **Chausse, Bruno**; Peloggia, Julia; Kowaltowski, Alicia J. Bioenergetic Profiling in the Skin. Experimental Dermatology. Submited.

2. Cerqueira, Fernanda; **Chausse, Bruno**; Liesa, Marc; Shirihai, Orian; Kowaltowski, Alicia J. Nutrient-dependent Versus -Independent Effects of Low and High Calorie Nutrition on Beta Cell Mitochondria. The FEBS Journal. Submited.

Congress presentations

1. Chausse, Bruno; Vieira-Lara, Marcel A.; Kowaltowski, Alicia J. Intermittent Fasting Results in Tissue-Specific Changes in Bioenergetics and Redox State. In: SFRBM's 21st Annual Meeting, 2014, Seattle - USA.

2. Vieira-Lara, Marcel A.; **Chausse, Bruno**; Kowaltowski, Alicia J. Intermittent Fasting Promotes Redox Changes in the Liver. In: XLIII Annual Meeting of the Brazilian Society for Biochemistry and Molecular Biology (SBBq), 2014, Foz do Iguaçu – Brazil.

3. Chausse, Bruno; Solon, Carina; Caldeira da Silva, Camille C.; Velloso, Licio Augusto; Kowaltowski, Alicia J. Intermittent Fasting Modulates Hypothalamic Control of Feeding and Body Mass. In: Keystone Symposia - C6: Neuronal Control of Appetite, Metabolism and Weight, 2013, Banff - Canada.

4. Chausse, Bruno; Solon, Carina; Caldeira da Silva, Camille C.; Velloso, Licio Augusto; Kowaltowski, Alicia J. Intermittent Fasting Modulates Hypothalamic Control of Feeding and Body Mass. In: XLII Annual Meeting of the Brazilian Society for Biochemistry and Molecular Biology, 2013, Foz do Iguaçu – Brazil.

5. Chausse, Bruno; Caldeira da Silva, Camille C.; Kowaltowski, Alicia J. Intermittent Feedings Promote Lower Body Weight Associated with Redox

Imbalance in Sprague Dowley Rats. In: XLI Reunião Anual da SBBq, 2012, Foz do Iguaçu – Brazil.

6. Chausse, Bruno; Caldeira da Silva, Camille C.; Kowaltowski, Alicia J. Bioenergetic and Redox Effects of Intermittent Feedings. In: VII Meeting of the SFRBM South American Group, 2011, São Pedro – Brazil.

7. Chausse, B.; Faheina-Martins, Gláucia V.; Silveira, A. L.; Araújo, Demétrius A. M. Evaluation of the Cytotoxic Activity of Carvacrol on Cell Line HL-60 and Primary Culture of Human Lymphocytes.. In: XV Meeting of the Brazilian Society for Cell Biology, 2010, São Paulo – Brazil.

8. Chausse, B.; Faheina-Martins, Gláucia V.; Araújo, Demétrius A. M. Avaliação do Potencial Citotóxico do Carvacrol Sobre as Linhagens Tumorais HL-60 e MCF-7. In: V Reunião Regional da Fesbe, 2010, Aracaju – Brazil.

9. Faheina-Martins, Gláucia V.; Silveira, A. L.; **Chausse, B**; Araújo, Demétrius A. M. Cytotoxicity of Lectins in Breast Cancer Cells: Influence of Fetal Bovine Serum Concentration. In: XIV Congresso da SBBC, 2008, São Paulo – Brazil.

7. Events

Participation in events

1. Society for Free Radical Biology and Medicine's (SFRBM) 21st Annual Meeting. Intermittent Fasting Results in Tissue-Specific Changes in Bioenergetics and Redox State. 2014. (Congress).

2. XLII Annual Meeting of the Brazilian Society for Biochemistry and Molecular Biology. Intermittent Fasting Modulates Hypothalamic Control of Feeding and Body Mass. 2013. (Congress).

3. Keystone Symposia - Neuronal Control of Appetite Metabolism and Weight. Intermittent Fasting Modulates Hypothalamic Control of Feeding and Body Mass. 2013. (Congress).

4. XLI Annual Meeting of the Brazilian Society for Bioquemistry and Molecular Biology. Intermittent Feedings Promote Lower Body Weight Associated With Redox Imbalance in Sprague Dowley Rats. 2012. (Congress).

5. VII Meeting of the Society for Free Radical Biology and Medicine (SFRBM) South American Group. Bioenergetic and Redox Effects of Intermittent Feedings. 2011. (Congress).

6. V Regional Meeting of Federação de Sociedades de Biologia Experimental (FeSBE). Avaliação do Potencial Citotóxico do Carvacrol Sobre as Linhagens Tumorais HL-60 e MCF-7. 2010. (Congress).

7. III Curso de Verão em Bioquímica e Biologia Molecular. 2008. (Course).

Event organization

1. Chausse, Bruno. VII Curso de Verão em Bioquímica e Biologia Molecular. 2012. (Course).

2. Chausse, Bruno. III Encontro da Pós-Graduação do Instituto de Química. 2011. (Congress).

Free Radical Biology and Medicine 52 (2012) 2201–2208

Contents lists available at SciVerse ScienceDirect

Free Radical Biology and Medicine

journal homepage: www.elsevier.com/locate/freeradbiomed

Review Article

Mitochondrial compartmentalization of redox processes

Ariel R. Cardoso [a,1], Bruno Chausse [a,1], Fernanda M. da Cunha [b,1], Luis A. Luévano-Martínez [a,1], Thire B.M. Marazzi [a,1], Phillipe S. Pessoa [a,1], Bruno B. Queliconi [a,1], Alicia J. Kowaltowski [a,*]

[a] Departamento de Bioquímica, Instituto de Química, Brazil
[b] Escola de Artes, Ciências e Humanidades, Universidade de São Paulo, 05508-900 São Paulo, SP, Brazil

ARTICLE INFO

Article history:
Received 16 January 2012
Received in revised form
5 March 2012
Accepted 6 March 2012
Available online 26 April 2012

Keywords:
Mitochondria
Compartments
Antioxidants
Mitochondrially-targeted probes
Mitochondrially-targeted antioxidants

ABSTRACT

Knowledge of location and intracellular subcompartmentalization is essential for the understanding of redox processes, because oxidants, owing to their reactive nature, must be generated close to the molecules modified in both signaling and damaging processes. Here we discuss known redox characteristics of various mitochondrial microenvironments. Points covered are the locations of mitochondrial oxidant generation, characteristics of antioxidant systems in various mitochondrial compartments, and diffusion characteristics of oxidants in mitochondria. We also review techniques used to measure redox state in mitochondrial subcompartments, antioxidants targeted to mitochondrial subcompartments, and methodological concerns that must be addressed when using these tools.

Contents

Introduction

Isolated mitochondria were first reported to release hydrogen peroxide in the late 1960s, and this oxidant was subsequently demonstrated to be a product of superoxide radical dismutation [8,19,37,53]. Since then, it has become clear that these organelles are a quantitatively relevant source of intracellular oxidants, produced mostly as by-products of electron transfer reactions.

The electron transfer reactions that generate oxidants are diverse in nature and occur in submitochondrial locations. This, added to specific characteristics of removal systems and differences in reactivity (and thus diffusion), may result in very distinct redox status in mitochondrial compartments. Because redox processes are highly dependent on local intracellular characteristics and targets, it is important to understand these environmental properties. This review focuses on current knowledge regarding the compartmentalization of mitochondrial redox processes.

Where are mitochondrial oxidants generated?

The electron transport chain is the most studied source of mitochondrial superoxide radicals ($O_2^{\bullet -}$), formed through one-electron reduction of molecular oxygen [1,66,108]. NADH-ubiquinone oxidoreductase (complex I) releases $O_2^{\bullet -}$ to the matrix, possibly through the flavin and iron–sulfur clusters into the hydrophilic arm [9,51,114]. Complex III (ubiquinone:cytochrome

* Corresponding author. Fax: +55 11 38155579.
E-mail address: alicia@iq.usp.br (A.J. Kowaltowski).
[1] These authors contributed equally to this work.

0891-5849/$ - see front matter © 2012 Elsevier Inc. All rights reserved.
http://dx.doi.org/10.1016/j.freeradbiomed.2012.03.008

c reductase), on the other hand, releases $O_2^{\bullet-}$ to both the intermembrane space and the matrix [9,114]. Although isolated succinate dehydrogenase (complex II) has been shown to release $O_2^{\bullet-}$ in the absence of added coenzyme Q [125], this complex seems to be of lesser importance considering total oxidant release in intact organelles and cells, perhaps because of structural characteristics of this enzyme [124]. Complex IV is not usually considered a quantitatively relevant source of mitochondrial $O_2^{\bullet-}$, because of its ability to bind tightly to partially reduced intermediates [9,48,60,114].

In addition to the electron transport chain, the importance of other mitochondrial enzymes, in particular flavoproteins, as $O_2^{\bullet-}$ sources has increasingly been recognized [1]. Two of these enzymes, pyruvate and α-ketoglutarate dehydrogenase, are located in the matrix and possess the same flavin subunit (dihydrolipoamide dehydrogenase or dihydrolipoyl dehydrogenase), which is the source of $O_2^{\bullet-}$ [102,106,111]. For reasons that are still unclear, $O_2^{\bullet-}$ generation is more pronounced in α-ketoglutarate dehydrogenase compared to pyruvate dehydrogenase [102]. Interestingly, α-ketoglutarate dehydrogenase is tightly associated with the matrix surface of the inner mitochondrial membrane [55] and, in yeast, is a component of the mitochondrial nucleoid [43,86]. This close proximity between an important source of mitochondrial oxidants and mitochondrial DNA (mtDNA) may explain why this enzyme is involved in mtDNA dysfunction [107] and is an oxidant source involved in aging in yeast [106].

Other sources of matrix $O_2^{\bullet-}$ include the electron-transferring flavoprotein Q oxidoreductase and possibly acyl-CoA dehydrogenases, although these sources still remain poorly explored [9,101,108]. Other mitochondrial flavoenzymes such as the branched-chain α-ketoacid dehydrogenase complex are possible and yet unstudied mitochondrial reactive oxygen species (ROS) sources.

Aconitase is a matrix enzyme commonly used as a marker for mitochondrial oxidant levels, because $O_2^{\bullet-}$ can oxidize its iron–sulfur clusters. Vasquez–Vivar and colleagues [117] reported that oxidized aconitase can produce hydroxyl radicals by the Fenton mechanism. Interestingly, aconitase is also a component of the nucleoid involved in the maintenance of mtDNA [107].

Enzymes on the outer surface of the inner mitochondrial membrane can contribute to oxidant release in the intermembrane space. Dihydroorotate dehydrogenase participates in the synthesis of pyrimidine nucleotides and donates electrons to coenzyme Q. In the absence of this electron acceptor, this enzyme has been shown to generate H_2O_2, although this remains to be further investigated [1,19]. α-Glycerophosphate dehydrogenase is an enzyme located on the outer surface of the inner mitochondrial membrane that has a clear role as a source of intermembrane space $O_2^{\bullet-}$ [9,60,108,112,129]. Moreover, topological measurements of $O_2^{\bullet-}$ generation originating from α-glycerophosphate dehydrogenase suggest radicals may be produced at both sides of the membrane [60], although the location of the flavin, far from the membrane, does not support this possibility [123]. Superoxide radical production within the mitochondrial matrix originating from glycerol phosphate may also be the result of reverse electron transfer to complex I [1,9,60,112,113,108].

Monoamino oxidase is an enzyme located on the outer face of the mitochondrial outer membrane. It can generate H_2O_2 at higher rates than the electron transfer chain, thus resulting in mtDNA damage [30,49,91].

Mitochondrial antioxidant compartmentalization

Considering the diverse and quantitatively significant sources of oxidants in the mitochondrial microenvironment described above, effective antioxidant mechanisms are necessary to maintain mitochondrial and cell function. Antioxidant systems vary greatly in each mitochondrial compartment and include many different strategies: (i) catalytic removal of free radicals and other ROS, (ii) reduction of free radicals by electron donors, (iii) chelating mechanisms for pro-oxidant metal ions, and (iv) repair mechanisms [25,48,50,114,116]. The antioxidant characteristics of the various mitochondrial subcompartments are described next.

$O_2^{\bullet-}$ in the matrix is dismutated into H_2O_2 either spontaneously or catalyzed by the MnSOD (SOD2). The high concentration and reaction rate of SOD2 suggest that the steady-state levels of mitochondrial $O_2^{\bullet-}$ are low, in keeping with the perceived importance of removing this oxidant [20,21,46,66,120].

H_2O_2 generated in the matrix can diffuse to other cellular compartments because of its high stability and membrane permeativity (as will be discussed below). Alternatively, H_2O_2 generated in the mitochondrial matrix will be removed by enzymatic systems in this compartment. These systems include glutathione peroxidases (GP*x*), thioredoxin peroxidases (TP*x*), and, in some tissues, catalase [18,48]. GP*x* and TP*x* convert hydrogen peroxide to H_2O at the expense of oxidizing glutathione (GSH) and thioredoxin (TR*x*), respectively. The ubiquity of both systems suggests the central importance of peroxide removal within cells, although simulations based on rate constants and concentrations suggest TP*x* is the premier enzyme responsible for H_2O_2 removal in mitochondria, mostly because of its relative abundance [15]. On the other hand, the rate constant of GP*x* and the concentrations of glutathione are higher. Differences also exist regarding substrate specificity: TP*x* also removes organic hydroperoxides [67]. Both TP*x* and GP*x* H_2O_2-removal systems use electrons from NADPH to regenerate reduced GSH and TR*x* [3,35,80]. NADPH in the mitochondrial matrix is regenerated from electrons donated by NADH, through the activity of the proton-translocating transhydrogenase [73], linking the presence of the inner membrane proton gradient to an effective removal of H_2O_2. Catalase has been found in heart and liver mitochondria [77,85], although it is probably not as effective as GP*x* and TP*x* in removing mitochondrial H_2O_2 at physiological levels [121]. Despite this, overexpression of catalase specifically in mitochondria significantly extends murine life span [90], indicating it is functionally relevant in this compartment.

Important nonenzymatic antioxidant systems also exist within the mitochondrial matrix: GSH is a powerful antioxidant itself. It is synthesized in the cytoplasm and imported into mitochondria by two electroneutral antiport carrier proteins, reaching concentrations as high as 11 mM in the matrix [22,34,38,57,116]. GSH scavenges hydroxyl radicals and singlet oxygen directly and can regenerate vitamins C and E to their reduced forms. The oxidized-to-reduced glutathione ratio is widely used as an indicator of the mitochondrial or cellular redox state. Ascorbate (vitamin C) is also an important electron donor in the mitochondrial matrix. It participates in the regeneration of oxidized vitamin E and is a radical scavenger. Ascorbate can also be a cofactor for one-Cys peroxiredoxins, which are located in yeast mitochondria, removing H_2O_2 [56,61,116].

Metal chelation is an essential antioxidant defense in the mitochondrial matrix, because the mitochondrion is a metal-rich organelle. Indeed, iron chelation prevents mitochondrial damage under conditions of oxidative stress [12,39]. Finally, mtDNA-repairing systems are essential for mtDNA integrity, ensuring efficient electron transport chain assembly that prevents further oxidant generation in mitochondria [29,48,114].

Hydrophobic antioxidant systems are located within the mitochondrial inner membrane, protecting both membrane integrity and inner membrane proteins. Phospholipid hydroperoxide glutathione peroxidase is a membrane-associated GP*x* that reacts with both hydrogen peroxide and lipid hydroperoxides. This enzyme protects against membrane-damaging lipid oxidation

and has been reported to be antiapoptotic, preventing the formation of cardiolipin hydroperoxide and cytochrome *c* release [70,109,115]. Vitamin E (α-tocopherol) is a relevant lipid-soluble antioxidant in the mitochondrial inner membrane, preventing the propagation of free radical-mediated chain reactions by trapping lipid peroxyl radicals [26,110]. Coenzyme Q is a recognized $O_2^{\bullet -}$ source when partially reduced but also represents an important inner membrane antioxidant when fully reduced. Ubiquinol inhibits lipid and protein oxidation by reducing perferryl radicals or eliminating lipid peroxyl radicals. Ubiquinol can also regenerate vitamin E from the α-tocopheroxyl radical [5,62].

In the mitochondrial intermembrane space, $O_2^{\bullet -}$ is dismutated to H_2O_2 by CuZnSOD (SOD1), the cytosolic isoform of SOD, also present in the intermembrane space [44,71]. Interestingly, targeting SOD1 specifically to the mitochondrial intermembrane space rescues the motor phenotype of SOD1 knockout animals, indicating that the mitochondrial location of this enzyme is essential for the maintenance of motor neuron integrity [17]. Cytochrome *c* is also an important mitochondrial antioxidant, oxidizing $O_2^{\bullet -}$ to O_2 and then transferring the electron to complex IV [74,93]. Finally, GSH is abundant in the intermembrane space; it is transported by voltage-dependent anion-selective channels located in the outer membrane [44].

Overall, mitochondrial antioxidant systems are so effective that it has been proposed that release of oxidants from mitochondria within cells under physiological conditions may not be significant [10,69,100].

Diffusion of oxidants and mitochondrial subcompartments

The presence of oxidants in various mitochondrial subcompartments depends not only on their generation properties, but also on their reactivity and diffusibility (see Fig. 1). Diffusion distance can be estimated by the Einstein–Schomulochowski equation,

$$\bar{x} = \sqrt{(6Dt)}, \tag{1}$$

where $\bar{x}$ is the quadratic mean of the diffusion distance in three-dimensional space, D is the diffusion coefficient, and t is the time, usually taken as the molecule half-life time. A half-life time is the time for a decrease in concentration of $1/e$, or 37%. The diffusion coefficient can be calculated using the Stokes–Einstein equation,

$$D = kT/6\pi\eta r, \tag{2}$$

where k represents the Boltzman constant, T is the absolute temperature, η is the viscosity of the biological matrix, and r is the hydrodynamic radius of the solute species. The diffusion coefficient was assumed to be $1 \times 10^{-9}\ s^{-1}$. Molecule half-life times are estimated considering all the rates at which a molecule reacts in the cell or tissue and reactant concentrations:

$$\tau = \ln 2/(k_d + k_1[M_1] + k_2[M_2] + \cdots + k_n[M_n]). \tag{3}$$

Chemical reactions in the condensed phase are limited by the solvent surrounding the reactants, which is usually water within cells. Encounters between reactants last about 10^{-8} to 10^{-10} s. If the probability of a reaction is high enough, the overall reaction rate will depend only on solvent diffusion, restricted by the diffusion limit (10^9–$10^{10}\ mol\ L^{-1}\ s^{-1}$).

Considering both the predicted short diffusion distances for $O_2^{\bullet -}$ and the limitations in measuring intracellular concentrations of this radical, the rates/concentrations of $O_2^{\bullet -}$ that leave or enter mitochondria remain a largely open question. Fig. 1 shows a schematic drawing of a 16 μm diameter cell and its mitochondria, with predicted diffusion distances of some ROS brought to scale. Fig. 2 shows ROS concentration evolutions based on their estimated lifetimes.

Superoxide diffusion distances and lifetimes are strongly dependent on the presence of superoxide dismutase and free metal ions. The high rate constant for the SOD reaction (about $5 \times 10^9\ L\ mol^{-1}\ s^{-1}$) reduces $O_2^{\bullet -}$ lifetime from 100 ms (in the absence of SOD) to 35 μs [59,84], whereas the diffusion distance changes from about 50 μm to 400 nm. Thus, in mitochondria, matrix and membrane SOD isoforms will remove most $O_2^{\bullet -}$ produced under physiological conditions [10]. Because superoxide is negatively charged, its diffusion through the lipid bilayer is unfavorable, and it is thus highly improbable that the radical generated in the mitochondrial matrix could leave this subcompartment. However, the protonated form of $O_2^{\bullet -}$, the perhydroxyl radical ($HOO^{\bullet}$; $pK_a = 4.7$), is potentially membrane-diffusible. Superoxide production occurring in the proton-rich intermembrane space could lead to the production of $HOO^{\bullet}$, which may diffuse into mitochondria (stimulated by the pH gradient) or to the immediate extramitochondrial space [23,52,84]. Intermembrane-space $O_2^{\bullet -}$ diffuses out

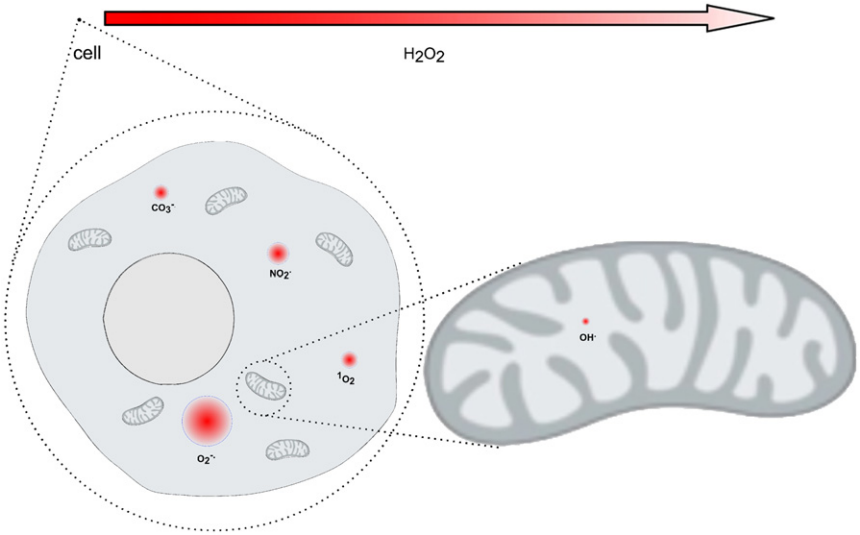

Fig. 1. Schematic representation of selected oxidant diffusion distances based on Einstein–Schomulochowski relations and $t = 3t_{1/2}$ accounting for ~95% decay of the initial concentration. Cell dimensions adopted were approximately 16 × 16 μm; mitochondrial dimensions were 2 × 1 μm; hydrogen peroxide diffusion radius (represented by the arrow) is ~3 mm. Half-life times: $CO_3^{\bullet -}$ 3.5 μs, $NO_2^{\bullet}$ 7 μs, $^1O_2$ 4 μs, $O_2^{\bullet -}$ 35 μs, $OH^{\bullet}$ 10 ns, H_2O_2 500 s.

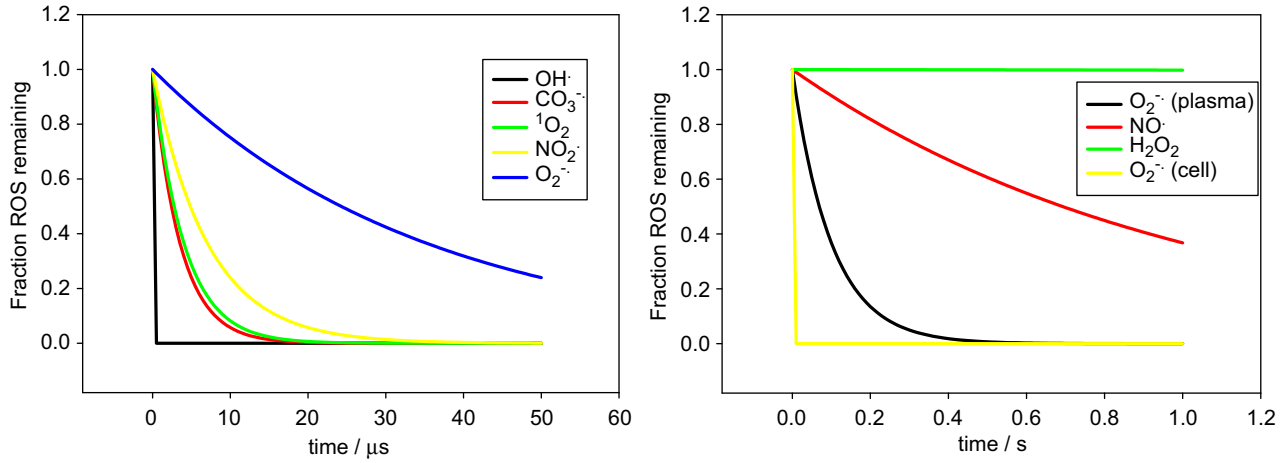

Fig. 2. Time evolution of selected oxidant species based on their estimated half-life times: $OH^{\bullet}$ 10 ns, $CO_3^{\bullet -}$ 3.5 µs, $^1O_2$ 4 µs, $NO_2^{\bullet}$ 7 µs, $O_2^{\bullet -}$ 35 µs (in the presence of SOD), $O_2^{\bullet -}$ 100 ms (in absence of SOD), $NO^{\bullet}$ 1 s, H_2O_2 500 s.

of the organelle through the outer membrane voltage-dependent anion channel [27].

Hydrogen peroxide is a relatively stable molecule in solution, with long lifetimes and large diffusion distances, mostly eliminated by thiol peroxidase and catalase activities, as described above. H_2O_2 is often believed to diffuse through membranes because of its lack of charge, small size, and physical properties similar to water [7]. However, biomembranes constitute a barrier to peroxide diffusion and lead to the formation of gradients. This was investigated experimentally in Jurkat cells by measuring H_2O_2 consumption rates by scavenging enzymes [2]. The magnitude of the H_2O_2 gradient is proportional to consumption rates in each compartment. Furthermore, the formation of the H_2O_2 gradient is determined by the size of the cell or organelle (smaller compartments are more permeable to H_2O_2) and expression levels of aquaporins known to transport H_2O_2 [6]. Membrane and/or cell wall composition also determines H_2O_2 permeability [98].

Hydroxyl radical lifetimes and diffusion distances in water are 10 ns and 5 nm, respectively [24,76]. Inside the cell, however, the lifetime may be much lower because of high reactivity toward cell components, and the diffusion distance in water should be considered an upper limit for diffusion in the cell. Singlet oxygen ($^1O_2$), which can be generated in various cellular locations by photosensitization, also has limited lifetime and diffusion (4 µs and 100 nm) in water and within cells [79].

Subcompartmentalized measurements of mitochondrial redox state and oxidants

Because the outcome of mitochondrial oxidant generation varies largely with the type, quantity, and location of ROS, gaining access to technologies that provide specific, localized, and quantitative measurements of these species is essential. Unfortunately, although considerable progress has been made, precise forms to measure mitochondrial redox state are still lacking, and all techniques should be used critically, include appropriate controls, and be associated with other mechanistically distinct techniques to confirm the findings [64]. We will first present techniques available and then discuss their shortcomings. Table 1 lists some commonly used mitochondrial redox probes, their strengths, and their weaknesses.

Probes available for measurements of mitochondrial redox state or oxidant levels can be separated into two main groups: protein and nonprotein probes. The majority of nonprotein probes are targeted to mitochondria through their coupling to the lipophilic triphenylphosphonium cation (TPP^+), a group that favors the accumulation of the probe (several hundreds of times) within mitochondria, driven by the membrane potential [65]. Mitochondrially targeted probes in this category include those designed for the detection of highly reactive oxygen/nitrogen species (MitoAR [45]), hydrogen peroxide/peroxynitrite (MitoPY1 [16]; MitoB [14]), superoxide (MitoSOX [41]), and lipid peroxides (MitoDPPP [89]; MitoFOX green, a diphenyl-1-pyrenylphosphine derivative available from Molecular Probes, Eugene, OR, USA, although a report describing its use could not be located).

Dichlorofluorescein (DCF) is another nonprotein probe that is not targeted to mitochondria, but we find important to mention because it is the most widely used fluorescent probe for ROS measurements, including mitochondrially derived oxidants. DCF has numerous artifacts and limitations [13,40,41], as discussed in the next section.

Recently, a hybrid probe, SPG2, was described by Srikun et al. [99]. This probe was designed to detect peroxynitrite/hydrogen peroxide and consists of a derivatized boronate bioconjugated to SNAP-tag fusion protein. This strategy allows the targeting of nonprotein compounds to various subcellular locations, a fact feasible only for protein probes so far.

Genetically encoded proteinaceous probes have been developed with a number of targeting sequences that promote their localization to specific mitochondrial compartments [28,32,54,83,118,119]. cpYFP, a circularly permuted yellow fluorescent protein that shifts its fluorescence emission under strong oxidizing conditions [118], was targeted to mitochondria through its fusion to the targeting sequence of subunit IV of cytochrome *c* oxidase [118]. HyPer, a genetically encoded biosensor for hydrogen peroxide based on cpYFP and the OxyR bacterial transcription factor [4], was targeted to the mitochondrial matrix or the intermembrane space through the use of the targeting sequence of subunit VIII of cytochrome *c* oxidase or a partial sequence of mouse mitochondrial glycerol phosphate dehydrogenase 2, respectively [54,83]. Finally, rxYFP [72] and roGFP [28], two fluorescent protein probes for measurement of thiol/disulfide intracellular redox state, were targeted to the mitochondrial matrix or the intermembrane space through the use of different leading sequences [32,119]. Quantitative measurements using rxYFP in yeast grown in high-glucose cultures (a condition that increases their H_2O_2 release [106]) suggest that GSH:GSSG ratios are in the range of 900:1 in the matrix and 250:1 in the intermembrane space. Both environments are thus distinct in redox state and more oxidized than the cytosol, in which the ratio is in the range of 3000:1 [32].

Table 1
Commonly used mitochondrial redox probes.

Probe	Characteristics	Cautionary notes	Refs.
Nonprotein probes			
MitoAR	High fluorescence intensity pH-independent fluorescence Tolerance to photobleaching Tolerance to autoxidation	Nonspecific Mitochondrial accumulation depends on membrane potential	[45]
MitoB1	More specific for mitochondrial H_2O_2 May be analyzed by mass spectrometry	Mitochondrial accumulation depends on membrane potential	[14]
MitoDPPP	Does not react with $O_2^{\bullet -}$ or $OH^{\bullet}$	Oxidized by various lipid peroxides, including those from other cellular sites	[89]
MitoPY	More specific for mitochondrial H_2O_2 than other nonprotein probes	Mitochondrial accumulation depends on membrane potential	[16]
MitoSOX	Reacts with $O_2^{\bullet -}$ to form a specific product (2-OH-Mito-E^+)	Reacts with other oxidants ($OH^{\bullet}$, $ONOO^-$) to form Mito-E^+ and dimers, which have similar spectral parameters Irreversible reaction—not suitable for transient measurements	[40,41,128]
$DCFH_2$	Easy manipulation Cheap Easily obtained	Nonspecific Dependent on pH, concentration of transition metals, and phenotype Modified by many biological molecules including GSH, NADH, and Ascorbate Autoxidation, photo-oxidation, autocatalysis, respiratory inhibition	[13,41,42,127]
Protein-based probes			
cpYFP	Can be targeted to specific mitochondrial compartments	Requires transfection and appropriate expression Very pH sensitive Suitability as a $O_2^{\bullet -}$ probe is under debate	[33,58,63,87,118]
HyPer	Ratiometric Specific for H_2O_2 Presents high sensitivity	Requires transfection and appropriate expression pH sensitive	[4,54,83]
rxYFP	Targeted	Not ratiometric High background noise Sensitive to pH and chloride	[32,58,72]
roGFP	Ratiometric Allows dynamic measurement of mitochondrial redox state Can be targeted to specific mitochondrial compartments	Limited sensitivity Biosynthesis of one mature molecule of GFP implies the release of one H_2O_2	[28,81,119]
Hybrid probe			
SPG2	Specific for H_2O_2 Can be targeted to specific mitochondrial compartments	Requires transfection Reaction with H_2O_2 is irreversible—not suitable for transient measurements Rate constant with H_2O_2 is lower than that of catalase, glutathione peroxidase, or peroxiredoxin	[81,99]

Mitochondrial probes: a few words of caution

Redox measurements in themselves are tricky, because of the reactive nature of oxidants, and localized measurements are even more so. Although most probes are designed to react preferentially with specific oxidants, they certainly react with other species, too [41,45,128], making specificity a rare quality. Furthermore, several important artifacts of these probes are particularly relevant to mitochondrial microenvironments.

Probes linked to TPP^+ [14,16,82] or any other lipophilic cation will accumulate in mitochondria in a manner related to the magnitude of the inner membrane potential. Thus, the first obvious point to be taken into account is that probe fluorescence both in the whole cell and in the mitochondria within the cell will vary with changes in the cellular and mitochondrial membrane potentials, independent of variations in oxidant levels. Because most changes in mitochondrial oxidant generation involve alterations of mitochondrial oxidative phosphorylation and energy metabolism, this is a central point that must always be considered and that precludes the use of these probes as sole measurements of mitochondrial oxidant levels. Furthermore, the accumulation of probes in the mitochondrial microenvironment does not increase proportionally to its localized fluorescence. Because the quantity of these probes in a small environment can be significant, both quenching [65,68] and mitochondrial uncoupling due to the accumulation of the indicator may occur. Uncoupling is a highly effective antioxidant strategy [11,95], so uptake of the probe is a possible mechanism in which the technique used to measure oxidants changes oxidant production. Finally, the presence of very high quantities of these chemicals in the mitochondrial microenvironment can lead to changes in mitochondrial function. It is worth noting that DCF, which can accumulate in mitochondria under some conditions, promotes mitochondrial respiratory inhibition when added to the extramitochondrial medium at micromolar concentrations [104]. Because these effects are certainly variable with cell type and loading conditions, it is recommended that mitochondrial functionality be verified as a control for the use of these indicators.

Protein-based probes [28,99,118] can be directed to specific compartments with low risk of quenching or interference with other proteins. Nonetheless, overexpression of any protein can change the normal physiology and morphology of the organelle. In addition, proteinaceous probes are based on cysteine redox chemistry [28,118] and are therefore limited to processes that affect thiols.

An issue that affects both protein and nonprotein probes is changes in mitochondrial quantity and morphology, which can affect probe signal [47]. Another central point for all probes is pH sensitivity. Mitochondria present substantial ΔpH across the inner mitochondrial membrane [78], and the pH in different mitochondrial environments is influenced by metabolic activity. Changes in pH can notably change the signal obtained with different probes [87,88,122], within the physiological range. For example, cpYFP fluorescence increases five times by shifting the pH from 7 to 8 [118], and clamping cytosolic pH has led to questions regarding $O_2^{\bullet -}$ measurements using this probe [87]. DCF presents at least threefold changes in fluorescence, with pH shifts between 7 and 8, and doubles its fluorescence emission with shifts of pH between 6 and 7 [122].

Targeted antioxidants and other "antioxidant strategies"

An effective way to demonstrate the participation of mitochondrial oxidants in pathophysiological processes is by verifying the effects of antioxidants designed to selectively remove ROS from mitochondrial microenvironments.

Lipophilic cationic antioxidants make use of the mitochondrial inner membrane potential, similar to TPP^+-bound probes, to promote the accumulation of antioxidants in the matrix. TPP^+-associated vitamin E (MitoVitE) and, especially, coenzyme Q (MitoQ) have been widely used and provide protection against many different oxidant-related forms of cell and organismal damage (reviewed by Smith and Murphy [96]). Both accumulate by more than 2 orders of magnitude in mitochondria, in a membrane-potential-dependent manner. The downfall of these probes is that they can cause uncoupling themselves [103], possibly preventing mitochondrial $O_2^{\bullet -}$ formation. These probes also undergo redox cycling that can generate $O_2^{\bullet -}$ and may be poor inhibitors of thiol oxidation [36]. Furthermore, MitoQ has been demonstrated to accept electrons before the rotenone-inhibitory site in complex I and to have its reduced form recycled by complex II, allowing it to act as an intracellular pro-oxidant under conditions under which electron flow through complex I is high [75].

SkQ_n compounds are similar to MitoQ in mitochondrial accumulation and protective properties, but are less prone to redox cycling because of the use of plastoquinones instead of the ubiquinone moiety present in MitoQ. The main pharmacological advantage of SkQ_n compounds over MitoQ is a larger window between their antioxidant and pro-oxidant effects (for review see [92,94]). Plastoquinones in vivo are located in thylakoid membranes, a highly oxidant environment, and present distinct redox properties: whereas the plastoquinone redox potential is around +110 mV, that of ubiquinone is +70 mV [97]. Moreover, SkQ_n compounds are reduced by mitochondrial cytochrome b_h, and the reduced form of SkQ_n compounds promptly reacts with superoxide produced in mitochondria. In addition, the $SkQH_2$ structure, especially $SkQH_21$, favors a direct interaction with cardiolipin molecules, hence avoiding oxidation of this lipid.

Cell-permeative mitochondrially targeted peptides have also been developed [105,126], and they mostly accumulate (by 3 or 4 orders of magnitude) in the inner mitochondrial membrane, without reaching the matrix, in a manner that is not highly dependent on the membrane potential. The differential location and accumulation properties of these mitochondrial antioxidants are interesting in terms of studying mitochondrial redox compartmentalization, but this possibility has not yet been fully explored. Membrane-potential-sensitive polycationic peptides that penetrate into the matrix have also been developed [31].

Conclusions

Because of the reactive nature of oxidants, their intracellular targets for both damaging and signaling effects must be within very specific constraints regarding the separation from their source. Given the importance of mitochondria as generators and targets of these oxidants, understanding the subcompartmentalization of mitochondrial redox processes is essential. In the past few years, a lot of knowledge has been gained regarding the characteristics and locations of mitochondrial oxidant generation, as well as more quantitative measurements of the antioxidant capacity and redox state of various mitochondrial subcompartments. A challenge for the area in the future will be the development of more trustworthy and specific mitochondrially targeted antioxidants, as well as mechanisms to conduct real-time, localized, specific, and quantitative measurements of oxidants in mitochondrial microenvironments in vivo.

References

[1] Andreyev, A. Y.; Kushnareva, Y. E.; Starkov, A. A. Mitochondrial metabolism of reactive oxygen species. *Biochemistry* **2:**200–214; 2005.

[2] Antunes, F.; Cadenas, E. Estimation of H_2O_2 gradients across biomembranes. *FEBS Lett.* **475:**121–126; 2000.

[3] Arnér, E. S. J.; Holmgren, A. Physiological functions of thioredoxin and thioredoxin reductase. *Eur. J. Biochem.* **267:**6102–6109; 2000.

[4] Belousov, V. V.; Fradkov, A. F.; Lukyanov, K. A.; Staroverov, D. B.; Shakhbazov, K. S.; Terskikh, A. V.; Lukyanov, S. Genetically encoded fluorescent indicator for intracellular hydrogen peroxide. *Nat. Methods* **3:**281–286; 2006.

[5] Bentinger, M.; Brismar, K.; Dallner, G. The antioxidant role of coenzyme Q. *Mitochondrion* **7:**41–50; 2007.

[6] Bienert, G. P.; Moller, A. L. B.; Kristiansen, K. A.; Schulz, A.; Moller, I. M.; Schjoerring, J. K.; Jahn, T. P. Specific aquaporins facilitate the diffusion of hydrogen peroxide across membranes. *J. Biol. Chem.* **282:**1183–1192; 2007.

[7] Bienert, G. P.; Schjoerring, J. K.; Jahn, T. P. Membrane transport of hydrogen peroxide. *Biochim. Biophys. Acta* **1758:**994–1003; 2006.

[8] Boveris, A.; Chance, B. The mitochondrial generation of hydrogen peroxide: general properties and effect of hyperbaric oxygen. *Biochem. J.* **134:** 707–716; 1973.

[9] Brand, M. D. The sites and topology of mitochondrial superoxide production. *Exp. Gerontol.* **45:**466–472; 2010.

[10] Brown, G. C.; Borutaite, V. There is no evidence that mitochondria are the main source of reactive oxygen species in mammalian cells. *Mitochondrion* **12:**1–4; 2012.

[11] Caldeira da Silva, C. C.; Cerqueira, F. M.; Barbosa, L. F.; Medeiros, M. H. G.; Kowaltowski, A. J. Mild mitochondrial uncoupling in mice affects energy metabolism, redox balance and longevity. *Aging Cell* **7:**552–560; 2008.

[12] Castilho, R. F.; Kowaltowski, A. J.; Meinicke, A. R.; Bechara, E. J.; Vercesi, A. E. Permeabilization of the inner mitochondrial membrane by Ca^{2+} ions is stimulated by t-butyl hydroperoxide and mediated by reactive oxygen species generated by mitochondria. *Free Radic. Biol. Med.* **18:**479–486; 1995.

[13] Chen, X.; Zhong, Z.; Xu, Z.; Chen, L.; Wang, Y. 2′,7′-Dichlorodihydrofluorescein as a fluorescent probe for reactive oxygen species measurement: forty years of application and controversy. *Free Radic. Res.* **44:**587–604; 2010.

[14] Cochemé, H. M.; Quin, C.; McQuaker, S. J.; Cabreiro, F.; Logan, A.; Prime, T. A.; Abakumova, I.; Patel, J. V.; Fearnley, I. M.; James, A. M.; Porteous, C. M.; Smith, R. A.; Saeed, S.; Carré, J. E.; Singer, M.; Gems, D.; Hartley, R. C.; Partridge, L.; Murphy, M. P. Measurement of H_2O_2 within living Drosophila during aging using a ratiometric mass spectrometry probe targeted to the mitochondrial matrix. *Cell Metab.* **13:**340–350; 2011.

[15] Cox, A. G.; Winterbourn, C. C.; Hampton, M. B. Mitochondrial peroxiredoxin involvement in antioxidant defence and redox signalling. *Biochem. J.* **425:**313–325; 2009.

[16] Dickinson, B. C.; Chang, C. J. A targetable fluorescent probe for imaging hydrogen peroxide in the mitochondria of living cells. *J. Am. Chem. Soc.* **130:**9638–9639; 2008.

[17] Fischer, L. R.; Igoudjil, A.; Magrané, J.; Li, Y.; Hansen, J. M.; Manfredi, G.; Glass, J. D. SOD1 targeted to the mitochondrial intermembrane space prevents motor neuropathy in the Sod1 knockout mouse. *Brain* **134:** 196–209; 2011.

[18] Forkink, M.; Smeitink, J. A. M.; Brock, R.; Willems, P. H. G. M.; Koopman, W. J. H. Detection and manipulation of mitochondrial reactive oxygen species in mammalian cells. *Biochim. Biophys. Acta* **1797:**1034–1044; 2010.

[19] Forman, H. J.; Kennedy, J. A. Role of superoxide radical in mitochondrial dehydrogenase reactions. *Biochem. Biophys. Res. Commun.* **60:**1044–1050; 1974.

[20] Forman, H. J.; Azzi, A. On the virtual existence of superoxide anions in mitochondria: thoughts regarding its role in pathophysiology. *FASEB J.* **11:**374–375; 1997.

[21] Fridovich, I. Superoxide radical and superoxide dismutases. *Annu. Rev. Biochem.* **64:**97–112; 1995.

[22] Griffith, O. W.; Meister, A. Origin and turnover of mitochondrial glutathione. *Proc. Nat. Acad. Sci. U.S.A.* **82:**4668–4672; 1985.

[23] Guidot, D. M.; Repine, J. E.; Kitlowski, A. D.; Flores, S. C.; Nelson, S. K.; Wright, R. M.; McCord, J. M. Mitochondrial respiration scavenges extramitochondrial superoxide anion via a nonenzymatic mechanism. *J. Clin. Invest.* **96:**1131–1136; 1995.

[24] Guo, Q. Q.; Yue, Q. L.; Zhao, J. J.; Wang, L.; Wang, H. S.; Wei, X. L.; Liu, J.; Jia, J. How far can hydroxyl radicals travel? An electrochemical study based on a DNA mediated electron transfer process *Chem. Commun.* **47:**11906–11908; 2011.

[25] Halliwell, B. Antioxidants: the basics—what they are and how to evaluate them. *Adv. Pharmacol.* **38:**3–20; 1997.

[26] Ham, A. J.; Liebler, D. C. Vitamin E oxidation in rat liver mitochondria. *Biochemistry* **34:**5754–5761; 1995.

[27] Han, D.; Antunes, F.; Canali, R.; Rettori, D.; Cadenas, E. Voltage-dependent anion channels control the release of the superoxide anion from mitochondria to cytosol. *J. Biol. Chem.* **278:**5557–5563; 2003.

[28] Hanson, G. T.; Aggeler, R.; Oglesbee, D.; Cannon, M.; Capaldi, R. A.; Tsien, R. Y.; Remington, S. J. Investigating mitochondrial redox potential with redox-sensitive green fluorescent protein indicators. *J. Biol. Chem.* **279:** 13044–13053; 2004.

[29] Hashiguchi, K.; Bohr, V. A.; Souza-Pinto, N. C. Oxidative stress and mitochondrial DNA repair: implications for NRTIs induced DNA damage. *Mitochondrion* **4:**215–222; 2004.

[30] Hauptmann, N.; Grimsby, J.; Shih, J. C.; Cadenas, E. The metabolism of tyramine by monoamine oxidase A/B causes oxidative damage to mitochondrial DNA. *Arch. Biochem. Biophys.* **335:**295–304; 1996.

[31] Horton, K. L.; Stewart, K. M.; Fonseca, S. B.; Guo, Q.; Kelley, S. O. Mitochondria-penetrating peptides. *Chem. Biol.* **15:**375–382; 2008.

[32] Hu, J.; Dong, L.; Outten, C. E. The redox environment in the mitochondrial intermembrane space is maintained separately from the cytosol and matrix. *J. Biol. Chem.* **283:**29126–29134; 2008.

[33] Huang, Z.; Zhang, W.; Fang, H.; Zheng, M.; Wang, X.; Xu, J.; Cheng, H.; Gong, G.; Wang, W.; Dirksen, R. T.; Sheu, S. S. Response to "A critical evaluation of cpYFP as a probe for superoxide". *Free Radic. Biol. Med.* **51:**1937–1940; 2011.

[34] Hurd, T. R.; Costa, N. J.; Dahm, C. C.; Beer, S. M.; Brown, S. E.; Filipovska, A.; Murphy, M. P. Glutathionylation of mitochondrial proteins. *Antioxid. Redox Signal* **8:**999–1010; 2005.

[35] Imai, H.; Nakagawa, Y. Biological significance of phospholipid hydroperoxide glutathione peroxidase (PHPGx, GPx4) in mammalian cells. *Free Radic. Biol. Med.* **34:**145–169; 2003.

[36] James, A. M.; Cochemé, H. M.; Smith, R. A.; Murphy, M. P. Interactions of mitochondria-targeted and untargeted ubiquinones with the mitochondrial respiratory chain and reactive oxygen species: implications for the use of exogenous ubiquinones as therapies and experimental tools. *J. Biol. Chem.* **280:**21295–21312; 2005.

[37] Jensen, P. K. Antimycin-insensitive oxidation of succinate and reduced nicotinamide-adenine dinucleotide in electron-transport particles. I. pH dependency and hydrogen peroxide formation. *Biochim. Biophys. Acta* **122:**157–166; 1966.

[38] Jocelyn, P. C. Some properties of mitochondrial glutathione. *Biochim. Biophys. Acta* **369:**427–436; 1975.

[39] Kakhlon, O.; Manning, H.; Breuer, W.; Melamed-Book, N.; Lu, C.; Cortopassi, G.; Munnich, A.; Cabantchik, Z. I. Cell functions impaired by frataxin deficiency are restored by drug-mediated iron relocation. *Blood* **112:**5219–5227; 2008.

[40] Kalyanaraman, B.; Darley-Usmar, V.; Davies, K. J.; Dennery, P. A.; Forman, H. J.; Grisham, M. B.; Mann, G. E.; Moore, K.; Roberts, L. J. 2nd; Ischiropoulos, H. Measuring reactive oxygen and nitrogen species with fluorescent probes: challenges and limitations. *Free Radic. Biol. Med.* **52:**1–6; 2012.

[41] Kalyanaraman, B. Oxidative chemistry of fluorescent dyes: implications in the detection of reactive oxygen and nitrogen species. *Biochem. Soc. Trans.* **39:**1221–1225; 2011.

[42] Karlsson, M.; Kurz, T.; Brunk, U. T.; Nilsson, S. E.; Frennesson, C. I. What does the commonly used DCF test for oxidative stress really show? *Biochem. J.* **428:**183–190; 2010.

[43] Kaufman, B. A.; Newman, S. M.; Hallberg, R. L.; Slaughter, C. A.; Perlman, P. S.; Butow, R. A. In organello formaldehyde crosslinking of proteins to mtDNA: identification of bifunctional proteins. *Proc. Nat. Acad. Sci. U.S.A.* **97:**7772–7777; 2000.

[44] Koehler, C. M.; Beverly, K. N.; Leverich, E. P. Redox pathways of the mitochondrion. *Antioxid. Redox Signal* **6:**813–822; 2006.

[45] Koide, Y.; Urano, Y.; Kenmoku, S.; Kojima, H.; Nagano, T. Design and synthesis of fluorescent probes for selective detection of highly reactive oxygen species in mitochondria of living cells. *J. Am. Chem. Soc.* **129:**10324–10325; 2007.

[46] Koopman, W. J.; Nijtmans, L. G.; Dieteren, C. E.; Roestenberg, P.; Valsecchi, F.; Smeitink, J. A.; Willems, P. H. Mammalian mitochondrial complex I: biogenesis, regulation and reactive oxygen species generation. *Antioxid. Redox Signal* **12:**1431–1470; 2010.

[47] Kowaltowski, A. J.; Cosso, R. G.; Campos, C. B.; Fiskum, G. Effect of Bcl-2 overexpression on mitochondrial structure and function. *J. Biol. Chem.* **277:**42802–42807; 2002.

[48] Kowaltowski, A. J.; Souza-Pinto, N. C.; Castilho, R. F.; Vercesi, A. E. Mitochondria and reactive oxygen species. *Free Radic. Biol. Med.* **47:**333–343; 2009.

[49] Kunduzova, O. R.; Bianchi, P.; Parini, A.; Cambon, C. Hydrogen peroxide production by monoamine oxidase during ischemia/reperfusion. *Eur. J. Pharmacol.* **448:**225–230; 2002.

[50] Limon-Pacheco, J.; Gonsebatt, M. E. The role of antioxidants and antioxidant-related enzymes in protective responses to environmentally induced oxidative stress. *Mutat. Res.* **674:**137–147; 2009.

[51] Liu, Y.; Fiskum, G.; Schubert, D. Generation of reactive oxygen species by the mitochondrial electron transport chain. *J. Neurochem.* **80:**780–787; 2002.

[52] Liu, S. S. Cooperation of a "reactive oxygen cycle" with the Q cycle and the proton cycle in the respiratory chain—superoxide generating and cycling mechanisms in mitochondria. *J. Bioenerg. Biomembr.* **31:**367–376; 1999.

[53] Loschen, G.; Azzi, A.; Richter, C.; Flohe, L. Superoxide radicals as precursors of mitochondrial hydrogen peroxide. *FEBS Lett.* **42:**68–72; 1974.

[54] Malinouski, M.; Zhou, Y.; Belousov, V. V.; Hatfield, D. L.; Gladyshev, V. N. Hydrogen peroxide probes directed to different cellular compartments. *PLoS One* **6:**e14564; 2011.

[55] Maas, E.; Bisswanger, H. Localization of the α-oxoacid dehydrogenase multienzyme complexes within the mitochondrion. *FEBS Lett.* **277:**189–190; 1990.

[56] Matés, J. M.; Pérez-Gómez, C.; Castro, I. N. Antioxidant enzymes and human diseases. *Clin. Biochem.* **32:**595–603; 1999.

[57] Meredith, M. J.; Reed, D. J. Status of the mitochondrial pool of glutathione in the isolated hepatocyte. *J. Biol. Chem.* **257:**3747–3753; 1982.

[58] Meyer, A. J.; Dick, T. P. Fluorescent protein-based redox probes. *Antioxid. Redox Signal* **13:**621–650; 2010.

[59] Mikkelsen, R. B.; Wardman, P. Biological chemistry of reactive oxygen and nitrogen and radiation-induced signal transduction mechanisms. *Oncogene* **22:**5734–5754; 2003.

[60] Miwa, S.; St-Pierre, J.; Partridge, L.; Brand, M. D. Superoxide and hydrogen peroxide production by Drosophila mitochondria. *Free Radic. Biol. Med.* **8:**938–948; 2003.

[61] Monteiro, G.; Horta, B. B.; Pimenta, D. C.; Augusto, O.; Netto, L. E. S. Reduction of 1-Cys peroxiredoxins by ascorbate changes the thiol-specific antioxidant paradigm, revealing another function of vitamin C. *Proc. Nat. Acad. Sci. U.S.A.* **104:**4886–4891; 2007.

[62] Mukai, K.; Kikuchi, S.; Urano, S. Stopped-flow kinetic study of the regeneration reaction of tocopheroxyl radical by reduced ubiquinone-10 in solution. *Biochim. Biophys. Acta* **1035:**77–82; 1990.

[63] Muller, F. L. A critical evaluation of cpYFP as a probe for superoxide. *Free Radic. Biol. Med.* **47:**1779–1780; 2009.

[64] Murphy, M. P.; Holmgren, A.; Larsson, N. G.; Halliwell, B.; Chang, C. J.; Kalyanaraman, B.; Rhee, S. G.; Thornalley, P. J.; Partridge, L.; Gems, D.; Nyström, T.; Belousov, V.; Schumacker, P. T.; Winterbourn, C. C. Unraveling the biological roles of reactive oxygen species. *Cell Metab.* **13:**361–366; 2011.

[65] Murphy, M. P.; Smith, R. A. Targeting antioxidants to mitochondria by conjugation to lipophilic cations. *Annu. Rev. Pharmacol. Toxicol.* **47:**629–656; 2007.

[66] Murphy, M. How mitochondria produce reactive oxygen species. *Biochem. J.* **417:**1–13; 2009.

[67] Netto, L. E.; de Oliveira, M. A.; Monteiro, G.; Demasi, A. P.; Cussiol, J. R.; Discola, K. F.; Demasi, M.; Silva, G. M.; Alves, S. V.; Faria, V. G.; Horta, B. B. Reactive cysteine in proteins: protein folding, antioxidant defense, redox signaling and more. *Comp. Biochem. Physiol. C: Toxicol. Pharmacol* **146:**180–193; 2007.

[68] Nicholls, D. G.; Ward, M. W. Mitochondrial membrane potential and neuronal glutamate excitotoxicity: mortality and millivolts. *Trends Neurosci.* **23:**166–174; 2000.

[69] Nohl, H.; Gille, L.; Kozlov, A.; Staniek, K. Are mitochondria a spontaneous and permanent source of reactive oxygen species? *Redox Rep.* **8:**135–141; 2003.

[70] Nomura, K.; Imai, H.; Koumura, T.; Kobayashi, T.; Nakagawa, Y. Mitochondrial phospholipid hydroperoxide glutathione peroxidase inhibits the release of cytochrome c from mitochondria by suppressing the peroxidation of cardiolipin in hypoglycaemia-induced apoptosis. *Biochem. J.* **351:**183–193; 2000.

[71] Okado-Matsumoto, A.; Fridovich, I. Subcellular distribution of superoxide dismutases (SOD) in rat liver: Cu,Zn-SOD in mitochondria. *J. Biol. Chem.* **276:**38388–38393; 2001.

[72] Østergaard, H.; Henriksen, A.; Hansen, F. G.; Winther, J. R. Shedding light on disulfide bond formation: engineering a redox switch in green fluorescent protein. *EMBO J.* **20:**5853–5862; 2001.

[73] Pedersen, A.; Karlsson, G. B.; Rydström, J. Proton-translocating transhydrogenase: an update of unsolved and controversial issues. *J. Bioenerg. Biomembr.* **40:**463–473; 2008.

[74] Pereverzev, M. O.; Vygodina, T. V.; Konstantinov, A. A.; Skulachev, V. P. Cytochrome c, an ideal antioxidant. *Biochem. Soc. Trans.* **31:**1312–1315; 2003.

[75] Plecitá-Hlavatá, L.; Jezek, J.; Jezek, P. Pro-oxidant mitochondrial matrix-targeted ubiquinone MitoQ10 acts as anti-oxidant at retarded electron transport or proton pumping within Complex I. *Int. J. Biochem. Cell Biol.* **41:**1697–1707; 2009.

[76] Pryor, W. A. Oxy-radicals and related species: their formation, lifetimes, and reactions. *Annu. Rev. Physiol.* **48:**657–667; 1986.

[77] Radi, R.; Turrens, J. F.; Chang, L. Y.; Bush, K. M.; Crapoll, J. D.; Freeman, B. A. Detection of catalase in rat heart mitochondria. *J. Biol. Chem.* **266:**22028–22034; 1991.

[78] Ramshesh, V. K.; Lemasters, J. J. Imaging of mitochondrial pH using SNARF-1. *Methods Mol. Biol.* **810:**243–248; 2012.

[79] Redmond, R. W.; Kochevar, I. E. Spatially resolved cellular responses to singlet oxygen. *Photochem. Photobiol.* **82:**1178–1186; 2006.

[80] Rhee, S. G.; Kang, S. W.; Chang, T.; Jeong, W.; Kim, K. Peroxiredoxin, a novel family of peroxidases. *IUBMB Life.* **52:**35–41; 2001.

[81] Rhee, S. G.; Chang, T. S.; Jeong, W.; Kang, D. Methods for detection and measurement of hydrogen peroxide inside and outside of cells. *Mol. Cells* **29:**539–549; 2010.

[82] Robinson, K. M.; Janes, M. S.; Pehar, M.; Monette, J. S.; Ross, M. F.; Hagen, T. M.; Murphy, M. P.; Beckman, J. S. Selective fluorescent imaging of superoxide in vivo using ethidium-based probes. *Proc. Nat. Acad. Sci. U.S.A.* **103:**15038–15043; 2006.

[83] Roma, L. P.; Duprez, J.; Takahashi, H. K.; Gilon, P.; Wiederkehr, A.; Jonas, J. C. Dynamic measurements of mitochondrial hydrogen peroxide concentration and glutathione redox state in rat pancreatic β-cells using ratiometric fluorescent proteins: confounding effects of pH with HyPer but not roGFP1. *Biochem. J.* **441:**971–978; 2012.

[84] Salvador, A.; Sousa, J.; Pinto, R. E. Hydroperoxyl, superoxide and pH gradients in the mitochondrial matrix: a theoretical assessment. *Free Radic. Biol. Med.* **31:**1208–1215; 2001.

[85] Salvi, M.; Battaglia, V.; Brunati, A. M.; La Rocca, N.; Tibaldi, E.; Pietrangeli, P.; Marcocci, L.; Mondovì, B.; Rossi, C. A.; Toninello, A. Catalase takes part in rat liver mitochondria oxidative stress defense. *J. Biol. Chem.* **282:**24407 24415; 2007.

[86] Sato, H.; Tachifuji, A.; Tamura, M.; Miyakawa, I. Identification of the YMN-1 antigen protein and biochemical analyses of protein components in the mitochondrial nucleoid fraction of the yeast *Saccharomyces cerevisiae*. *Protoplasma* **219:**51–58; 2002.

[87] Schwarzländer, M.; Logan, D. C.; Fricker, M. D.; Sweetlove, L. J. The circularly permuted yellow fluorescent protein cpYFP that has been used as a superoxide probe is highly responsive to pH but not superoxide in mitochondria: implications for the existence of superoxide 'flashes'. *Biochem. J.* **437:**381–387; 2011.

[88] Selivanov, V. A.; Zeak, J. A.; Roca, J.; Cascante, M.; Trucco, M.; Votyakova, T. V. The role of external and matrix pH in mitochondrial reactive oxygen species generation. *J. Biol. Chem.* **283:**29292–29300; 2008.

[89] Shioji, K.; Oyama, Y.; Okuma, K.; Nakagawa, H. Synthesis and properties of fluorescence probe for detection of peroxides in mitochondria. *Bioorg. Med. Chem. Lett.* **20:**3911–3915; 2010.

[90] Schriner, S. E.; Linford, N. J.; Martin, G. M.; Treuting, P.; Ogburn, C. E.; Emond, M.; Coskun, P. E.; Ladiges, W.; Wolf, N.; Van Remmen, H.; Wallace, D. C.; Rabinovitch, P. S. Extension of murine life span by overexpression of catalase targeted to mitochondria. *Science* **308:**1909–1911; 2005.

[91] Simonson, S. G.; Zhang, J.; Canada Jr. A. T.; Su, Y. F.; Benveniste, H.; Piantadosi, C. A. Hydrogen peroxide production by monoamine oxidase during ischemia–reperfusion in the rat brain. *J. Cereb. Blood Flow Metab.* **13:**125–134; 1993.

[92] Skulachev, M. V.; Antonenko, Y. N.; Anisimov, V. N.; Chernyak, B. V.; Cherepanov, D. A.; Chistyakov, V. A.; Egorov, M. V.; Kolosova, N. G.; Korshunova, G. A.; Lyamzaev, K. G.; Plotnikov, E. Y.; Roginsky, V. A.; Savchenko, A. Y.; Severina, I. I.; Severin, F. F.; Shkurat, T. P.; Tashlitsky, V. N.; Shidlovsky, K. M.; Vyssokikh, M. Y.; Zamyatnin Jr A. A.; Zorov, D. B.; Skulachev, V. P. Mitochondrial-targeted plastoquinone derivatives: effect on senescence and acute age-related pathologies. *Curr. Drug Targets* **12:**800–826; 2011.

[93] Skulachev, V. P. Cytochrome c in the apoptotic and antioxidant cascades. *FEBS Lett.* **423:**275–280; 1998.

[94] Skulachev, V. P.; Antonenko, Y. N.; Cherepanov, D. A.; Chernyak, B. V.; Izyumov, D. S.; Khailova, L. S.; Klishin, S. S.; Korshunova, G. A.; Lyamzaev; Pletjushkina, O. Y.; Roginsky, V. A.; Rokitskaya, T. I.; Severin, F. F.; Severina, I. I.; Simonyan, R. A.; Skulachev, M. V.; Sumbatyan, N. V.; Sukhanova, E. I.; Tashlitsky, V. N.; Trendeleva, T. A.; Vyssokikh, M. Y.; Zvyagilskaya, R. A. Prevention of cardiolipin oxidation and fatty acid cycling as two antioxidant mechanisms of cationic derivatives of plastoquinone (SkQs). *Biochim. Biophys. Acta* **1797:**878–889; 2010.

[95] Skulachev, V. P. Uncoupling: new approaches to an old problem of bioenergetics. *Biochim. Biophys. Acta* **1363:**100–124; 1998.

[96] Smith, R. A.; Murphy, M. P. Animal and human studies with the mitochondria-targeted antioxidant MitoQ. *Ann. N. Y. Acad. Sci.* **1201:**96–103; 2010.

[97] Song, Y.; Garry, R. B. Thermodynamic and kinetic considerations for the reaction of semiquinone radicals to form superoxide and hydrogen peroxide. *Free Radic. Biol. Med.* **49:**919–962; 2010.

[98] Sousa-Lopes, A.; Antunes, F.; Cyrne, L.; Marinho, H. S. Decreased cellular permeability to H_2O_2 protects *Saccharomyces cerevisiae* cells in stationary phase against oxidative stress. *FEBS Lett.* **578:**152–156; 2004.

[99] Srikun, D.; Albers, A. E.; Nam, C. I.; Iavarone, A. T.; Chang, C. J. Organelle-targetable fluorescent probes for imaging hydrogen peroxide in living cells via SNAP-Tag protein labeling. *J. Am. Chem. Soc.* **132:**4455–4465; 2010.

[100] Staniek, K.; Nohl, H. Are mitochondria a permanent source of reactive oxygen species? *Biochem. Biophys. Acta* **1460:**268–275; 2000.

[101] St-Pierre, J.; Buckingham, J. A.; Roebuck, S. J.; Brand, M. D. Topology of superoxide production from different sites in the mitochondrial electron transport chain. *J. Biol. Chem.* **277:**44784–44790; 2002.

[102] Starkov, A. A.; Fiskum, G.; Chinopoulos, C.; Lorenzo, B. J.; Browne, S. E.; Patel, M. S.; Beal, M. F. Mitochondrial α-ketoglutarate dehydrogenase complex generates reactive oxygen species. *J. Neurosci.* **24:**7779–7788; 2004.

[103] Sukhanova, E. I.; Trendeleva, T. A.; Zvyagilskaya, R. A. Interaction of yeast mitochondria with fatty acids and mitochondria-targeted lipophilic cations. *Biochem. (Moscow)* **75:**139–144; 2010.

[104] Swift, L. M.; Sarvazyan, N. Localization of dichlorofluorescin in cardiac myocytes: implications for assessment of oxidative stress. *Am. J. Phys.* **278:**H982–H990; 2000.

[105] Szeto, H. H. Mitochondria-targeted peptide antioxidants: novel neuroprotective agents. *AAPS J.* **8:**E521–E531; 2006.

[106] Tahara, E. B.; Barros, M. H.; Oliveira, G. A.; Netto, L. E. S.; Kowaltowski, A. J. Dihydrolipoyl dehydrogenase as a source of reactive oxygen species inhibited by caloric restriction and involved in *Saccharomyces cerevisiae* aging. *FASEB J.* **21:**274–283; 2007.

[107] Tahara, E. B.; Cezário, K.; Souza-Pinto, N. C.; Barros, M. H.; Kowaltowski, A. J. Respiratory and TCA cycle activities affect *S. cerevisiae* lifespan, response to caloric restriction and mtDNA stability. *J. Bioenerg. Biomembr.* **43:**483–491; 2011.

[108] Tahara, E. B.; Navarete, F. D.; Kowaltowski, A. J. Tissue-, substrate-, and site-specific characteristics of mitochondrial reactive oxygen species generation. *Free Radic. Biol. Med.* **9:**1283–1297; 2009.

[109] Thomas, J. P.; Maiorino, M.; Ursini, F.; Girotti, A. W. Protective action of phospholipid hydroperoxide glutathione peroxidase against membrane-damaging lipid peroxidation. *J. Biol. Chem.* **265:**454–461; 1990.

[110] Thomas, S. M.; Gebicki, J. M.; Dean, R. T. Radical initiated α-tocopherol depletion and lipid peroxidation in mitochondrial membranes. *Biochim. Biophys. Acta* **1002:**189–197; 1989.

[111] Tretter, L.; Adam-Vizi, V. Generation of reactive oxygen species in the reaction catalyzed by α-ketoglutarate dehydrogenase. *J. Neurosci.* **24:**7771–7778; 2004.

[112] Tretter, L.; Takacs, K.; Kövér, K.; Adam-Vizi, V. Stimulation of H_2O_2 generation by calcium in brain mitochondria respiring on α-glycerophosphate. *J. Neurosci. Res.* **15:**3471–3479; 2007.

[113] Tretter, L.; Takacs, K.; Hegedus, V.; Adam-Vizi, V. Characteristics of α-glycerophosphate-evoked H_2O_2 generation in brain mitochondria. *J. Neurochem.* **3:**650–663; 2007.

[114] Turrens, J. F. Mitochondrial formation of reactive oxygen species. *J. Physiol.* **552:**335–344; 2003.

[115] Ursini, F.; Maiorino, M.; Gregolin, C. The selenoenzyme phospholipid hydroperoxide glutathione peroxidase. *Biochim. Biophys. Acta* **839:**62–70; 1985.

[116] Valko, M.; Leibfritz, D.; Moncol, J.; Cronin, M. T. D.; Mazur, M.; Telser, J. Free radicals and antioxidants in normal physiological functions and human disease. *Int. J. Biochem. Cell Biol.* **39:**44–84; 2007.

[117] Vasquez-Vivar, J.; Kalyanaraman, B.; Kennedy, M. C. Mitochondrial aconitase is a source of hydroxyl radical: an electron spin resonance investigation. *J. Biol. Chem.* **19:**14064–14069; 2000.

[118] Wang, W.; Fang, H.; Groom, L.; Cheng, A.; Zhang, W.; Liu, J.; Wang, X.; Li, K.; Han, P.; Zheng, M.; Yin, J.; Wang, W.; Mattson, M. P.; Kao, J. P.; Lakatta, E. G.; Sheu, S. S.; Ouyang, K.; Chen, J.; Dirksen, R. T.; Cheng, H. Superoxide flashes in single mitochondria. *Cell* **134:**279–290; 2008.

[119] Waypa, G. B.; Marks, J. D.; Guzy, R.; Mungai, P. T.; Schriewer, J.; Dokic, D.; Schumacker, P. T. Hypoxia triggers subcellular compartmental redox signaling in vascular smooth muscle cells. *Circ. Res.* **106:**526–535; 2010.

[120] Weisiger, R. A.; Fridovich, I. Superoxide dismutase: organelle specificity. *J. Biol. Chem.* **248:**3582–3592; 1973.

[121] Winterbourn, C. C.; Hampton, M. B. Thiol chemistry and specificity in redox signaling. *Free Radic. Biol. Med.* **45:**549–561; 2008.

[122] Wrona, M.; Wardman, P. Properties of the radical intermediate obtained on oxidation of 2′,7′-dichlorodihydrofluorescein, a probe for oxidative stress. *Free Radic. Biol. Med.* **41:**657–667; 2006.

[123] Yeh, J. I.; Chinte, U.; Du, S. Structure of glycerol-3-phosphate dehydrogenase, an essential monotopic membrane enzyme involved in respiration and metabolism. *Proc. Nat. Acad. Sci. U.S.A.* **105:**3280–3285; 2008.

[124] Yankovskaya, V.; Horsefield, R.; Törnroth, S.; Luna-Chavez, C.; Miyoshi, H.; Léger, C.; Byrne, B.; Cecchini, G.; Iwata, S. Architecture of succinate dehydrogenase and reactive oxygen species generation. *Science* **299:**700 704; 2003.

[125] Zhang, L.; Yu, L.; Yu, C. A. Generation of superoxide anion by succinate-cytochrome c reductase from bovine heart mitochondria. *J. Biol. Chem.* **273:**33972–33976; 1998.

[126] Zhao, K.; Zhao, G. M.; Wu, D.; Soong, Y.; Birk, A. V.; Schiller, P. W.; Szeto, H. H. Cell-permeable peptide antioxidants targeted to inner mitochondrial membrane inhibit mitochondrial swelling, oxidative cell death, and reperfusion injury. *J. Biol. Chem.* **279:**34682–34690; 2004.

[127] Zhou, M.; Diwu, Z.; Panchuk-Voloshina, N.; Haugland, R. P. A stable nonfluorescent derivate of resorufin for the fluorometric determination of trace hydrogen peroxide: applications in detecting the activity of phagocyte NADPH oxidase and other oxidases. *Anal. Biochem.* **253:**162–168; 1997.

[128] Zielonka, J.; Kalyanaraman, B. Hydroethidine- and MitoSOX-derived red fluorescence is not a reliable indicator of intracellular superoxide formation: another inconvenient truth. *Free Radic. Biol. Med.* **48:**983–1001; 2010.

[129] Zoccarato, F.; Cavallini, L.; Deana, R.; Alexandre, A. Pathways of hydrogen peroxide generation in guinea pig cerebral cortex mitochondria. *Biochem. Biophys. Res. Commun.* **2:**727–734; 1988.

Free Radical Biology & Medicine 51 (2011) 1454–1460

Contents lists available at ScienceDirect

Free Radical Biology & Medicine

journal homepage: www.elsevier.com/locate/freeradbiomed

Original Contribution

Long-term intermittent feeding, but not caloric restriction, leads to redox imbalance, insulin receptor nitration, and glucose intolerance

Fernanda M. Cerqueira, Fernanda M. da Cunha, Camille C. Caldeira da Silva, Bruno Chausse, Renato L. Romano, Camila C.M. Garcia, Pio Colepicolo, Marisa H.G. Medeiros, Alicia J. Kowaltowski *

Departamento de Bioquímica, Instituto de Química, Universidade de São Paulo, 05508–900 São Paulo, SP, Brazil

ARTICLE INFO

Article history:
Received 6 June 2011
Accepted 8 July 2011
Available online 2 August 2011

Keywords:
Calorie restriction
Free radicals
Insulin receptor
Glucose tolerance
Nitration
Nitric oxide synthase

ABSTRACT

Calorie restriction is a dietary intervention known to improve redox state, glucose tolerance, and animal life span. Other interventions have been adopted as study models for caloric restriction, including nonsupplemented food restriction and intermittent, every-other-day feedings. We compared the short- and long-term effects of these interventions to ad libitum protocols and found that, although all restricted diets decrease body weight, intermittent feeding did not decrease intra-abdominal adiposity. Short-term calorie restriction and intermittent feeding presented similar results relative to glucose tolerance. Surprisingly, long-term intermittent feeding promoted glucose intolerance, without a loss in insulin receptor phosphorylation. Intermittent feeding substantially increased insulin receptor nitration in both intra-abdominal adipose tissue and muscle, a modification associated with receptor inactivation. All restricted diets enhanced nitric oxide synthase levels in the insulin-responsive adipose tissue and skeletal muscle. However, whereas calorie restriction improved tissue redox state, food restriction and intermittent feedings did not. In fact, long-term intermittent feeding resulted in largely enhanced tissue release of oxidants. Overall, our results show that restricted diets are significantly different in their effects on glucose tolerance and redox state when adopted long-term. Furthermore, we show that intermittent feeding can lead to oxidative insulin receptor inactivation and glucose intolerance.

McCay [1] first demonstrated that rats restricted in caloric intake exhibited extended life spans. Subsequently, calorie restriction (CR) was shown to extend life span in many animal models [2–4] and attracted the attention of researchers uncovering mechanisms involved in animal aging. Unfortunately, studies involving dietary limitations and their biological effects have diverged over the years regarding the protocol adopted. Today, many diets commonly referred to as CR in the literature involve intermittent feeding and fasting cycles (IF), also known as every-other-day feedings, or food restriction (FR) without micronutrient supplementation (incurring malnutrition [5]). Although some metabolic changes similar to those observed in CR are present in FR or IF [6–9], there is little or inconsistent evidence to date that these interventions promote life-span benefits [10–14; reviewed in 5,6,15]. Furthermore, most studies adopt a single nutritional protocol, precluding side-by-side comparisons between these clearly distinct diets.

Of the many effects of CR, two are widely accepted to be connected with extended longevity: redox changes and alterations in insulin signaling pathways [16–18]. CR limits mitochondrial generation of reactive oxygen species (ROS), alters the expression and activity of antioxidant pathways, and prevents oxidative modifications of biomolecules during aging [4,18,19]. CR also prevents the loss of peripheral sensitivity to insulin, precluding many of the effects of aging associated with insulin resistance [16,17]. Changes in redox state and insulin signaling may be linked, although this cross talk is still poorly explored. Insulin receptor sensitivity has been shown to increase in response to mild oxidative imbalance [20,21], whereas excessive ROS production in diabetes and obesity can impair insulin signaling [22,23].

Here, we compare the short- and long-term effects of ad libitum feeding (AL), CR, and IF on body weight, intra-abdominal fat accumulation, glucose tolerance, and insulin signaling. We find that, although IF and CR are similar in short-term studies, they are strikingly different in long-term interventions. Long-term IF promotes redox imbalance, oxidative modification of the insulin receptor, and glucose intolerance.

Experimental procedures

Animals

All experiments were conducted in agreement with the National Institutes of Health guidelines for humane treatment of animals and were reviewed and approved by the local Animal Care and Use Committee. For short-term studies, male, 4-week-old Sprague–Dawley rats were separated into three groups: AL, fed ad libitum with an

Abbreviations: AL, ad libitum; CR, calorie restriction; FR, food restriction; IR, insulin receptor; IF, intermittent feeding/fasting; NOS, nitric oxide synthase; ROS, reactive oxygen species.

* Corresponding author. Fax: +55 11 38155579.
E-mail address: alicia@iq.usp.br (A.J. Kowaltowski).

0891-5849 © 2011 Elsevier Inc. Open access under the Elsevier OA license.
doi:10.1016/j.freeradbiomed.2011.07.006

AIN-93-M diet prepared by Rhoster (Campinas, SP, Brazil); CR, fed daily with 60% of a diet supplemented with micronutrients, to reach the vitamin and mineral levels consumed by AL animals; and IF, which had ad libitum access to the AIN-93-M diet on alternating days. Body mass and food consumption were recorded weekly. In the long-term study, the FR group was added (FR, fed daily with 60% weight of the same diet offered to AL animals), and the rats were divided into groups at 8 weeks of age. Food was offered to FR and CR rats at 6:00 PM, the same time at which IF chow was alternately placed or removed. FR and CR feedings were adjusted weekly by weight, based on AL food consumption measured 1 week prior. The animals were lodged three individuals per cage, in 12-h light/dark cycles, and given water ad libitum.

After 4 weeks or 8 months of dietary intervention, the rats were sacrificed after 12 h of overnight fasting and tissues were dissected and weighed. Total hindlimb skeletal muscle and intra-abdominal fat deposits were pooled and homogenized together. To ensure that all rats presented comparable feeding statuses, food was placed at 6:00 PM for all groups. Food was removed at 8:00 PM, and the animals were sacrificed at 8:00 AM the following day. During the long-term dietary intervention, 2 of 8 animals in the FR group and 1 of 15 AL rats died spontaneously, 2 of 16 animals from the IF group were removed because of locomotive alterations, and 1 was eliminated because of the presence of tumors. No animals were eliminated from the CR group (18 in total).

Glucose levels and glucose tolerance tests

Peripheral blood was collected from the tail of 8- or 40-week-old animals fasted for 12 h and immediately used for glucose analysis using a glucose analyzer (Accu-Check Performa, São Paulo, SP, Brazil). For glucose tolerance tests, rats were anesthetized with isoflurane (5%) using a calibrated vaporizer (35–50% O_2; 50–65% N_2O), at the end of the dietary intervention and after an overnight fasting period. A 200 g/L glucose solution was injected ip at a final dose of 2 g kg^{-1} [24], and blood samples for glycemic determinations were obtained from the paw at 0, 30, 60, and 120 min after the challenge and analyzed using a glucose analyzer.

Immunoprecipitations

Intra-abdominal adipose tissue and skeletal muscle samples were homogenized using an electric potter in lysis buffer (50 mM sodium phosphate, pH 7.4, 10% glycerol, 1% octyl phenol ethoxylate, 10 mM sodium orthovanadate, 10 mM sodium fluoride, 10 mM sodium pyrophosphate, supplemented with a Sigma protease inhibitor mixture). After 30 min on ice, tissue lysates were centrifuged (13,000 *g*, 20 min, 4 °C), and the resulting supernatants were collected. Solubilized proteins, at final concentration of 1 (adipose tissue) or 2 mg/ml (muscle), were incubated with anti-insulin receptor (IR) β subunit (4 μg/ml) or anti-insulin receptor substrate 1 (IRS1) (3 μg/ml) antibodies at 4 °C overnight. Protein A–agarose (Sigma) beads were added, and the incubation was continued at 4 °C for 2 h. The beads were centrifuged (13,000 *g*, 1 min, 4 °C), washed five times in lysis buffer, and suspended in Laemmli sample buffer containing 5% 2-mercaptoethanol. Immunoprecipitation specificity was verified through SDS–PAGE separation of precipitated samples followed by silver-stained polyacrylamide gels.

Western blots

Proteins from tissue lysates or protein agarose beads conjugated with IR or IRS1 were diluted in Laemmli sample buffer containing 5% 2-mercaptoethanol. After heating at 90 °C for 15 min, proteins were separated by SDS–PAGE and transferred onto nitrocellulose membranes. After membranes were blocked with 5% bovine serum albumin, detection of individual proteins was carried out by blotting with specific primary antibodies against adiponectin (Abcam; 0.5 μg ml^{-1}), IR (Upstate; 1:1000), IRS1 (Upstate; 0.54 μg ml^{-1}), phosphotyrosine (Upstate; 0.5 μg ml^{-1}), nitrotyrosine (OxisResearch; 1:2000), dinitrophenylhydrazine (Sigma; 1:5000), endothelial nitric oxide synthase (eNOS; Sigma; 1:3000), phospho-eNOS^{Ser1177} (Cell Signaling; C9C3 clone, 1:1000), inducible NOS (iNOS; Alexis Biochemicals; 1:750), catalase (Abcam; 1:1000), superoxide dismutase 2 (Abcam; 0.5 μg ml^{-1}), or γ-actin (Sigma; 1:2000), a loading control. Chemiluminescence detection using a secondary peroxidase-linked anti-rabbit (Calbiochem; 1:10,000) or anti-sheep IgG (Calbiochem; 1:13,000) and a detection system from Pierce KLP (Rockford, IL, USA) was performed. Signals were quantified by densitometry using ImageQuant (Amersham Biosciences) and corrected to actin levels. Adiponectin and dinitrophenylhydrazine were corrected using Ponceau red staining. Phospho-eNOS, phospho-Tyr-IR, phospho-Tyr-IRS1, and NO_2-Tyr-IR were corrected to the total amount of immunoprecipitate.

H_2O_2 release

Tissues were extracted and immediately segmented into fine pieces (~1 mm) in PBS (137 mM NaCl, 10 mM phosphate, 2.7 mM KCl, pH 7.4) supplemented with 10 mM glucose, 50 μM Amplex red, and 1 U ml^{-1} horseradish peroxidase. Amplex red reacts with peroxidase–H_2O_2 complexes producing fluorescent resorufin [25]. Fluorescence was measured at ex 563 nm and em 587 nm, using 5-nm slits, within 1 h of tissue preparation. Baseline fluorescence in the same medium was subtracted from all measurements. A calibration curve was constructed using commercial H_2O_2.

Statistical analysis

Data were analyzed using GraphPad Prism and Origin software. Figures represent averages ± SEM of 3–12 measurements and were compared using ANOVA. Two-tailed p values under 0.05 were considered significant.

Results

Fig. 1 compares the effects of short- (4 weeks) and long- (32 weeks) term dietary interventions on animal weight and intra-abdominal adiposity. FR, CR, and IF animals presented lower body weights compared to AL at both time points (Fig. 1A and B), although total food ingestion per week in IF animals was equal to that of AL (Fig. 1C and D) due to overeating during the feeding period. We found that IF animals ingested approximately 60% of their 24-h food consumption within the first 2 h after chow placement, a consumption rate of 19 g h^{-1} rat^{-1}, whereas FR and CR animals presented food intake rates of 9 g h^{-1} rat^{-1}.

Although body weights were lower in all restricted groups, IF rats presented high intra-abdominal adiposity at both time points (Fig. 1E and F). FR and CR animals, in turn, presented low levels of abdominal adiposity. Consistently, serum adiponectin levels, which are typically inversely proportional to abdominal adiposity [26], were low in AL and IF at both time points and high in CR and FR animals (Fig. 1G and H). Altogether, these results suggest that, although all feeding strategies led to weight reductions compared to AL animals, IF differs significantly from FR and CR in terms of energy intake and balance.

Short-term dietary interventions did not alter fasting glucose levels (Fig. 2A). Long-term maintenance on an AL diet led to increased fasting glucose levels, which only CR prevented significantly (Fig. 2B). Glucose levels 2 h after food was offered were in the range of 240 mg dl^{-1} in IF animals, whereas FR and CR levels were approximately 150 and 130 mg dl^{-1}, respectively, versus 150 mg dl^{-1} in AL (measured after 2 h in the dark period in 40-week-old rats).

Because of the changes observed in fasting glucose levels, we performed a glucose tolerance test. We found that short-term IF and CR improve glucose clearance (Fig. 2C and E). The same was not verified in

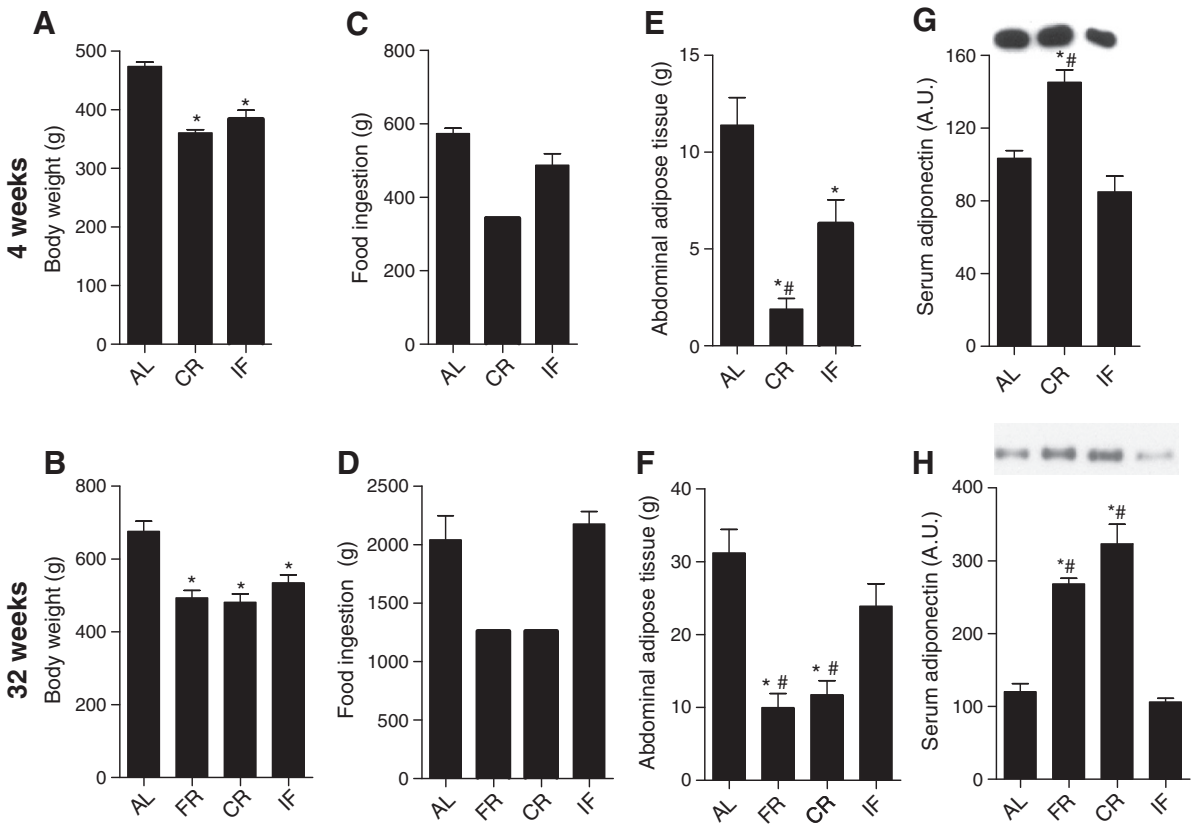

Fig. 1. IF decreases body weight, but not food ingestion or intra-abdominal adiposity. Animals were subjected to AL, FR, CR, or IF diet. Body mass after (A) 4 or (B) 32 weeks of dietary intervention, food consumption per animal over (C) 4 or (D) 32 weeks, intra-abdominal fat mass per animal after (E) 4 or (F) 32 weeks, and serum adiponectin quantifications after (G) 4 or (H) 32 weeks are shown. $^{*}p<0.05$ versus control; $^{\#}p<0.05$ versus IF, $n=15$.

the long-term experiments (Fig. 2D and F): surprisingly, whereas CR maintained good glucose tolerance long term, IF animals had significantly worse glucose clearance than AL.

To understand the changes in glucose tolerance, we measured IR expression and activation by determining Tyr phosphorylation levels in two insulin-responsive tissues: intra-abdominal adipose tissue and skeletal muscle. Short-term IF and CR strongly increased IR expression (not shown) and IR-Tyr phosphorylation in the abdominal adipose tissue and skeletal muscle (Fig. 3A and C). Long-term dietary interventions also significantly increased IR expression in the skeletal muscle (Supplementary Fig. 1) and phospho-Tyr-IR in the adipose tissue (Fig. 3B). In skeletal muscle, IR phosphorylation was increased by FR and CR, but not IF (Fig. 3D). Whereas the short-term IR phosphorylation results are consistent with glucose tolerance tests, the same was not observed in long-term results, in which IF animals presented impaired glucose clearance but not decreased IR phosphorylation relative to AL. We hypothesized that a different modification unrelated to phosphorylation could be impairing IR function.

In vitro studies have previously shown that Tyr nitration can decrease the function of this receptor [27–31]. We thus investigated whether IR nitration could explain the physiological differences between the long-term experimental groups we observed. We found (Fig. 4A and B) that CR consistently prevented IR nitration relative to AL diets. Furthermore, IF strongly increased nitration levels in the adipose tissue and muscle, and FR increased nitration in the muscle. The effect of short-term interventions on IR nitration was also measured and indicated that young rats present very low levels of this modification, virtually undetectable under our conditions (results not shown).

To verify the downstream results on IR function of the changes observed in phosphorylation and nitration, we measured the phosphorylation of the IR substrate IRS1. Expression levels of IRS1 are included in Supplemental Fig. 1C and D. Phospho-Tyr-IRS1 levels (Fig. 5A and B) were increased specifically in CR in muscle and were decreased by IF in both tissues relative to AL. The changes observed in IRS1 phosphorylation are compatible with glucose clearance, which is improved by CR and decreased in IF. We propose that the overall function of the IR is the result of both phosphorylation (activating) and nitration (inhibitory) of this receptor, as will be further discussed below.

Tyr nitration is promoted by peroxynitrite, the reaction product of superoxide radicals and nitric oxide [32]. Accordingly, we investigated whether the diets produced changes in NOS levels and the generation of ROS. We found that eNOS activation through phosphorylation was enhanced significantly relative to AL only in CR muscle samples (Fig. 6A and B), which may explain enhanced oxygen consumption levels (Supplementary Fig. 2), because mitochondrial biogenesis is stimulated by eNOS-derived nitric oxide [33–35]. iNOS expression was enhanced in all restricted diets (Figs. 6C and 4D). Overall, nitric oxide synthesis pathway activities do not explain the IR nitration patterns.

On the other hand, tissue H_2O_2 release was markedly enhanced in IF, both in muscle and in adipose tissue, and decreased in CR in muscle (Fig. 6E and F), a pattern very similar to IR nitration levels observed in Fig. 4. H_2O_2 is a relatively stable and membrane-diffusible product of superoxide radical dismutation, thus often used as a marker for ROS levels in biological samples [36] in which reliable measurements of the production of nondiffusible and unstable species such as superoxide radicals is not possible. The large increases observed in H_2O_2 diffusion from the IF tissues may represent enhanced tissue ROS generation and/or a decrease in antioxidant capacity. We measured quantities of the major antioxidants glutathione, superoxide dismutase, and catalase in these tissues (Supplementary Fig. 3). In most cases, IF increased the levels of the antioxidants measured, with the exception of catalase and glutathione in skeletal muscle. Thus, if anything, IF improved antioxidant capacity, especially in the abdominal adipose tissue. Thus, increased levels of H_2O_2 release from IF

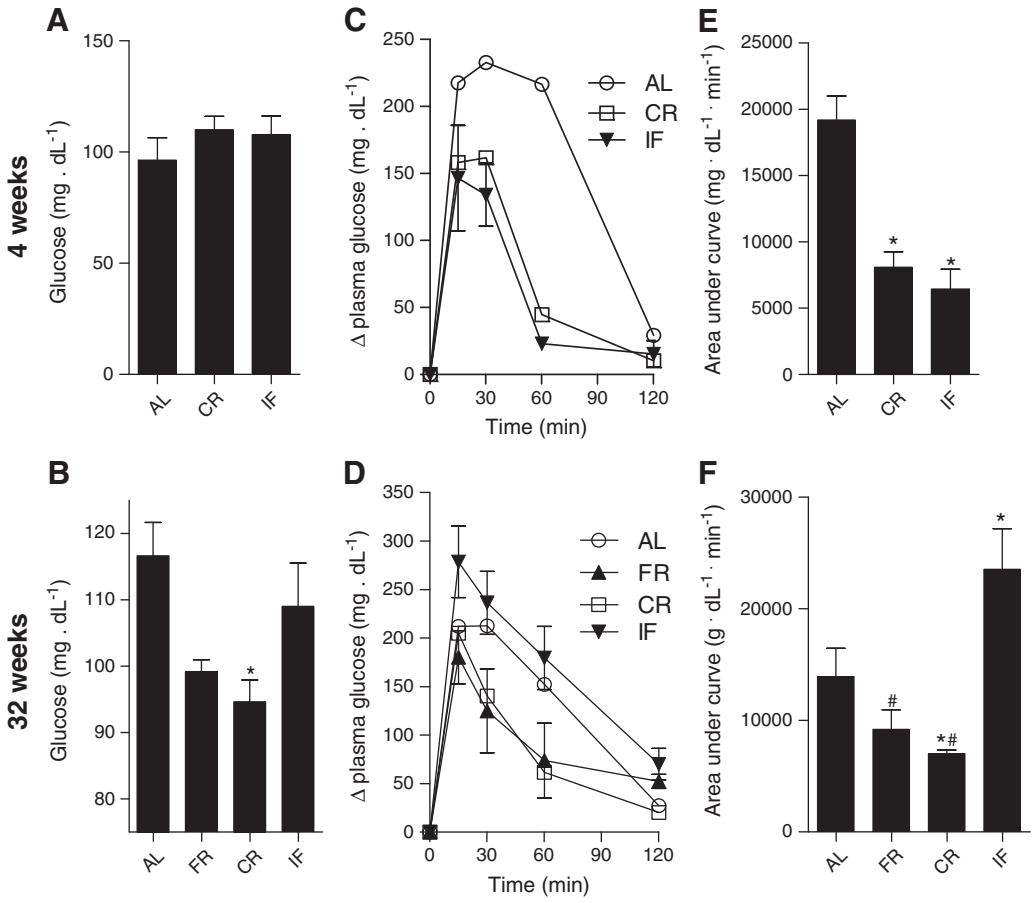

Fig. 2. Long-term, but not short-term IF leads to glucose intolerance. Rats were tested for fasting glucose after (A) 4 or (B) 32 weeks of dietary intervention. Blood glucose after a 2 g kg^{-1} intraperitoneal glucose injection after (C) 4 or (D) 32 weeks is shown. (E and F) Areas under the glucose curve in (C) and (D), respectively. $^{*}p<0.05$ vs control; $^{\#}p<0.05$ vs IF, $n=15$.

tissues probably reflects mostly enhanced ROS generation, although this point still remains to be verified directly.

Discussion

Dietary interventions such as FR and IF have been used interchangeably in the literature as equivalent to CR [5], although little is known about the long-term impact of these interventions. In this article, we compared short- and long-term effects of these diets and found that, despite some similarities, there are very significant differences that warrant attention. The most immediate difference between CR and IF is that intermittent ad libitum feeding does not limit total food intake, as reported here (Fig. 1) and in previous studies [5,6]. Some studies measured reductions in spontaneous feedings with IF [37,38], although the protocols differ in the onset of the adopted diet, which may influence feeding patterns and result in differences in food ingestion.

Despite equal food ingestion, IF animals maintained lower weights compared to animals fed ad libitum (Fig. 1), but with an interesting characteristic: abdominal fat deposits and adiponectin levels in long-term IF animals were equal to those of AL. It should be stressed that our studies involved obesity-prone Sprague–Dawley rats, previously used in IF protocols [38,39], and that further studies are necessary to determine if the results obtained here would also occur in other animal models. Despite this limitation, the use of obesity-prone animals is interesting as a model, considering human tendencies toward weight gain. In this sense, it is interesting to note that our study shows that weight loss on a restricted diet can be deceptive as a sole measurement and can occur in the presence of high abdominal fat levels and low adiponectin, risk factors in metabolic diseases associated with aging such as diabetes [40,41].

Short-term effects of CR and IF on glucose tolerance were similar and involved more favorable glucose clearance, enhanced IR expression, and phosphorylation. CR has been widely shown to promote glucose tolerance [42,43], and some short-term IF studies present similar results [44,45], even when animals were maintained on the diet for 6 months [39]. Surprisingly, however, we found that the long-term (8 months) effects of CR and IF were quite different. Only CR prevented increments in fasting glucose levels in aged rats and improved the response in glucose tolerance tests (Fig. 2). In fact, IF animals presented glucose intolerance relative to AL, as indicated by tolerance tests and hyperglycemia after feeding. Although this finding was surprising, it does have a precedent: Simon and Rosselin [45] demonstrated that glucose and insulin levels fluctuate largely in IF and can be reduced during the fasting period, but significantly increased during feeding, compared to AL animals. In this particular study, we chose to measure parameters in all animals when fasted for 12 h after a typical feeding period (see a full description under Experimental procedures), to analyze the animals under comparable conditions, which should reflect the effects of the diet on overall metabolic alterations relative to the specific feeding status.

Despite glucose intolerance in IF, phospho-Tyr-IR levels were increased in all diets (Fig. 3), demonstrating that glucose clearance did not mirror IR phosphorylation in response to insulin in FR and IF rats. Interestingly, whereas IR phosphorylation levels were not compatible with physiological measurements of glucose clearance in animals on long-term dietary interventions, IRS1 phosphorylation levels were, presenting significant increases in CR and decreases in IF relative to AL (Fig. 5). In view of this result, we speculated that in IF, and to a lesser extension in FR, IR receptors are not functionally controlled solely in response to phosphorylation levels.

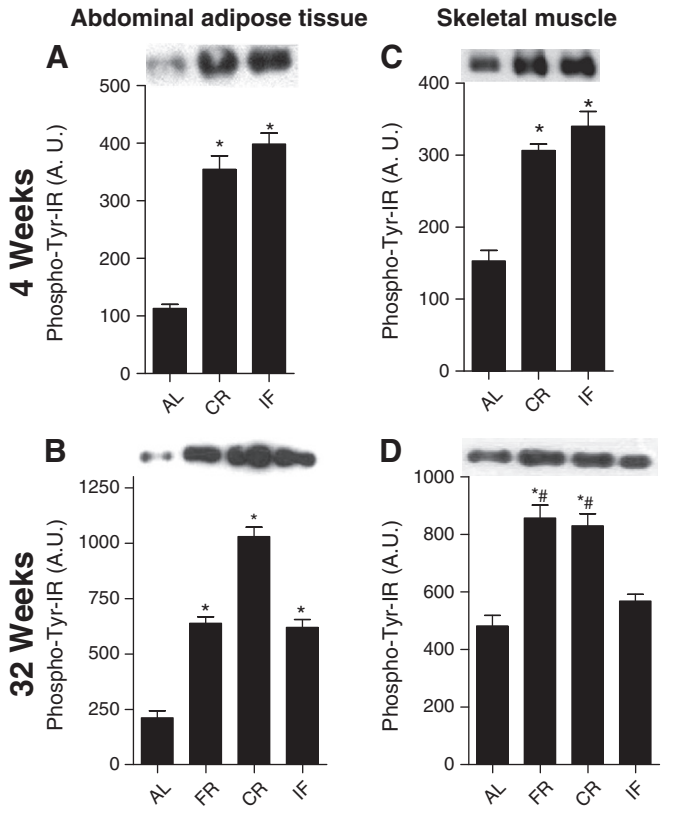

Fig. 3. FR, CR, and IF increase insulin receptor phosphorylation levels. IR from muscle and intra-abdominal adipose tissue was immunoprecipitated and blotted. Typical blots are shown above the average densitometric results. Phospho-Tyr-IR levels in intra-abdominal adipose tissue from rats in the (A) short- and (B) long-term dietary interventions and phospho-Tyr-IR in skeletal muscle from rats in the (C) short- and (D) long-term dietary interventions are shown. $^{*}p<0.05$ vs control; $^{\#}p<0.05$ vs IF, $n=4$.

A known modification that impairs IR function is tyrosine nitration [27–32], which has been previously observed in animals fed a high-fat diet [29]. We propose that phospho-Tyr sites coexist with NO_2-Tyr and that the concerted effect of both modifications determines IRS1 phosphorylation and glucose clearance. Indeed, we found that, whereas NO_2-Tyr-IR was virtually undetectable in short-term-treated animals (results not shown), older animals accumulate NO_2-Tyr-IR significantly in a manner prevented by CR (Fig. 4). IF animals exhibited large quantities of NO_2-Tyr-IR in both insulin-sensitive tissues analyzed, and FR led to an accumulation of the modified receptor in the skeletal muscle. Thus, in animals on long-term interventions, nitration of the IR

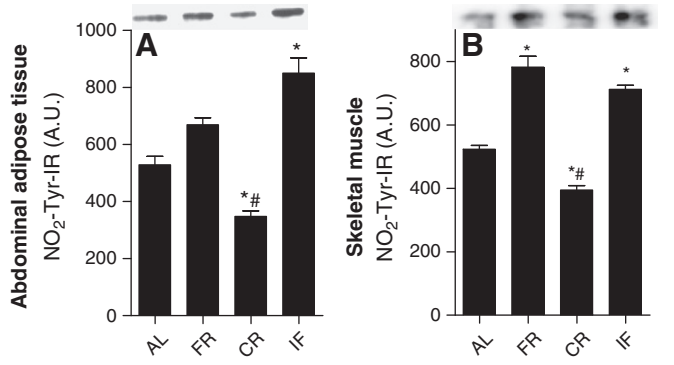

Fig. 4. IR nitration is prevented by long-term CR and enhanced by FR and IF. IR from the (A) intra-abdominal adipose tissue and (B) skeletal muscle of animals 32 weeks on the dietary interventions were immunoprecipitated and blotted. Typical blots are shown above the average densitometric results. $^{*}p<0.05$ vs control; $^{\#}p<0.05$ vs IF, $n=4$.

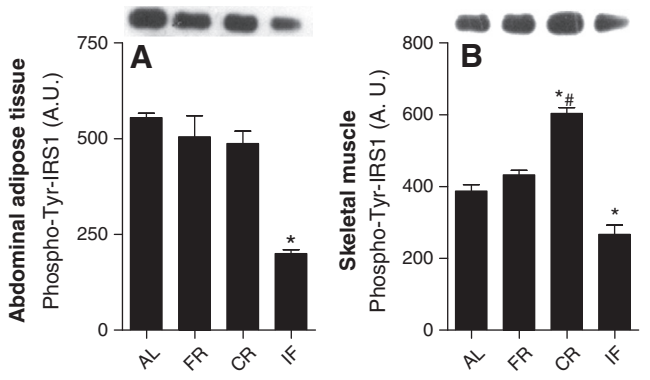

Fig. 5. IRS1 phosphorylation is enhanced by long-term CR, but decreased in IF. The IRS1 from the (A) intra-abdominal adipose tissue and (B) skeletal muscle of animals 32 weeks on the dietary interventions was immunoprecipitated and blotted for phospho-Tyr. Typical blots are shown above the average densitometric results. $^{*}p<0.05$ vs control; $^{\#}p<0.05$ vs IF, $n=4$.

is modified by the dietary protocol and, in concerted action with IR phosphorylation, can determine the activation of the downstream pathway and glucose clearance.

We conducted further experiments to determine why the dietary interventions differ in promoting IR nitration over time. Nitration is promoted by peroxynitrite, a product of nitric oxide and superoxide radicals [32]. We measured increases in eNOS phosphorylation and iNOS expression, but found that overall there was no IF- and FR-specific increase in these nitric-oxide generating systems (Fig. 6).

On the other hand, H_2O_2 release rates (Fig. 6) from both tissues closely resembled nitration patterns (Fig. 4) and were strikingly enhanced in IF. H_2O_2 release from tissues reflects overall production of this ROS versus its removal and was used as a general marker of redox state in our study because of difficulties in measuring superoxide radicals in situ in animal tissues [46]. Confirming that IF causes redox imbalance, we found that IF animals presented significantly higher oxidized glutathione levels (4939 ± 396 pmol mg protein^{-1}) than AL animals (1942 ± 648 pmol mg protein^{-1}, methods used are described in the supplementary material). Interestingly, enhanced production of ROS in IF promotes mainly oxidative modifications in proteins. IF did not increase levels of malondialdehyde, a product of lipid oxidation, relative to CR diet (results not shown, methods in supplementary materials), but resulted in strikingly higher levels of IR modification (Fig. 4) and protein carbonylation (Supplementary Fig. 3).

The opposite results of CR and IF with regard to ROS release and oxidative modifications of proteins are particularly worrisome because IF is often considered equivalent to CR in studies uncovering the impact of dietary restriction on aging [5]. On the other hand, our results show that from a redox standpoint, these diets are very distinct. Indeed, we are unaware of any other dietary intervention capable of increasing tissue ROS release under physiological conditions at this magnitude.

Overall, we find that long-term FR, CR, and IF promote different changes in energy metabolism and redox states, parameters strongly associated with life-span extension [3,4]. CR is clearly the most beneficial intervention in terms of maintaining glucose tolerance, increasing antioxidant defenses, and preventing the release of ROS from tissues. FR presents some of the benefits of CR, although the redox balance is not as favorable, possibly because of micronutrient malnutrition [5]. On the other hand, long-term IF unexpectedly leads to glucose intolerance and strongly increases ROS release rates compared to AL. This is, to our knowledge, the first report that a restrictive dietary intervention can have a negative effect on glucose tolerance associated with oxidative modifications of the IR and suggests that frequent feeding/fasting cycles may be a risk factor for age-associated obesity and insulin resistance leading to diabetes. Furthermore, the differences between CR and IF indicate that, unlike daily

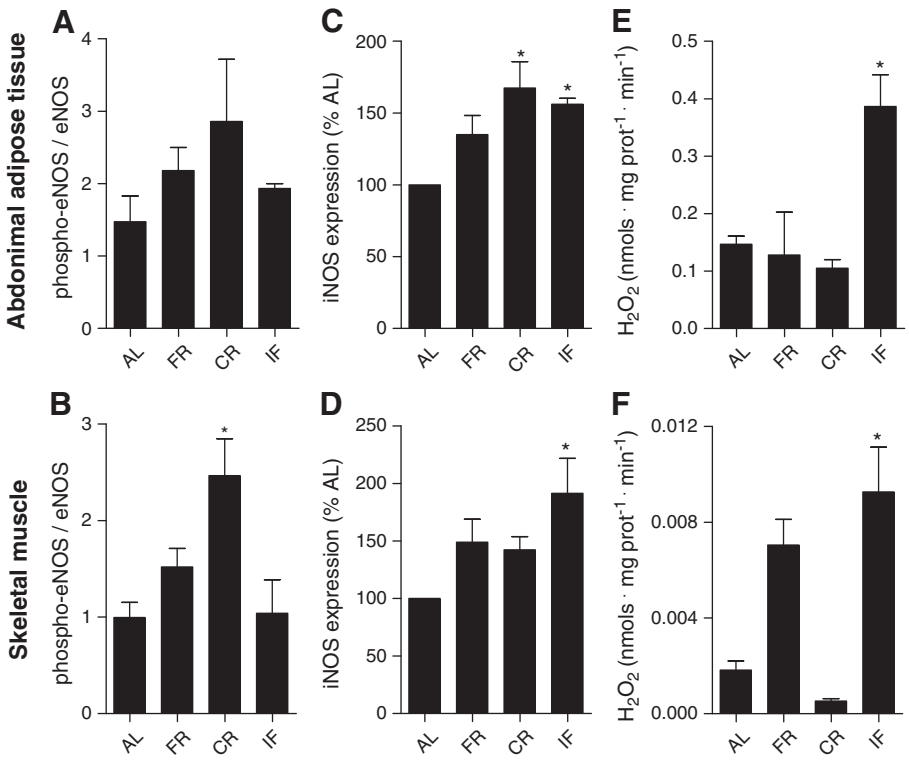

Fig. 6. Long-term IF leads to enhanced tissue reactive oxygen species release. Densitometric analysis of (A) intra-abdominal adipose tissue and (B) skeletal muscle phospho-eNOS^{Ser1177}/eNOS, densitometric analysis of (C) intra-abdominal adipose tissue and (D) skeletal muscle iNOS expression, and (E) intra-abdominal adipose tissue and (F) skeletal muscle H_2O_2 release rates are shown. $^*p<0.05$ vs control, $n=8$.

limitations of caloric intake, alternating feeding and starvation cycles in laboratory animals probably constitute an unhealthy long-term dietary intervention.

Acknowledgments

The authors are in debt to Silvania M.P. Neves, Renata S. Fontes, Flavia M.P. Ong, and Maria de Fátima Rodrigues for excellent animal care. This work was supported by grants from the Fundação de Amparo à Pesquisa do Estado de São Paulo, Instituto Nacional de Ciência e Tecnologia de Processos Redox em Biomedicina, Conselho Nacional de Desenvolvimento Científico e Tecnológico, Coordenação de Aperfeiçoamento do Pessoal de Nível Superior, and John Simon Guggenheim Memorial Foundation.

Appendix A. Supplementary data

Supplementary data to this article can be found online at doi:10.1016/j.freeradbiomed.2011.07.006.

References

[1] McCay, C. M. The effect of retarded growth upon the length of life and upon ultimate size. *J. Nutr.* **10:**63–79; 1935.
[2] Blagosklonny, M. V.; Campisi, J.; Sinclair, D. A.; Bartke, A.; Blasco, M. A.; Bonner, W. M.; Bohr, V. A.; Brosh Jr., R. M.; Brunet, A.; Depinho, R. A.; Donehower, L. A.; Finch, C. E.; Finkel, T.; Gorospe, M.; Gudkov, A. V.; Hall, M. N.; Hekimi, S.; Helfand, S. L.; Karlseder, J.; Kenyon, C.; Kroemer, G.; Longo, V.; Nussenzweig, A.; Osiewacz, H. D.; Peeper, D. S.; Rando, T. A.; Rudolph, K. L.; Sassone-Corsi, P.; Serrano, M.; Sharpless, N. E.; Skulachev, V. P.; Tilly, J. L.; Tower, J.; Verdin, E.; Vijg, J. Impact papers on aging in 2009. *Aging* **3:** 111–121; 2010.
[3] Partridge, L.; Gems, D. Mechanisms of ageing: public or private? *Nat. Rev. Genet.* **3:** 165–175; 2002.
[4] Sohal, R. S.; Weindruch, R. Oxidative stress, caloric restriction, and aging. *Science* **273:** 59–63; 1996.
[5] Cerqueira, F. M.; Kowaltowski, A. J. Commonly adopted caloric restriction protocols often involve malnutrition. *Ageing Res. Rev.* **7:**552–560; 2010.
[6] Anson, R. M.; Jones, B.; de Cabo, R. The diet restriction paradigm: a brief review of the effects of every-other-day feeding. *Age* **27:**17–25; 2005.
[7] Boily, G.; Seifert, E. L.; Bevilacqua, L.; He, X. H.; Sabourin, G.; Estey, C.; Moffat, C.; Crawford, S.; Saliba, S.; Jardine, K.; Xuan, J.; Evans, M.; Harper, M. E.; McBurney, M. W. SirT1 regulates energy metabolism and response to caloric restriction in mice. *PLoS One* **12:**e1759; 2008.
[8] Bonelli, M. A.; Desenzari, S.; Cavallini, G.; Donati, A.; Romani, A. A.; Bergamini, E.; Borghetti, A. F. Low-level caloric restriction rescues proteasome activity and Hsc70 level in liver of aged rats. *Biogerontology* **9:**1–10; 2008.
[9] Mager, D. E.; Wan, R.; Brown, M.; Cheng, A.; Wareski, P.; Abernethy, D. R.; Mattson, M. P. Caloric restriction and intermittent fasting alter spectral measures of heart rate and blood pressure variability in rats. *FASEB J.* **20:**631–637; 2006.
[10] Duffy, P. H.; Lewis, S. M.; Mayhugh, M. A.; McCracken, A.; Thorn, B. T.; Reeves, P. G.; Blakely, S. A.; Casciano, D. A.; Feuers, R. J. Effect of the AIN-93 M purified diet and dietary restriction on survival in Sprague–Dawley rats. *J. Nutr.* **132:**101–107; 2002.
[11] Goodrick, C. L.; Ingram, D. K.; Reynolds, M. A.; Freeman, J. R.; Cider, N. Effects of intermittent feeding upon body weight and life span in inbred mice: interaction of genotype and age. *Mech. Ageing Dev.* **55:**69–87; 1990.
[12] Keenan, K. P.; Laroque, P.; Ballam, G. C.; Soper, R.; Dixit, R.; Mattson, B. A.; Adams, S. P.; Coleman, J. B. The effects of diet, ad lib overfeeding, and moderate dietary restriction on the rodent bioassay. *Toxicol. Pathol.* **24:**757–768; 1996.
[13] Pearson, K. J.; Baur, J. A.; Lewis, K. N.; Peshkin, L.; Price, N. L.; Labinskyy, N.; Swindell, W. R.; Kamara, D.; Minor, R. K.; Perez, E.; Jamieson, H. A.; Zhang, Y.; Dunn, S. R.; Sharma, K.; Pleshko, N.; Woollett, L. A.; Csiszar, A.; Ikeno, Y.; Le Couteur, D.; Elliott, P. J.; Becker, K. G.; Navas, P.; Ingram, D. K.; Wolf, N. S.; Ungvari, Z.; Sinclair, D. A.; de Cabo, R. Resveratrol delays age-related deterioration and mimics transcriptional aspects of dietary restriction without extending lifespan. *Cell Metab.* **8:**157–168; 2008.
[14] Valle, A.; Guevara, R.; García-Palmer, F. J.; Roca, P.; Oliver, J. Caloric restriction retards the age related decline in mitochondrial function of brown adipose tissue. *Rejuvenation Res.* **11:**597–604; 2008.
[15] Pugh, T. D.; Klopp, R. G.; Weindruch, R. Controlling caloric consumption: protocols for rodents and rhesus monkeys. *Neurobiol. Aging* **20:**157–165; 1999.
[16] Hayashi, H.; Yamaza, H.; Komatsu, T.; Park, S.; Chiba, T.; Higami, Y.; Nagayasu, T.; Shimokawa, I. Calorie restriction minimizes activation of insulin signaling in response to glucose. *Exp. Gerontol.* **43:**827–832; 2008.
[17] Lambert, A. J.; Merry, B. J. Effect of caloric restriction on mitochondrial reactive oxygen species production and bioenergetics. *Am. J. Physiol.* **286:**R71–R79; 2004.
[18] Merry, B. Oxidative stress and mitochondrial function with aging—the effects of calorie restriction. *Aging Cell* **3:**7–12; 2004.
[19] Marzetti, E.; Wohlgemuth, S. E.; Anton, S. D.; Bernabei, R.; Carter, C. S.; Leewenburgh, C. Cellular mechanisms of cardioprotection by calorie restriction. *Clin. Geriatr. Med.* **25:**715–732; 2009.
[20] Mahadev, K.; Motoshima, H.; Wu, X.; Russy, M. J.; Arnold, R. S.; Cheng, G.; Lambeth, J. D.; Goldstein, B. J. The NAD(P)H oxidase homolog Nox4 modulates

insulin-stimulated generation of H_2O_2 and plays an integral role in insulin signal transduction. *Mol. Cell. Biol.* **24:**1844–1854; 2004.
[21] Ristow, M.; Zarse, K.; Oberbach, A.; Klöting, N.; Birringer, M.; Michael, K.; Stumvoll, M.; Kahn, R. C.; Blüher, M. Antioxidants prevent health-promoting effects of physical exercises in humans. *Proc. Natl. Acad. Sci. USA* **106:**8665–8670; 2009.
[22] Ceriello, A.; Motz, E. Is the oxidative stress the pathogenic mechanism underlying insulin resistance, diabetes, and cardiovascular disease? The common soil hypothesis revisited. *Arterioscler. Thromb. Vasc. Biol.* **24:**816–823; 2004.
[23] Evans, J. L.; Goldfine, I. D.; Maddux, B. A.; Grodsky, G. M. Oxidative stress and stress-activated signaling pathways: a unifying hypothesis of type 2 diabetes. *Endrocr. Rev.* **23:**599–622; 2002.
[24] De Campos, K. E.; Sinzato, Y. K.; Pimenta, W. de P.; Rugde, M. V. C.; Damasceno, D. C. Effect of maternal obesity on diabetes development in adult rat offspring. *Life Sci.* **81:**1473–1478; 2007.
[25] Zhou, M.; Diwu, Z.; Panchuk-Voloshina, N.; Haugland, R. P. A stable nonfluorescence derivative of resorufin for the fluorimetric determination of trace hydrogen peroxide: applications in detecting the activity of phagocyte NADPH oxidase and other oxidases. *Anal. Biochem.* **253:**162–168; 1997.
[26] Masaki, T.; Chiba, S.; Yasuda, T.; Tsubone, T.; Kakuma, T.; Shimomura, I.; Funahashi, T.; Matsuzawa, Y.; Yoshimatsu, H. Peripheral, but not central, administration of adiponectin reduces intra-abdominal adiposity and upregulates the expression of uncoupling protein in agouti yellow (Ay/a) obese mice. *Diabetes* **52:**2266–2273; 2003.
[27] Carpenter, F. H.; Boesel, R. W.; Sakai, D. D. Tetrakis(3-nitrotyrosine)insulin. *Biochemistry* **19:**5926–5931; 1980.
[28] Morris, J. W. S.; Mercola, D. A.; Arquilla, E. R. Preparation and properties of 3-nitrotyrosine insulins. *Biochemistry* **9:**3930–3937; 1970.
[29] Duplain, H.; Sartori, C.; Dessen, P.; Jayet, P. Y.; Schwab, M.; Bloch, J.; Nicod, P.; Scherrer, U. Stimulation of peroxynitrite catalysis improves insulin sensitivity in high fat diet-fed mice. *J. Physiol.* **586:**4011–4016; 2008.
[30] Zhou, J.; Huang, K. Peroxynitrite mediates muscle insulin resistance in mice via nitration of IRβ/IRS-1 and Akt. *Toxicol. Appl. Pharmacol.* **241:**101–110; 2009.
[31] Charbonneau, A.; Marette, A. Inducible nitric oxide synthase induction underlies lipid-induced hepatic insulin resistance in mice: potential role of tyrosine nitration of insulin signaling proteins. *Diabetes* **59:**861–871; 2010.
[32] Ischiropoulos, H.; Zhu, L.; Chen, J.; Tsai, J. H. M.; Martin, J. C.; Smith, C. D.; Beckman, J. S. Peroxynitrite-mediated tyrosine nitration catalyzed by superoxide dismutase. *Arch. Biochem. Biophys.* **298:**431–437; 1992.
[33] Nisoli, E.; Clementi, E.; Tonello, C.; Sciorati, C.; Briscini, L.; Carruba, M. O. Effects of nitric oxide on proliferation and differentiation of rat brown adipocytes in primary cultures. *Br. J. Pharmacol.* **125:**888–894; 1998.
[34] Nisoli, E.; Clementi, E.; Paolucci, C.; Cozzi, V.; Tonello, C.; Sciorati, C.; Bracale, R.; Valerio, A.; Francolini, M.; Moncada, S.; Carruba, M. O. Mitochondrial biogenesis in mammals: the role of endogenous nitric oxide. *Science* **299:**896–899; 2003.
[35] Cerqueira, F. M.; Laurindo, F. R.; Kowaltowski, A. J. Mild mitochondrial uncoupling and calorie restriction increase fasting eNOS, akt and mitochondrial biogenesis. *PLoS One* **6:**e18433; 2011.
[36] Kowaltowski, A. J.; de Souza-Pinto, N. C.; Castilho, R. F.; Vercesi, A. E. Mitochondria and reactive oxygen species. *Free Radic. Biol. Med.* **47:**333–343; 2009.
[37] Caro, J.; López-Torres, M.; Sánchez, I.; Naudi, A.; Portero-Otín, M.; Pamplona, R.; Barja, G. Effect of every other day feeding on mitochondrial free radical production and oxidative stress in mouse liver. *Rejuvenation Res.* **74:**621–629; 2008.
[38] Martin, B.; Pearson, M.; Brenneman, R.; Golden, E.; Keselman, A.; Iyun, T.; Carlson, O. D.; Egan, J. M.; Becker, K. G.; Wood III, W.; Prabhu, V.; de Cabo, R.; Maudsley, S.; Mattson, M. P. Conserved and differential effects of dietary energy intake on the hippocampal transcriptomes of females and males. *PLoS One* **3:**e2398; 2008.
[39] Martin, B.; Pearson, M.; Kebejian, L.; Golden, E.; Keselman, A.; Bender, M.; Carlson, O.; Egan, J.; Ladenheim, B.; Cadet, J. L.; Becker, K. G.; Wood, W.; Duffy, K.; Vinayakumar, P.; Maudsley, S.; Mattson, M. P. Sex-dependent metabolic, neuroendocrine, and cognitive responses to dietary energy restriction and excess. *Endocrinology* **148:**4318–4333; 2007.
[40] Yatagai, T.; Nagasaka, S.; Taniguchi, A.; Fukushima, M.; Nakamura, T.; Kuroe, A.; Nakai, Y.; Ishibashi, S. Hypoadiponectinemia is associated with visceral fat accumulation and insulin resistance in Japanese men with type 2 diabetes mellitus. *Metabolism* **52:**1274–1278; 2003.
[41] Matsuzawa, Y. The metabolic syndrome and adipocytokines. *FEBS Lett.* **580:** 2917–2921; 2006.
[42] Wang, Z. Q.; Floyd, Z. E.; Qin, J.; Liu, X.; Yu, Y.; Zhang, X. H.; Wagner, J. D.; Cefalu, W. T. Modulation of skeletal muscle insulin signaling with chronic caloric restriction in cynomolgus monkeys. *Diabetes* **59:**1488–1498; 2009.
[43] Zhu, M.; de Cabo, R.; Anson, R. M.; Ingram, D. K.; Lane, M. A. Caloric restriction modulates insulin receptor signaling in liver and skeletal muscle of rat. *Nutrition* **21:** 378–388; 2005.
[44] Anson, R. M.; Guo, Z.; de Cabo, R.; Lyun, T.; Rios, M.; Hagepanos, A.; Ingram, D. K.; Lane, M. A.; Mattson, M. P. Intermittent fasting dissociates beneficial effects of dietary restriction on glucose metabolism and neuronal resistance to injury from calorie intake. *Proc. Natl. Acad. Sci. USA* **100:**6216–6220; 2003.
[45] Simon, J.; Rosselin, G. Effect of intermittent feeding on glucose–insulin relationship in the chicken. *J. Nutr.* **109:**631–641; 1979.
[46] Wardman, P. Fluorescent and luminescent probes for measurement of oxidative and nitrosative species in cells and tissues: progress, pitfalls, and prospects. *Free Radic. Biol. Med.* **43:**995–1022; 2007.

Experimental Dermatology ADF

Bioenergetic Profiling in the Skin

Journal:	*Experimental Dermatology*
Manuscript ID:	EXD-15-0175.R1
Manuscript Type:	Methods Letter to the Editors
Date Submitted by the Author:	n/a
Complete List of Authors:	Forni, Maria Fernanda Chausse, Bruno Peloggia, Julia Kowaltowski, Alicia; Universidade de São Paulo, Departamento de Bioquímica
Keywords:	bioenergetic profiling, mitochondrial isolation, epidermis, dermis, respiratory rates

Experimental Dermatology Letter to Editor

Title: Bioenergetic Profiling in the Skin

Authors:

Maria Fernanda Forni [1]

Bruno Chausse [1]

Julia Peloggia [1]

Alicia J. Kowaltowski [1*]

Affiliation:

[1]Departamento de Bioquímica, Instituto de Química, Universidade de São Paulo. Avenida Prof. Lineu Prestes, 748 sala 1065, bloco 10 superior, 05508-900, São Paulo, SP, Brazil

***Corresponding Author:** e-mail: alicia@iq.usp.br

Conflict of interest

The authors declare no conflict of interest

Acknowledgments

The authors are in debt to Silvania M.P. Neves, Renata S. Fontes, Flavia M.P. Ong, and Maria de Fátima Rodrigues for animal care, and Camille C. Caldeira da Silva and Edison Alves Gomes for technical support. Funded by *Fundação de Amparo à Pesquisa do Estado de São Paulo* (FAPESP, 10/51906-1, 13/04871-6, 14/17270-3), *Centro de Pesquisa, Inovação e Difusão de Processos Redox em Biomedicina* (13/07937-8), Núcleo de Pesquisa em Processos Redox em Biomedicina (NAP-Rexodoma), Instituto Nacional de Ciência e Technologia de Processos Redox em Biomedicina (INCT Redoxoma) and *Conselho Nacional de Pesquisa e Desenvolvimento* (CNPq, 153560/2011-8, 302898/2013-1).

Background

The skin is a large organ which presents important thermoregulatory and metabolic functions (1,2), and should thus be a focus of studies involving energy metabolism. Nevertheless, bioenergetic studies in epithelia-containing organs such as the skin are rare (3,4), probably due to difficulties in organelle isolation (5) or *in situ* studies in these tissues, added to the lack of published protocols. Furthermore, the skin is subdivided into two tissues: the dermis and the epidermis, as is typical in the structure of composite organs with an epithelial tissue on top of a mesenchymal layer. Results obtained with whole organ homogenates in composite tissues such as the skin tend to be the average of the individual responses of the different types of cells resident in the tissue (6). It is thus also important to establish techniques that allow for measurements of bioenergetic characteristics in different tissues of the skin.

Questions Addressed

We established techniques to study skin mitochondrial bioenergetics in isolated organelles and *in situ* in different cell types, producing a bioenergetic profile of this tissue.

Experimental Design

Tecniques used are described in detail in the Supplementary Material.

Mitochondrial isolation and oxygen consumption

Mitochondria were isolated from mouse skin samples using an adaptation of standard differential centrifugation methods. Oxygen concentrations and consumption rates (OCR) was measured using Oroboros high-resolution respirometry (3).

Cell isolation, culture and oxygen consumption

The dermis and epidermis of mouse backskins were separated by scraping, and the two tissues were cultured separately. The epidermal fraction consisted mainly of keratinocytes (89% ± 2.2) and the dermal fraction of fibroblasts (88% ± 1.6, Supplementary Table 1). OCR and extracellular

acidification rates (ECAR) were determined using an XF24 extracellular flux analyzer (Seahorse Bioscience).

Results

By adding trypsin digestion and fur-filtering steps to standard differential centrifugation protocols, we were able to isolate highly functional mitochondria from murine whole skin samples. Fig. 1 shows a typical oxygen tension trace (Panel A) and quantified ADP-maximized OCR (Panel B) supported by different respiratory substrates (NADH-linked pyruvate and malate, complex II electron donor succinate and Complex IV electron donor TMPD). The relative contribution of each respiratory complex was uncovered using specific inhibitors: rotenone for Complex I and antimycin A for Complex III. Skin mitochondria respire well both with pyruvate plus malate or succinate as substrates.

To assess the quality of the preparations, we measured respiration in the presence and absence of ATP synthesis (7). Figs. 1C and 1D indicate that skin mitochondria are highly coupled, presenting a large increase in OCR when ADP is added, in a manner inhibited by oligomycin, an ATP synthase inhibitor. The respiratory control ratio was on average 4.39, a value similar to that obtained in preparations from mesenchymal tissues (7) and indicating that integrity was maintained. The addition of the protonophore CCCP stimulated the oligomycin-inhibited OCR, further indicating that these mitochondria were fully coupled. Overall, we find that the method described provides adequate quantities of high quality mitochondria.

Although it is useful to study many mitochondrial characteristics, isolation of this organelle from the whole skin does not adequately assess differences that may exist between the tissues that the skin is composed of. Thus, we also measured mitochondrial bioenergetics in intact cells isolated from the epidermis and dermis using extracellular flux measurements (8). Figure 2A shows typical *in situ* bioenergetic measurements. The basal OCR, which represents O_2 consumption under physiological conditions, was substantially higher in the dermis (Fig 2B), indicating that these cells present a more respiratory phenotype than epidermal cultures. After oligomycin was added, a decrease in basal respiration proportional to ATP-generating mitochondrial activity is observed (Fig. 2A). Dermal cells displayed higher ATP production-dependent OCR (Fig. 2C), suggesting that epidermal cells rely more on glycolysis. Extracellular acidification (ECAR) was significantly higher in the epidermis than in the dermis (Fig. 2H), corroborating the suggestion that the epidermis has higher glycolytic activity than the dermis. CCCP-stimulated maximal respiration is higher in the dermis (Fig. 2D), but no significant changes were evident in the reserve capacity, or the difference between basal and

maximal respiration (Fig. 2E). This leads to the speculation that, when challenged, both tissues are equally capable of responding with increased respiration to compensate for a higher ATP demand (8). The proton leak across the inner membrane, estimated in the presence of oligomycin, was significantly increased in the epidermis (Fig. 2F). To determine the extent of non-mitochondrial oxygen consumption, the respiratory chain was inhibited with antimycin A and rotenone. This non-mitochondrial OCR was subtracted from all rates calculated previously, is linked to the activity of non-mitochondrial oxidases present in the cell, and was increased in the dermis (Fig. 2G).

Conclusions

Overall, our data show that it is possible to reliably measure mitochondrial characteristics as isolated organelles and *in situ*, both in the dermis and epidermis, which present distinctive bioenergetic profiles. The same experimental approaches can be adapted for human skin explants and help elucidate metabolic alterations associated with clinical conditions of the skin.

Figure Legends

Figure 1: Isolated skin mitochondrial respiration. Mitochondria (0.25 mg/mL) were incubated as described in the Supplementary Methods and oxygen tensions were followed over time. **(A)** Oxygen consumption maximized by ADP. Pyruvate plus malate, rotenone, succinate, antimycin A and TMPD plus ascorbate were added where indicated. **(B)** OCR from experiments such as those depicted in Panel A. **(C)** Oxygen consumption measured in different respiratory states. Pyruvate and malate, ADP, oligomycin and CCCP were added where indicated. **(D)** Quantification of experiments such as those in panel C.

Figure 2: Bioenergetic profile of primary dermis and epidermis cultures. Cells (60,000 per well) were treated with respiratory inhibitors and uncoupler, at the concentrations described in the Supplementary Methods. **(A)** OCR from dermal (□) and epidermal (•) cells. Oligomycin, CCCP and Antimycin A plus rotenone were added where indicated. **(B)** Basal OCR, **(C)** ATP production-dependent OCR, **(D)** Maximal OCR, **(E)** Spare respiratory capacity, **(F)** H^+ leakiness and **(G)** Non-mitochondrial respiration calculated from experiments such as those depicted in Panel A, as described in the Supplementary Methods. **(H)** Extracellular acidification rate (ECAR). *$p \leq 0.05$; **$p < 0.001$.

References

1. Fuchs E, Raghavan S Getting under the skin of epidermal morphogenesis. Nat Rev Genet 2002: 3: 199-209.
2.Forni M F, Trombetta-Lima M, Sogayar M C Stem cells in embryonic skin development. Biol Res 2012: 45: 215-222.
3. Hutter E, Unterluggauer H, Garedew A *et al.* High-resolution respirometry-a modern tool in aging research. Exp Gerontol 2006: 41: 103-109.
4. Gerencser A A, Neilson A, Choi S W, *et al.* Quantitative microplate-based respirometry with correction for oxygen diffusion. Anal Chem 2009: 81: 6868-6878.
5. Nicholls D G, Ferguson S J Bioenergetics 4. In: Bioenergetics 2013: 1-419.
6. Schubert C Single-cell analysis: The deepest differences. Nature 2011: 480: 133-137.
7. Tahara E B, Navarete F D, Kowaltowski A J Tissue-, substrate-, and site-specific characteristics of mitochondrial reactive oxygen species generation. Free Radic Biol Med 2009: 46: 1283-1297.
8. Brand M D, Nicholls D G Assessing mitochondrial dysfunction in cells. Biochem J 2011: 435: 297-312.

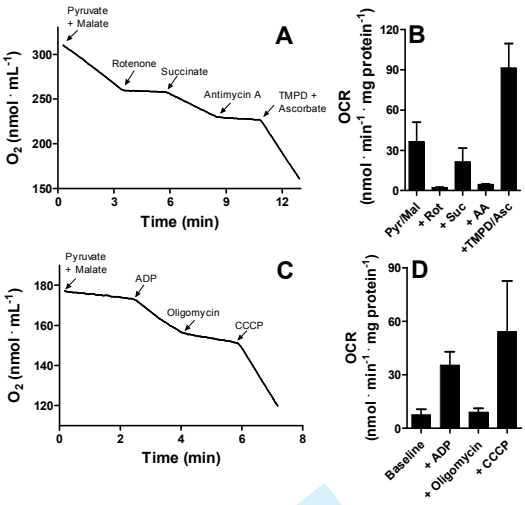

Forni et al., 2015, Fig. 1

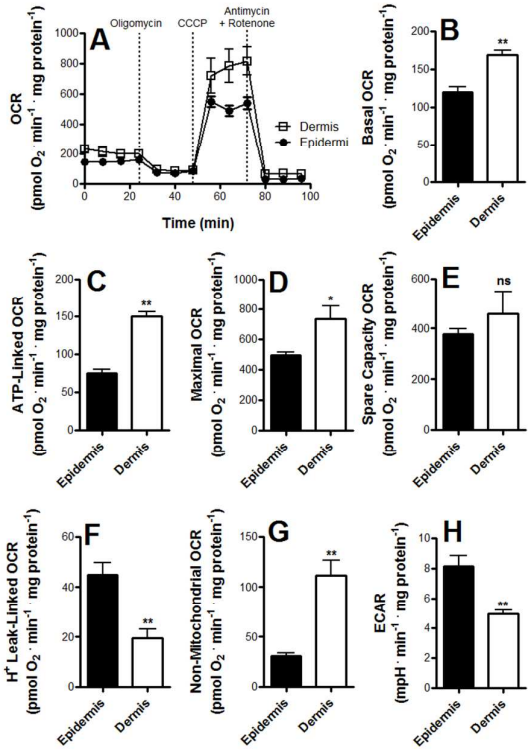

Forni et al., 2015, Fig. 2

Supplementary Material - Experimental Dermatology Letter to Editor

Title: Bioenergetic Profiling in the Skin

Authors:

Maria Fernanda Forni [1]

Bruno Chausse [1]

Julia Peloggia [1]

Alicia J. Kowaltowski [1*]

Affiliations:

[1]Departamento de Bioquímica, Instituto de Química, Universidade de São Paulo. Avenida Prof. Lineu Prestes, 748 sala 1065, bloco 10 superior, 05508-900, São Paulo, SP, Brazil

***Corresponding Author:** e-mail: alicia@iq.usp.br

Complete Experimental Design

Isolation of skin mitochondria

Adapted from reference (16). All experiments were approved by the local animal ethics committee and follow international animal care and use guidelines. After euthanasia by cervical dislocation (the use of anesthetics was avoided due to the effects on membrane ionic permeability), dorsal skins of five female Swiss mice were shaved to remove the fur and separated from contaminant tissues. The resultant skin pool was incubated in 20 mL of 0.25% trypsin-EDTA (Gibco) for 1 hour, at 37ºC. The tissue was finely minced in isolation buffer (250 mM sucrose, 10 mM Hepes, 1 mM EGTA and 0.1% BSA, pH 7.2), at 4°C. All subsequent procedures were conducted over ice. The tissue was processed for 5 s with a Polytron homogenizer and then transferred to a mechanized potter with a Teflon pestle and homogenized. This digestion and suspension procedure was found to provide the highest mitochondrial yield without compromising quality, after multiple trials with different experimental

conditions. The suspension was sifted using a 70 μm cell strainer to remove fur and centrifuged at 2,000 g for 5 min. The supernatant was centrifuged again at 10,000 g for 5 min and the pellet was resuspended and centrifuged again at 10,000 g for 5 min. The final mitochondrial pellet was resuspended in 200 μL of isolation buffer. Protein quantification was conducted using the Bradford method.

Isolated mitochondrial respiration

Respiration was followed using an Oroboros high-resolution respirometry system (17). O_2 consumption was monitored using 0.250 mg protein/mL isolated mitochondrial suspensions in experimental buffer containing 150 mM KCl, 10 mM Hepes, 2 mM KPi, 2 mM $MgCl_2$, and 0.1% BSA (pH 7.2), at 37ºC. Different substrates and respiratory inhibitors were used as described in the figure legend, at the following concentrations: 5 mM pyruvate, 3 mM malate, 1 μM rotenone, 1 mM succinate, 1 μg/mL antimycin A, 200 μM N,N,N′,N′-tetramethyl-p-phenylenediamine (TMPD), 2 mM ascorbate, 1 mM ADP, 0.5 μg/mL oligomycin and 1 μM carbonyl cyanide m-chloro phenyl hydrazone (CCCP). Respiratory control ratios (RCR) were calculated using malate/pyruvate as substrates, by dividing rates in the presence of ADP (state 3 respiration) by respiration in the presence of oligomycin (state 4 respiration).

Cell isolation and culture

The backskins of Swiss mice were washed in 70% ethanol and collected in a sterile environment. Subcutaneous fat was removed from the skin with a scalpel, and the whole skin was placed, dermis down, on 0.25% trypsin-EDTA (Gibco) at 37^{o}C for 1 h. After scraping the epidermis away, single cell suspensions were obtained from both the dermis and epidermis through mechanical dissociation. The dermal cells were then filtered with strainers (70 μm, followed by 40 μm), washed twice with phosphate buffered saline without calcium, pH 7.4 (PBSA), and plated in DMEM (Gibco, Rockville, MD) containing 10% Fetal Bovine Serum (FBS) and 1% ampicilin/streptomycin in adherent flasks. The same procedure was followed for the espidermis and the resulting cells were plated in Keratinocyte Serum Free Medium (KSFM) (Gibco, Rockville, MD), supplemented with Bovine Pituitary Extract (BPE; 50 μg/mL) and Epidermal Growth Factor (EGF; 5 μg/mL), both from Gibco. Cells were maintained at 37^{0}C, with 5% CO_2 and controlled humidity.

Characterization of epidermal and dermal primary cultures

Cells were detached with versene (50 mM EDTA in PBSA, pH 7.4) and fixed with 4% buffered paraformaldehyde for 15 min. After blocking for non-specific binding sites with 2% bovine serum

albumin (BSA) for 1 h at room temperature, the cells were exposed for 1 h to the specific antibodies, namely Pancytokeratin (keratinocytes and epidermal precursors), Vimentin (fibroblasts) and MiTF (melanocytes), all from AbCam and CD3/CD4/CD8 (lymphocytes), CD11b and F4/80 (macrophages), from BD Biosciences at concentrations previously validated ranging from 1:500 to 1:1000. Experiments were performed using an Attune Cytometer. At least 50,000 events/duplicate were recorded (Life Technologies). Negative controls were used and comprised of the same class IgG isotype controls. Compensation and analysis were performed using FlowJo X (TriStar Inc). Results are depicted in Supplementary Table 1.

Intact cell oxygen consumption rate (OCR) and extracellular acidification rate (ECAR) measurements

OCR and ECAR were measured in primary cultures of the epidermis and dermis using an XF24 extracellular flux analyzer (Seahorse Bioscience), as previously described (15). An assay medium composed of 114 mM NaCl, 4.7 mM KCl, 1.2 mM KH_2PO_4, 1.16 mM $MgSO_4$, 2.5 mM $CaCl_2$, pH 7.2, and 2.8 mM glucose was used. The cells were seeded in an XF24 24 well cell culture microplate at 60,000 cells per well (0.32 cm^2 growth area) in 500 µL of growth medium and incubated overnight at 37°C in a humidified atmosphere of 95% air and 5% CO_2. This cell density was chosen because it provided constant and reliable readings, while higher cell densities were found to change cellular differentiation properties, as assessed by filaggrin staining. Wells were checked for homogeneous plating of the cells and eliminated if they presented clumps or uneven areas. Prior to the assays, the growth medium was replaced by 500 µL of assay medium for 1 h at 37°C without CO_2 in the air. H^+ leak-linked and ATP production-linked OCR were determined by the addition of oligomycin (5 µg/mL), which inhibits the ATP synthase. After 3 measurement cycles, 4 µM of the uncoupler CCCP was added to determine maximal respiratory capacity. After a further 3 measurement cycles, 1 µM rotenone in addition to 1 µM antimycin A were added to ablate mitochondrial oxygen consumption. After each experiment, the plate was retrieved, washed with PBSA, and the protein content of each well was estimated after lysis in RIPA+ buffer through the Bradford methodology.

Statistical analysis

Data were analyzed using GraphPad Prism and Origin software. Figures represent averages ± SEM of 3-12 measurements consisting of four individual mice in each experiment and were compared using ANOVA. Two-tailed p values under 0.05 were considered significant.

Supplementary References

1. Fuchs E, Raghavan S Getting under the skin of epidermal morphogenesis. Nat Rev Genet 2002: 3: 199-209.
2. Schneider M R, Schmidt-Ullrich R, Paus R The hair follicle as a dynamic miniorgan. Curr Biol 2009: 19: 132-142.
3. Watt F M Mammalian skin cell biology: at the interface between laboratory and clinic. Science 2014: 346: 937-940.
4. Driskell R R, Watt F M Understanding fibroblast heterogeneity in the skin. Trends Cell Biol 2015: 25: 92-99.
5. Koster M I, Roop D R Mechanisms regulating epithelial stratification. Annu Rev Cell Dev Biol 2007: 23: 93-113.
6. Oroboros Instrument wiki: Applications. http://wiki.oroboros.at/index.php/O2k-Publications: Topics. pp. Compilation of articles published in the bioenergetic area.
7. Seahorse Biosciences Applications http://www.seahorsebio.com/applications/overview.php. pp. Compilation of articles published with the Seahorse Apparatus.
8. Nicholls D G, Ferguson S J Bioenergetics 4. In: Bioenergetics 2013: 1-419.
9. Casasnovas C, Banchs I, Cassereau J *et al.* Phenotypic spectrum of MFN2 mutations in the Spanish population. J Med Genet 2010: 47: 249-256.
10. Konieczny P, Fuchs P, Reipert S *et al.* Myofiber integrity depends on desmin network targeting to Z-disks and costameres via distinct plectin isoforms. J Cell Biol 2008: 181: 667-681.
11. Kunz D, Luley C, Fritz S *et al.* Oxygraphic evaluation of mitochondrial function in digitonin-permeabilized mononuclear cells and cultured skin fibroblasts of patients with chronic progressive external ophthalmoplegia. Biochem Mol Med 1995: 54: 105-111.
12. Nochez Y, Arsene S, Gueguen N *et al.* Acute and late-onset optic atrophy due to a novel OPA1 mutation leading to a mitochondrial coupling defect. Molecular Vision 2009: 15: 598-608.
13. Vielhaber S, Winkler K, Kirches E *et al.* Visualization of defective mitochondrial function in skeletal muscle fibers of patients with sporadic amyotrophic lateral sclerosis. J Neurol Sci 1999: 169: 133-139.
14. Schubert C Single-cell analysis: The deepest differences. Nature 2011: 480: 133-137.
15. Forni M F, Trombetta-Lima M, Sogayar M C Stem cells in embryonic skin development. Biol Res 2012: 45: 215-222.
16. Tahara E B, Navarete F D, Kowaltowski A J Tissue-, substrate-, and site-specific characteristics of mitochondrial reactive oxygen species generation. Free Radic Biol Med 2009: 46: 1283-1297.
17. Hutter E, Unterluggauer H, Garedew A *et al.* High-resolution respirometry-a modern tool in aging research. Exp Gerontol 2006: 41: 103-109.
18. Brand M D, Nicholls D G Assessing mitochondrial dysfunction in cells. Biochem J 2011: 435: 297-312.
19. Green H, Kehinde O, Thomas J Growth of cultured human epidermal-cells into multiple epithelia suitable for grafting. Proc Nat Acad Sci USA 1979: 76: 5665-5668.
20. Frisch S M, Francis H Disruption of epithelial cell-matrix interactions induces apoptosis. J Cell Biol 1994: 124: 619-626.
21. Balda M S, Garrett M D, Matter K The ZO-1-associated Y-box factor ZONAB regulates epithelial cell proliferation and cell density. J Cell Biol 2003: 160: 423-432.
22. Gordillo G M, Sen C K Revisiting the essential role of oxygen in wound healing. Am J Surg 2003: 186: 259-263.

Supplementary Table 1 - Immunophenotypic Characterization of Primary Epidermal and Dermal Cultures: The mixed population isolation presented is relative to a mixed population of 5 animals (10^6 cells/point), in duplicate (nd = not detected). All time points were compared to isotypic immunoglobulin controls tagged with the same fluorophore as the antibody of interest.

Specific Marker	Cell Type	% Epidermal Fraction	% Dermal Fraction
Pan-cytokeratin	Keratinocytes/epidermal precursors	89 ± 2.2	nd
Vimentin	Fibroblasts	1.6 ± 0.3	88 ± 1.6
MiTF	Melanocytes	2.2 ± 0.5	1.4 ± 0.4
CD3	Lymphocytes (CD4+CD8)	2.3 ± 0.3	3.2 ± 0.2
CD4	T Lymphocytes	1.8 ± 0.5	1.2 ± 0.7
CD8	T Lymphocytes	nd	2.1 ± 0.5
CD11b	Macrophages	3.4 ± 0.3	4.8 ± 0.5
F4/80	Macrophages (Langerhans cells)	2 ± 0.6	nd

Serum from Calorically-Restricted Animals Enhances Glucose Responses in Insulin-Secreting Cells

Fernanda M. Cerqueira[1,2,3] Bruno Chausse[3], Marc Liesa[2], Orian S. Shirihai[1,2*], Alicia J. Kowaltowski[3]

[1]Department of Medicine, Boston University School of Medicine, USA; [2]Department of Biochemistry, Ben Gurion University, Israel; [3]Departamento de Bioquímica, Universidade de São Paulo, Brazil

*Corresponding author: shirihai@bu.edu, Department of Medicine, Boston University School of Medicine, Boston, MA, USA.

Abstract

Caloric restriction (CR) is a well-established intervention to prevent age-associated diseases, including obesity and diabetes. This nutritional intervention, which consists of limiting caloric but not micronutrient intake, has been shown to change mitochondrial function as well as PGC-1 and nitric oxide signaling, which regulate mitochondrial mass and morphology. We have previously shown that soluble factors from the sera of CR animals are responsible for at least part of these mitochondrial effects, since these are reproduced in cell cultures incubated with sera from CR animals. Here we studied the effect of CR serum versus serum from animals fed *ad libitum* (AL) on INS1 beta cell insulin secretion. INS1 cells incubated with CR sera presented higher levels of PGC-1-alpha and active nitric oxide synthase. Mitochondrial mass was unaltered by CR serum, but the expression of Mitofusin-2 (Mfn2) and OPA-1, proteins involved in mitochondrial fusion, were increased, while the levels of mitochondrial fission mediator, DRP-1, were reduced. Consistent with changes in mitochondrial dynamics proteins levels, CR sera treatment increased mitochondrial fusion rates, as well as their length and connectivity. These changes in mitochondrial morphology were associated with higher glucose-stimulated insulin secretion and mitochondrial respiration. Importantly, CR sera prevented mitochondrial alterations promoted by glucolipotoxicity, an *in vitro* model of type II diabetes. Overall, our results show that soluble serum factors present in restricted diets promote mitochondrial alterations which are associated with enhanced insulin secretion, including under acute stress promoted high nutrient overload.

Introduction

Calorie restriction (CR) has been shown to extend the lifespan of a wide range of organisms, from yeasts to mammals (1, 2). Furthermore, CR prevents or delays the onset of age-related diseases in non-human primates, although its effects on lifespan are still debatable (3,4).

Type II diabetes is an age-related disease associated with high caloric intake (5-8). This disease involves widespread changes in the response to insulin and progresses toward a pancreatic failure to adequately secrete insulin in response to high circulating glucose levels (9, 10). Multiple cellular pathways are compromised in β-cells upon insulin secretion failure, and mitochondrial dysfunction has being largely implicated in this phenomenon (11, 12). Indeed, mitochondria present a critical role in the regulation of insulin secretion, and have gained strong attention in studies uncovering the pathophysiology and seeking new therapeutic targets for type II diabetes (13-15).

Human and murine β-cells present limited replication capacity (16-18) and rely on organelle maintenance to ensure their functionality over time, which can be quite high (up to 30 years in humans; 18). These cells present progressive mitochondrial dysfunction over time, displaying an ATP production deficit (19, 20) which contributes toward diet-induced diabetes progression (21). In a high nutrient environment, mitochondria from β-cells become fragmented and present reduced glucose-stimulated insulin secretion capacity (22). On the other hand, limiting nutrient intake through CR preserves insulin secretion in aged animals (23).

It is thus possible that CR may prevent β-cell functional decay by modulating mitochondrial function. Indeed, CR has been shown to prevent mitochondrial functional decay during aging in several tissues and organisms (24-25), stimulating mitochondrial biogenesis and enhancing their oxidative function (26-30). An important regulator of mitochondrial physiology which has emerged recently is mitochondrial morphology, as well as dynamic changes in this morphology. Indeed, starvation increases mitochondrial length by decreasing mitochondrial fission, a process associated with higher

mitochondrial ATP synthesis capacity (31, 32, Liesa & Shirihai) and CR has been shown to increase the expression levels of the mitochondrial fusion protein mitofusin 2 (33; 26-27), suggesting that limited nutrient availability might be regulating mitochondrial dynamics by different mechanisms.

In this study we sought to understand the impact of CR on β-cell functionality and the potential dependency of CR-mediated changes on mitochondrial function and morphology. As a model of caloric restriction, we treated β-cells with sera from rats maintained on CR or *ad libitum* (AL) diets. Our results show that soluble factors in the serum from CR mammals enhance mitochondrial elongation and fusion, an effect associated with higher mitochondrial respiratory capacity and insulin secretion. Furthermore, we demonstrate that CR serum protects against the toxicity of a high nutrient environment, maintaining mitochondrial structure and β-cell function in an *in vitro* model of type II diabetes.

Methodology

Animals and serum collection

All experiments were conducted in agreement with National Institutes of Health guidelines for humane treatment of animals and were approved by the local Animal Care and Use Committee. Male, 8-week-old, Sprague-Dawley rats were separated into 2 groups: AL, fed *ad libitum* with an AIN-93-M diet prepared by Rhoster (Campinas, SP, Brazil) and CR, fed at 60% levels of AL-ingested amounts a diet supplemented with micronutrients to reach the same vitamin and mineral levels (34). The animals were lodged 3 per cage and given water *ad libitum*. At 34 weeks (26 weeks on the diet), rats were sacrificed after 12 hours fasting and serum was obtained as described in (35), allowed to clot for 20-30 min at 25°C and centrifuged for 20 min at 300 *g*. The supernatant was collected and stored at -20°C. Sera were thawed and heat-inactivated at 56°C for 30 min prior to use.

Cell culture, acute glucose and glucolipotoxicity experiments

INS1 cells were cultured with 100 IU/mL penicillin/streptomycin in RPMI media (12 mM glucose, 10% fetal bovine serum, 1 mM pyruvic acid, 10 mM Hepes, 2 mM glutamine and 0.1% β-mercaptoethanol) at 37°C and 5% CO_2. Cells were plated at 50% confluence for all the experiments. After 24 h of cell seeding, regular RPMI media was replaced by media containing 10% of AL or CR rat serum instead of fetal bovine serum. All experiments were performed after 24 h of the media exchange.

The effects of an acute glucose load were tested by incubating cells in DMEM minimum media with 2 mM glucose for 2.5 h, followed by increasing the glucose concentration to 12 mM. Insulin secretion was evaluated one hour after the change in glucose levels. Control cells were kept in 2 mM glucose media for the same time period.

Glucolipotoxicity (GLT) was performed by incubating cells for 24 h under standard conditions with 10% AL or CR serum, followed by changing the media to RPMI with 20 mM added glucose, 0.4 mM palmitate-conjugated BSA (4:1) and 1% serum (AL or CR). Control cells were incubated in 2 mM glucose with 1% BSA and no added palmitate. Experiments were conducted 24 hours after GLT was initiated.

Mitochondrial morphology and dynamics

INS1 cells expressing photo-activatable-GFP (mt-PA-GFP) and mitochondrial Ds-Red were imaged live using a Zeiss LSM 710 microscope with a x63 oil immersion objective and 463/543 nm helium-neon laser with a 650 to 710 nm bandpass filter. Five confocal plane pictures were taken from each image. Image J 1.41o software was used to distinguish mitochondrial structures and analyze morphological characteristics. The aspect ratio (AR) was calculated using the ratio of major and minor axes of the ellipse equivalent to the mitochondrion. The form factor (FF) was measured through the degree of branching (FF = perimeter^2/4π*area).

Mitochondrial dynamics were followed after 2-foton laser photoactivation of mt-PA-GFP, as described in Lovy *et al.* (36). Briefly, around 30% of the mitochondrial area visualized by mitochondrially-targeted Ds-Red fluorescence was bleached and the dilution of GFP through the mitochondrial network was followed during 48 min, in 12 min intervals. The average fluorescence intensity within the photo-activated area was calculated for every time point. Finally, the percentage of GFP fluorescence decay in the photoactivable area was plotted as a function of time, considering the fluorescence at time zero of photoactivation = 100%.

Western blots

Cell lysates were diluted in Laemmli sample buffer (100 mM Tris–HCl, 2% SDS, 10% glycerol, 0.1% bromophenol blue) containing 5% β-mercaptonoethanol. After heating at 95°C for 5 min, proteins were separated by SDS-PAGE and transferred onto PVDF membranes. Membranes were blocked with 5% non-fat milk and detection of individual proteins was carried out by blotting with specific primary antibodies against Mitofusin 2, VDAC (Abcam, 1:1,000), PGC-1-α (Santa Cruz, 1:500), DRP1, OPA1, eNOS (BD Bioscience, 1:1,000), phospho-eNOS^{1177} (Cell Signaling 1:1,000) or actin (Novus Biologicals; 1:2,000). Chemiluminescence detection using a secondary peroxidase-linked anti-rabbit (Calbiochem; 1:10,000) or anti-mouse (Calbiochem; 1:10,000) and a detection system from Pierce KLP (Rockford, IL, USA) was performed. Image J (NIH software) was used for densitometry and detected proteins were normalized to actin.

Cellular oxygen consumption

An hour before oxygen consumption measurements, cell media was replaced by assay media (2 mM glucose, 0.8 mM Mg^{2+}, 1.8 mM Ca^{2+}, 143 mM NaCl, 5.4 mM KCl, 0.91 mM NaH_2PO_4, and 15 mg/mL Phenol red) for 60 min at 37°C (no CO_2) before loading into the Seahorse Bioscience XF96 extracellular analyzer (37). During these 60 min, the ports of the cartridge containing the oxygen probes were loaded with the compounds to be injected during the assay (25 µL/port) and the cartridge was calibrated. Glucose was injected at a final concentration of 12 mM. FCCP was used at final concentrations of 4 µM and injected with sodium pyruvate (Sigma) at a final concentration of 5 mM. Oligomycin and antimycin were used at final concentrations of 5 and 2 µM, respectively. All respiratory modulators were used at ideal concentrations titrated during preliminary experiments (not shown).

Insulin secretion

Insulin released into the media after acute glucose stimulation was measured through by Fret using a HTRF CisBio kit and a TECAN M1000 plate reader. Insulin content was normalized by cell number.

Data analysis

Data represent means ± SEM or representative blots of at least three equal repetitions. Morphological analyses were performed in 10-20 cells. Statistical comparisons were conducted using ANOVA and GraphPad Prism software.

RESULTS

CR serum modulates insulin release and respiratory responses

Previous studies have documented that the serum obtained from rodents or humans on caloric restriction (CR) diets changes multiple characteristics of cultured cells, many of which involve energy metabolism (29, 35, 38). Beta-cells respond to blood glucose fluctuations by secreting insulin, and we sought to investigate how this secretion was affected by sera from CR or AL animals (Fig. 1). In INS1 cells (insulinoma β-cells) we found that CR serum significantly decreased basal insulin secretion (Fig. 1A, full columns), observed under low (2 mM) glucose, relative to AL serum-treated INS1 cells (open columns). On the other hand, CR sera resulted in a larger increase in glucose-stimulated (12 mM) insulin secretion when compared to AL-treated INS1 cells (Figure 1A). This effect was reproduced in primary mouse islets (Fig. 1B). These results indicate that a soluble factor (or factors) in the serum from CR animals increases glucose-sensitive insulin secretion while decreasing basal insulin secretion.

Hormone release in insulin-secreting cells is regulated by an increase in oxidative metabolism (39). In order to uncover possible changes in this process in INS1 cells treated with CR sera, we followed mitochondrial respiration in intact cells using a Seahorse Bioanalyzer (Fig. 2; reference 37). Representative respiratory traces are shown in Fig. 2A. While oxygen consumption rates were similar in 2 mM glucose, the addition of 12 mM glucose (where indicated) increased respiratory rates more significantly in cells cultured in CR sera (•) than in cells in AL sera (◊). Indeed, the respiratory rates promoted by high glucose, quantified as the last measurement before oligomycin addition, as indicated schematically by the letter “C” in Fig. 2B and depicted in Panel C, were 25% larger in CR cells than in AL cells. When oligomycin, which inhibits mitochondrial ATP synthesis, was added, absolute respiratory rates were similar (Fig. 2A). However, ATP-linked respiration (the difference between respiratory rates before and after the addition of oligomycin) was significantly higher in CR samples when compared to AL (Fig. 2D). Altogether, these results demonstrate that CR sera-treated INS1 cells present higher ATP-generating respiratory responses to high glucose. Finally, maximal respiratory rates measured in the presence of the mitochondrial uncoupler FCCP were larger in CR cells (Figs. 2A and 2E), but non-mitochondrial respiration observed in the presence of antimycin was equal (Fig. 2A). Overall, these results show CR serum increases glucose-stimulated respiration rates in INS1 cells, probably through a mechanism involving higher electron transport chain capacity.

CR serum changes mitochondrial morphology and dynamics

The enhanced respiratory rates observed in Fig. 2 could be due to an increase in mitochondrial mass. In fact, *in vivo* and *in vitro* CR has been widely shown to increase mitochondrial biogenesis, resulting in higher mitochondrial protein contents per cell in a variety of tissues (26-28, 35, 38). We thus sought to test whether CR treatment increased mitochondrial mass in INS1 cells (Fig. 3). We first measured the levels of PGC-1-α, a transcriptional co-activator of mitochondrial biogenesis, (40) and the activation of eNOS, which produces the PGC-1-α activator nitric oxide (41). The active phosphorylated form of eNOS was largely increased by CR, and PGC-1-α levels were strongly induced by CR serum (Fig. 3A, B and C). However, mitochondrial mass quantification through Mitotracker green staining (Fig. 3D), and mitochondrial area measured through mitochondrially targeted Ds-Red fluorescence (results not shown) did not uncover an increase in mitochondrial mass in CR serum treated cells, although a small increase in the expression of VDAC, an outer membrane protein often used as a marker for mitochondrial mass, was detected (Fig. 3E). Thus, although mitochondrial biogenesis pathways are activated by CR serum in insulin-secreting cells, their activation does not appear to be related to overt increases in mitochondrial mass under these growth conditions.

Other aspects of mitochondrial physiology regulated by PGC-1 coactivators are mitochondrial morphology and dynamics. Indeed, we found that the expression levels of Mitofusin-2 and OPA-1, which mediate mitochondrial fusion (42), were significantly increased by CR sera (Fig. 3A, F and G). Meanwhile, DRP-1, a mediator of mitochondrial fission, was decreased (Fig. 3A and H).

In order to verify if the changes in expression of these proteins altered mitochondrial morphology, cells expressing mitochondrial Ds-Red were imaged (Fig. 4). We found that cells incubated in CR serum presented more elongated mitochondria (a typical image is shown in Fig. 4A). Quantification of the mitochondrial form factor, a measure of mitochondrial elongation (Fig. 4B) and the aspect ratio, a measure of mitochondrial branching (Fig. 4C), demonstrated that CR serum induced an elongation and branching of mitochondria, a result that closely mirrors the increase in mitochondrial fusion protein expression observed in Fig. 3.

In order to discern whether this elongation and branching was associated with dynamic changes in mitochondrial morphology, we quantified mitochondrial fusion rates using a photo-activatable mitochondrial GFP (mt-PA-GFP, 43, Fig 5). By promoting photoactivation of this

protein in one portion of the cell and following the diffusion of the GFP across the non-photoactivated mitochondria over time, mitochondrial fusion rates can be quantified. We found that matrix content diffusion between mitochondria in CR cells was strikingly increased relative to AL cells (typical images are shown in Panel A, and GFP dilution is quantified in Panel B).

CR serum protects INS1 cells from fatty acid plus glucose toxicity

Exposure to high levels of fatty acids and glucose has a toxic effect on insulin-secreting cells known as glucolipotoxicity and considered an *in vitro* model for diabetes (22, 44). Since CR serum enhanced insulin secretion under normal growth conditions, we thus sought to verify the effects of this serum on cells submitted to glucolipotoxicity (GLT, Fig. 6). After 24 hours in CR or AL sera, cells were submitted to GLT (20 mM glucose, 4 mM palmitate:BSA and 1% of either AL or CR sera) for a further 24 hours. As reported previously (22), GLT promoted mitochondrial fragmentation in AL INS1 cells, as evidenced by mitochondrial matrix targeted Ds-Red fluorescence imaging (Fig. 6A). On the other hand, CR sera preserved mitochondrial mass and structure in GLT-treated INS1 cells (Fig. 6A and B). Furthermore, the decrease in mitochondrial fusion promoted by GLT (22) was prevented by CR serum (Fig. 6C and D), as evidenced by photo-GFP experiments. Overall, these results show that CR serum preserves mitochondrial morphology, mass and dynamics under GLT conditions.

GLT not only affects mitochondrial structure, but also reduces respiratory function (44). Indeed, as depicted in Fig. 7, respiratory rates of AL cells are strongly blunted by GLT (in Fig. 7A, compare the AL BSA control ◊, to the AL GLT trace, △). CR serum (▼) almost completely prevented the effects of GLT, preserving glucose-enhanced respiration (Fig. 7A and B), ATP-linked respiration (Fig. 7A and C) and maximal respiratory rates (Fig. 7A and D).

DISCUSSION

Studies using heterochronic parabiosis in which young-to-old or old-to-young systemic circulations of two animals are joined (48-50) pioneered the concept that circulatory factors are involved in cellular aging (50). Indeed, more recent studies have also implicated circulating components in the blood to cellular rejuvenation (51-53). In keeping with these findings, the *ex vivo* use of serum from calorically-restricted animals reproduces many CR effects in cell cultures (29, 35, 54-56), demonstrating that these effects are linked to serum components, and not the chronology of the cells themselves.

Mitochondrial dysfunction and impaired organellar turnover is a commonfinding in aging and many age-related diseases that can be prevented by CR (57-58). We have previously shown that sera from CR animals leads to the activation of the eNOS pathway and increased mitochondrial biogenesis in vascular cells and neurons, suggesting these mitochondrial effects are mediated by soluble factors, including adiponectin (28, 29).

Despite their undeniable impact on aging and age-related diseases, surprisingly little attention has been focused on insulin-secreting cells when studying the effects of CR. In order to address this knowledge gap, we compared the effects of sera from control AL and CR animals on insulin-secreting cell cultures. Interestingly, although we found that CR serum promoted the activation of the eNOS and PGC-1-α pathway, we could not find an overt increase in mitochondrial mass under basal conditions (Fig. 3), but did see a preservation of mitochondrial mass under nutrient overload (Fig. 6). This indicates that the effects of CR on mitochondrial mass are specific to nutrient overload conditions.

Nonetheless, mitochondrial fusion, another mitochondrial feature regulated by the PGC-1-α pathway, was strongly altered by CR sera, both under control (Figs. 3, 4) and under GLT (Fig. 6) conditions. Prior studies have uncovered links between energy availability and mitochondrial architecture: Under starvation, limited nutrient supply or acidic conditions, mitochondria typically become more elongated and tubular, an effect associated with more efficient ATP production (31-32, 59). Indeed, we found that the mitochondrial elongation promoted by CR serum was associated with an increased respiratory response to glucose, higher ATP-linked respiration and higher maximal respiratory capacity (Fig. 2). Since maximal respiratory rates were enhanced without measurable changes in overall mitochondrial mass (Fig. 3B), the enhanced respiratory capacity observed under CR culture conditions is most probably

attributable to changes in mitochondrial morphology and dynamics. Mitochondrial fusion can enhance respiratory function by providing higher oxygen availability throughout the mitochondrial network, allowing faster substrate cycling and altering respiratory complex assembly and interaction (60, 61). The result of the higher maximal respiratory rates observed is that CR INS1 cells also exhibit higher spare respiratory capacity (the difference between basal respiration and maximal respiratory rates), a feature that has been proposed to be important under stressful conditions, allowing for more adequate responses toward increases in energy demand (62, 63).

As fuel sensors, β-cells respond quickly to changes in nutrients (64). However, the *in vitro* CR model used here does not limit glucose availability nor promote direct changes in medium pH (both CR and AL serum were added to buffered media with equal glucose availability). Indeed, CR sera can also preserve cellular respiratory function and glucose responses under nutrient toxicity conditions, demonstrating that the effects are not linked to energy availability (GLT, Figs. 6, 7). Indeed, our findings suggest that circulatory factors in CR lead to bioenergetic changes in insulin-secreting cells directly, not through changes in nutrient availability.

In prior studies, we have demonstrated that mitochondrial dynamics control insulin secretion in β-cells (22, 43). Here, we add to these findings by showing that soluble factors in the sera from CR animals modify mitochondrial morphology and dynamics and acutely affect insulin-secreting cells. This suggests that mitochondrial morphological manipulation may be a useful therapeutic target in type II diabetes. Additionally, the identification of the factors involved in the preservation of the insulin-secreting function present in CR sera may open even more targetable intervention opportunities in this disease.

Figure Legends

Figure 1. CR serum increases glucose-stimulated insulin secretion. (A) INS1 or (B) dispersed murine β-cells were adapted in 2 mM glucose. After 2.5 h, glucose levels were raised to 12 mM (control cells were kept in 2 mM of glucose) and insulin released into the cell culture media was measured by ELISA within 1.5 h. *p < 0.05 *vs*. AL.

Figure 2. CR serum increases glucose-stimulated respiration and maximum respiratory capacity. (A) Representative oxygen consumption rates (OCR) of INS1 cells under basal condition (2 mM glucose) and after the subsequent addition of 10 mM glucose, 4 μM oligomicin, 5 μM FCCP and 2 μM antimycin. (B) Representation of the values shown in Panels C, D and E: glucose-stimulated OCR (last measurement after glucose addition), ATP-linked OCR (glucose-stimulated OCR minus oligomycin-insensitive-OCR) and maximal OCR (highest OCR after FCCP addition), respectively. OCR values in the presence of antimycin (non-mitochondrial respiration) were subtracted from all quantifications. *p < 0.05 *vs*. AL.

Figure 3. CR serum increases the expression of proteins involved in mitochondrial fusion. INS1 cells were cultured for 24 h with 10% serum from AL or CR rats. (A) Representative blots for the indicated proteins. (B, C) Quantifications of Western Blot bands obtained from independent experiments and normalized to actin or eNOS. (D) Mitotracker green fluorescence evaluated through FACS analysis. (E-H) Quantifications of Western Blot bands obtained from independent experiments and normalized to actin. *p < 0.05 *vs*. AL.

Figure 4. CR serum alters mitochondrial morphology, promoting elongation and branching. After 24 h incubation with AL or CR serum, INS1 cells stably expressing mitochondrial DS-Red were imaged with a 100 x lens. (A) Maximum z projection of mitochondrial DS-red fluorescence. (B) Form Factor analysis (FF = $perimeter^2/4\pi*area$), threshold of 3. (C) Aspect ratio analysis (AR = minimum / major axes of the ellipse equivalent to the mitochondrion), threshold of 0.45. *p < 0.05 *vs*. AL.

Figure 5. CR serum increases mitochondrial fusion rates. INS1 cells stably expressing mitochondrial DS-Red and photo-activable-GFP (mtPA-GFP) were imaged with a 63 x lens. 5 stacks were obtained for each image. (A) Representative Z-projection Images; at time point 0, mt-Pa-GFP was activated using a two-photon laser. Fusion of the photoactivated fraction (~30%) with the rest of the mitochondrial web, leading to a dilution in fluorescence intensity, was followed at 12 min intervals. (*B)* Time-dependent average dilution of GFP; 100% is the GFP fluorescence soon after activation.

Figure 6. CR serum protects against mitochondrial mass and dynamics loss promoted by glucolipotoxicity. After 24 h incubation in media with 10% AL or CR serum, cells were challenged with glucolipotoxic (GLT) media (0.4 mM palmitate, 20 mM glucose, 1% AL or CR serum). (A) z-projection images of mitochondrial Ds-Red staining. (B) Mitochondrial area quantified from Mito-DsRed images using Image J. (C) INS1 cells stably expressing mitochondrial DS-Red and photo-activable-GFP (mtPA-GFP) were imaged with 63 x lens to follow mitochondrial dynamics. 5 stacks were obtained for each image. Representative Z-projections images are shown. At time 0, mt-Pa-GFP was activated using a two-photon laser.

Fusion of the photoactivated fraction (~30%) with the rest of the mitochondrial web leading to fluorescence dilution was followed in 12 min intervals. (D) Time-dependent average dilution of GFP from multiple cells; 100% is the GFP fluorescence soon after activation. *$p < 0.05$ *vs*. AL; #$p < 0.05$ *vs*. BSA.

Figure 7. CR serum protects mitochondrial function from glucolipotoxicity. After 24 h incubation in media with 10% AL or CR serum, cells were challenged with the GLT media described for Fig. 6. (A) Representative respiration chart of INS1 cells under basal conditions (2 mM glucose) and after the subsequent additions of 10 mM glucose, 4 μM oligomicin, 5 μM FCCP and 2 μM antimycin, as indicated by the arrows. (B) Glucose-stimulated OCR (last measurement after glucose addition) (C) ATP-linked OCR (glucose stimulated OCR minus OCR in the presence of the ATP inhibitor oligomycin), (D) Maximum respiratory capacity (highest OCR value after FCCP addition). OCR values in the presence of antimycin were subtracted from all quantifications. *$p < 0.05$ *vs*. AL; $^{\#}p < 0.05$ *vs*. BSA.

References

1. Sinclair, D. A. (2005) Toward a unified theory of caloric restriction and longevity regulation. *Mech. Ageing Dev.* **126**, 987-1002.
2. Anderson R. M., Weindruch R. (2010) Metabolic reprogramming, caloric restriction and aging. *Trends Endocrinol. Metab.* **21**, 134-141.
3. Mattison J. A., Roth G. S., Beasley T. M., Tilmont E. M., Handy A. M., Herbert R. L., Longo D. L., Allison D. B., Young J. E., Bryant M, Barnard D., Ward W. F., Qi W., Ingram D. K., de Cabo R., Mattison J. A. (2012) Impact of calorie restriction on health and survival on rhesus monkeys from NIA study. *Nature* **489**, 318-321.
4. Redman L. M., Ravussin E. (2011) Caloric restriction in humans: impact on physiological, psychological, and behavioral outcomes. *Antioxid. Redox Signal.* **14**, 275-287.
5. Horwitz D. L. (1982) Diabetes and aging. *Am. J. Clin. Nutr*. **36**, 803-808.
6. Morley J. E. (2008) Diabetes and aging: epidemiologic overview. *Clin. Geriatr. Med.* **24**, 395-405.
7. Bennett P. H. (1976) Report of work group on epidemiology. Natural Commission on Diabetes. Vol III. Part I, Washington, DC: Department of Health, Education and Welfare, publ (NIH), 76-1021, 1976:65-133.
8. Koopman R. J., Mainous A. G. 3rd, Diaz V. A., Geesey M. E. (2005) Changes in age at diagnosis of type 2 diabetes mellitus in the United States, 1988 to 2000. *Ann. Fam. Med.* **3**, 60–63.
9. Kahn S. E. (2003) The relative contributions of insulin resistance and beta-cell dysfunction to the pathophysiology of Type 2 diabetes. *Diabetologia* **46**, 3-19.
10. Weir G. C. Bonner-Weir S. (2004) Five stages of evolving beta cells dysfunction during progression to diabetes. *Diabetes* **53**, S16-21.
11. Lowell B. B., Shulman G. I. (2005) Mitochondrial Dysfunction and Type 2 Diabetes. *Science* **307**, 384-387.
12. Maechler P., Wollheim C. B. (2001) Mitochondrial function in normal and diabetic β-cells. *Nature* **414**, 807-812.
13. Pi J., Bai Y., Zhang Q., Wong V., Floering L.M., Daniel K., Reece J. M., Deeney J. T., Andersen M. E., Corkey B. E., Collins S. (2007) Reactive oxygen species as a signal in glucose-stimulated insulin secretion. *Diabetes* **56**, 1783-1791.
14. Wolheim C. B. (2000) Beta-cell mitochondria in the regulation of insulin secretion: a new culprit in type II Diabetes. *Diabetologia* **43**, 265-277.
15. Green K., Brand M. D., Murphy M. P. (2004) Prevention of mitochondrial oxidative damage as a therapeutic strategy in diabetes. *Diabetes* **5**, S110-118.
16. Teta M., Long S. Y., Wartschow L. M., Rankin M. M., Kushner J. A. (2005) Very slow turnover of beta-cells in aged adult mice. *Diabetes* **54**, 2557–2567**.**
17. Cnop M., Hughes S. J., Igoillo-Esteve M., Hoppa M. B., Sayyed F., van de Laar L., Gunter J. H., de Koning E. J., Walls G. V., Gray D. W., Johnson P. R., Hansen B. C., Morris J. F.,Pipeleers-Marichal M., Cnop I., Clark A. (2010) The long lifespan and low turnover of human islet beta cells estimated by mathematical modelling of lipofuscin accumulation. *Diabetologia* **53**, 321–330.

18. Cnop M., Igoillo-Esteve M., Hughes S. J., Walker J. N., Cnop I., Clark A. (2011) Longevity of human islet alpha- and beta-cells. *Diabetes Obes. Metab.* **13**, S39–S46.
19. Terman A., Kurz T., Navratil M., Arriaga E. A., Brunk U.T. (2010) Mitochondrial turnover and aging of long-lived postmitotic cells: the mitochondrial-lysosomal axis theory of aging. *Antioxid. Redox Signal.* **12**, 503-535.
20. Simmons R. A., Suponitsky-Kroyter I., Selak M. A. (2005) Progressive accumulation of mitochondrial DNA mutations and decline in mitochondrial function lead to beta-cell failure. *J. Biol. Chem*. **280**, 28785-28791.
21. Sone H., Kagawa Y. (2005) Pancreatic beta cell senescence contributes to the pathogenesis of type 2 diabetes in high-fat diet-induced diabetic mice. *Diabetologia* **48**, 58-67.
22. Molina A. J., Wikstrom J. D., Stiles L., Las G., Mohamed H., Elorza A., Walzer G., Twig G., Katz S., Corkey B. E., Shirihai O. S. (2009) Mitochondrial networking protects beta-cells from nutrient-induced apoptosis. *Diabetes* **58**, 2303-2315.
23. He X. Y., Zhao X. L., Gu Q., Shen J. P., Hu Y., Hu R. M. (2012) Calorie restriction from a young age preserves the functions of pancreatic β cells in aging rats. *Tohoku J. Exp. Med.* **227**, 245-252.
24. Hepple R. T., Baker D. J., McConkey M., Murynka T., Norris R. (2006) Caloric restriction protects mitochondrial function with aging in skeletal and cardiac muscles*. Rejuvenation Res.* **9**, 219-222.
25. Lanza I. R., Zabielski P., Klaus K. A., Morse D. M., Heppelmann C. J., Bergen H. R. 3rd., Dasari S., Walrand S., Short K. R., Johnson M. L., Robinson M. M., Schimke J. M., Jakaitis D. R., Asmann Y. W., Sun Z., Nair K. S. (2012) Chronic calorie restriction preserves mitochondrial function in senescence without increasing mitochondrial biogenesis. *Cell Metab*. **16**, 777-188.
26. Nisoli E., Tonello C., Cardile A., Cozzi V., Bracale R., Tedesco L., Falcone S., Valerio A., Cantoni O., Clementi E., Moncada S., Carruba M. O. (2005) Calorie restriction promotes mitochondrial biogenesis by inducing the expression of eNOS. *Science* **310**, 314-317.
27. Cerqueira F. M., Laurindo F. R., Kowaltowski A. J. (2011) Mild mitochondrial uncoupling and calorie restriction increase fasting eNOS, akt and mitochondrial biogenesis. *PLoS One* **31**, e18433.
28. Cerqueira F. M., Brandizzi L. I., Cunha F. M., Laurindo F. R., Kowaltowski A. J. (2012) Serum from calorie-restricted rats activates vascular cell eNOS through enhanced insulin signaling mediated by adiponectin. *PLoS One* **7**, e31155.
29. Cerqueira F. M., Cunha F. M., Laurindo F. R., Kowaltowski A. J. (2012) Calorie restriction increases cerebral mitochondrial respiratory capacity in a NO•-mediated mechanism: impact on neuronal survival. *Free Radic. Biol. Med.* **52**, 1236-1241.
30. Lin S. J., Kaeberlein M., Andalis A. A., Sturtz L. A., Defossez P. A., Cullota V. C., Fink G. R., Guarente L. (2002) Calorie restriction extends *Saccharomyces cerevisae* lifespan by increasing respiration. *Nature* **418**, 344-348.

31. Rambold A. S., Kostelecky B., Elia N., Lippincott-Schwartz J. (2011) Tubular network formation protects mitochondria from autophagosomal degradation during nutrient starvation. *Proc. Natl. Acad. Sci. USA* **108**, 10190-10195.
32. Liesa M., Shirihai O. S. (2013) Mitochondrial dynamics in the regulation of nutrient utilization and energy expenditure. *Cell Metab*. **17**, 491-506.
33. Civitarese A. E., Carling S., Heilbronn L. K., Hulver M. H., Ukropcova B., Deutsh W. A., Smith S. R., Ravussin E., CALERIE Pennington Team (2007) Calorie restriction increases muscle mitochondrial biogenesis in healthy humans. *Plos Med.* **4**, e76.
34. Cerqueira F. M., Kowaltowski A.J. (2010) Commonly adopted caloric restriction protocols often involve malnutrition. *Ageing Res. Rev.* **9**, 424–430.
35. de Cabo R., Fürer-Galbán S., Anson R. M., Gilman C., Gorospe M., Lane M. A. (2003) An in vitro model of caloric restriction. *Exp. Gerontol.* **38**, 631-639.
36. Lovy A., Molina A. J., Cerqueira F. M., Trudeau K., Shirihai O. S. (2012) A faster, high resolution, mtPA-GFP-based mitochondrial fusion assay acquiring kinetic data of multiple cells in parallel using confocal microscopy. *J. Vis. Exp.* **20**, e3991.
37. Wu M., Neilson A., Swift A. L., Moran R., Tamagnine J., Parslow D., Armistead S., Lemire K., Orrell J., Teich J., Chomicz S., Ferrick D. A. (2007) Multiparameter metabolic analysis reveals a close link between attenuated mitochondrial bioenergetic function and enhanced glycolysis dependency in tumor cells. *Am. J. Physiol. Cell Physiol.* **292**, C125-136.
38. López-Lluch G., Hunt N., Jones B., Zhu M., Jamieson H., Hilmer S., Cascajo M. V., Allard J., Ingram D. K., Navas P., de Cabo R. (2006) Calorie restriction induces mitochondrial biogenesis and bioenergetic efficiency. *Proc. Natl. Acad. Sci. USA.* **103**, 1768-1763.
39. Patterson J. N., Cousteils K., Lou J. W., Manning Fox J. E., MacDonald P. E., Joseph J. W. (2014) Mitochondrial metabolism of pyruvate is essential for regulating glucose-stimulated insulin secretion. *J. Biol. Chem.* **289**, 13335-13346.
40. Scarpulla R. C. (2011) Metabolic control of mitochondrial biogenesis through the PGC-1 family regulatory network. *Biochim. Biophys. Acta*. **1813**, 1269-1278.
41. Ventura-Clapier R., Garnier A., Veksler V. (2008) Transcriptional control of mitochondrial biogenesis: the central role of PGC-1-alpha. *Cardiovasc. Res.* **79**, 208-217.
42. Chan D. C. (2006) Mitochondrial fusion and fission in mammals. *Annu. Cell Dev. Biol.* **22**, 79-99.
43. Twig G., Graf S. A., Wikstrom J. D., Mohamed H., Haigh S. E., Elorza A., Deutsch M., Zurgil N., Reynolds N., Shirihai O. S. (2006) Tagging and tracking individual networks within a complex mitochondrial web with photoactivatable GFP. *Am. J. Physiol. Cell Physiol.* **291**, C176-184.
44. Las G., Serada S. B., Wikstrom J. D., Twig G., Shirihai O. S.(2011) Fatty acids suppress autophagic turnover in b-cells. *J. Biol. Chem.* **286**, 42534-42544.
45. Chen H., Chomyn A., Chan D. C. (2005) Disruption of fusion results in mitochondrial heterogeneity and dysfunction. *J. Biol. Chem.* **280**, 26185-26192.
46. Wikstrom J. D., Mahdaviani K., Liesa M., Sereda S. B., Si Y., Las G., Twig G., Petrovic N., Zingaretti C., Graham A., Cinti S., Corkey B. E., Cannon B., Nedergaard J., Shirihai O. S. (2014) Hormone-induced mitochondrial fission is utilized by brown adipocytes as an amplification pathway for energy expenditure. *EMBO J.* **33**, 418-436.

47. Bach D., Pich S., Soriano F. X., Vega N., Baumgartner B., Oriola J., Daugaard J. R., Lloberas J., Camps M., Zierath J. R., Rabasa-Lhoret R., Wallberg-Henriksson H., Laville M., Palacín M., Vidal H., Rivera F., Brand M., Zorzano A. (2003) Mitofusin-2 determines mitochondrial network architeture and mitochondrial metabolism. A novel regulatory mechanism altered in obesity. *J. Biol. Chem*. **278**, 17190-17197.
48. Bunster E., Meyer R. K. (1933) An improved method of parabiosis. *Anat. Rec*. **57**, 339–343.
49. Finerty J. C. (1952) Parabiosis in physiological studies. *Physiol. Rev.* **32**, 277-302.
50. Tauchi H., Hasegawa K. (1977) Change of the hepatic cells in parabiosis between old and young rats. *Mech. Ageing Dev*. **6**, 333-339.
51. Conboy I. M., Conboy M. J., Wagers A. J., Girma E. R., Weissman I. L., Rando T. A. (2005) Rejuvenation of aged progenitor cells by exposure to a young systemic environment. *Nature* **433**, 760-764.
52. Villeda S. A., Plambeck K. E., Middeldorp J., Castellano J.M., Mosher K. I., Luo J., Smith L. K., Bieri G., Lin K., Berdnik D., Wabl R., Udeochu J., Wheatley E. G. Zou B., Simmons D. A., Xie X. S., Longo F. M., Wyss-Coray T. (2014) Young blood reverses age-related impairments in cognitive function and synaptic plasticity in mice. *Nature Med.* **20**, 659-663.
53. Kaiser J. (2014) Aging. 'Rejuvenation factor' in blood turns back the clock in old mice. *Science* **344**, 570-571.
54. Omodei D., Licastro D., Salvatore F., Crosby S. D., Fontana L. (2013) Serum from humans on long-term calorie restriction enhances stress resistance in cell culture. *Aging (Albany NY)* **5**, 599-606.
55. Allard J. S., Heilbroon L. K., Smith C., Hunt N. D., Ingram D. K., Pennington CALERIE Team, de Cabo R. (2008) In vitro cellular adaptations of indicators of longevity in response to treatment with serum collected from humans on calorie restricted diets. *Plos One* **3**, e3211.
56. Csiszar A., Labinskyy N., Jimenez R., Pinto J. T., Ballabh P., Losonczy G., Pearson K. J., de Cabo R., Ungvari Z. (2009) Anti-oxidative and anti-inflammatory vasoprotective effects of calorie restriction in aging: role of circulating factors and Sirt1. *Mech. Ageing Dev.* **130**, 518-527.
57. Merry B. J. (2004) Oxidative stress and mitochondrial function with aging – the effects of calorie restriction. *Aging Cell* **3**, 7-12.
58. Cuervo A. M. (2008) Calorie restriction and aging: the ultimate “cleasing diet”. *J. Gerontol. A Biol. Sci. Med. Sci.* **63**, 547-549.
59. Khacho M., Tarabay M., Patten D., Khacho P., MacLaurin J. G., Guadagno J., Bergeron R., Cregan S. P., Harper M. E., Park D. S., Slack R. S. (2014) Acidosis overrides oxygen deprivation to maintain mitochondrial function and cell survival. *Nat. Commun*. **5**, 1-15.
60. Nakada K., Inoue K., Ono T., Isobe K., Ogura A., Goto Y. I., Nonaka I., Hayashi J. I. (2001) Inter-mitochondrial complementation: mitochondria-specific system preventing mice from expression of disease phenotypes by mutant mtDNA. *Nat. Med*. **7**, 934–940.
61. Partikian A., Olveczky B., Swaminathan S., Li Y., Verkman A. S. (1998) Rapid diffusion of green fluorescent protein in the mitochondrial matrix. *J. Cell Biol*. **140**, 821–829.

62. van der Windt G. J., Everts B., Chang C. H., Curtis J. D., Freitas T. C., Amiel E., Pearce E. J., Pearce E. L. (2012) Mitochondrial respiratory capacity is a critical regulator of CD8+ T cell memory development. *Immunity* **36**, 68-78.
63. Keuper M., Jastroch M., Yi C. X., Fischer-Posovszky P., Wabitsch M., Tschöp M. H., Hofmann S. M. (2014) Spare mitochondrial respiratory capacity permits human adipocytes to maintain ATP homeostasis under hypoglycemic conditions. *FASEB J.* **28**, 761-770.
64. Rorsman P. (1997) The pancreatic beta-cells as a fuel sensor: an electrophysiologist`s viewpoint. *Diabetologia* **40**, 487-495.

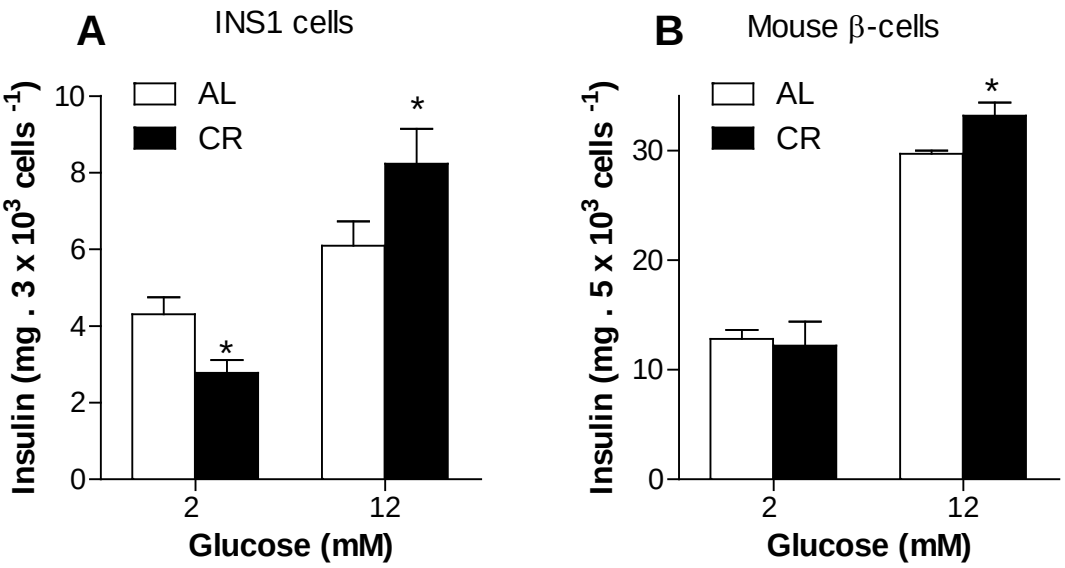

Cerqueira et al., 2014, Figure 1

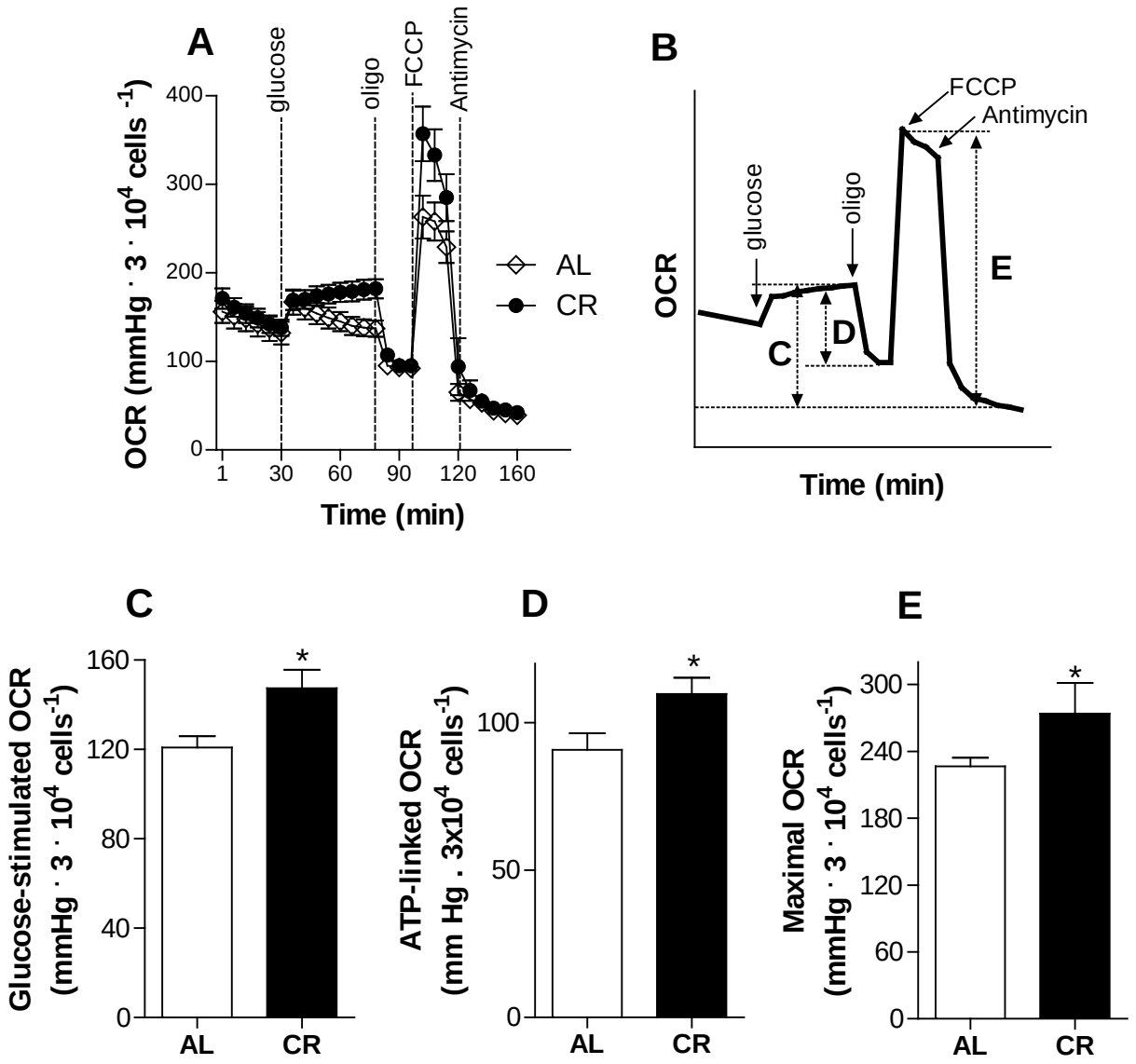

Cerqueira et al., 2014, Figure 2

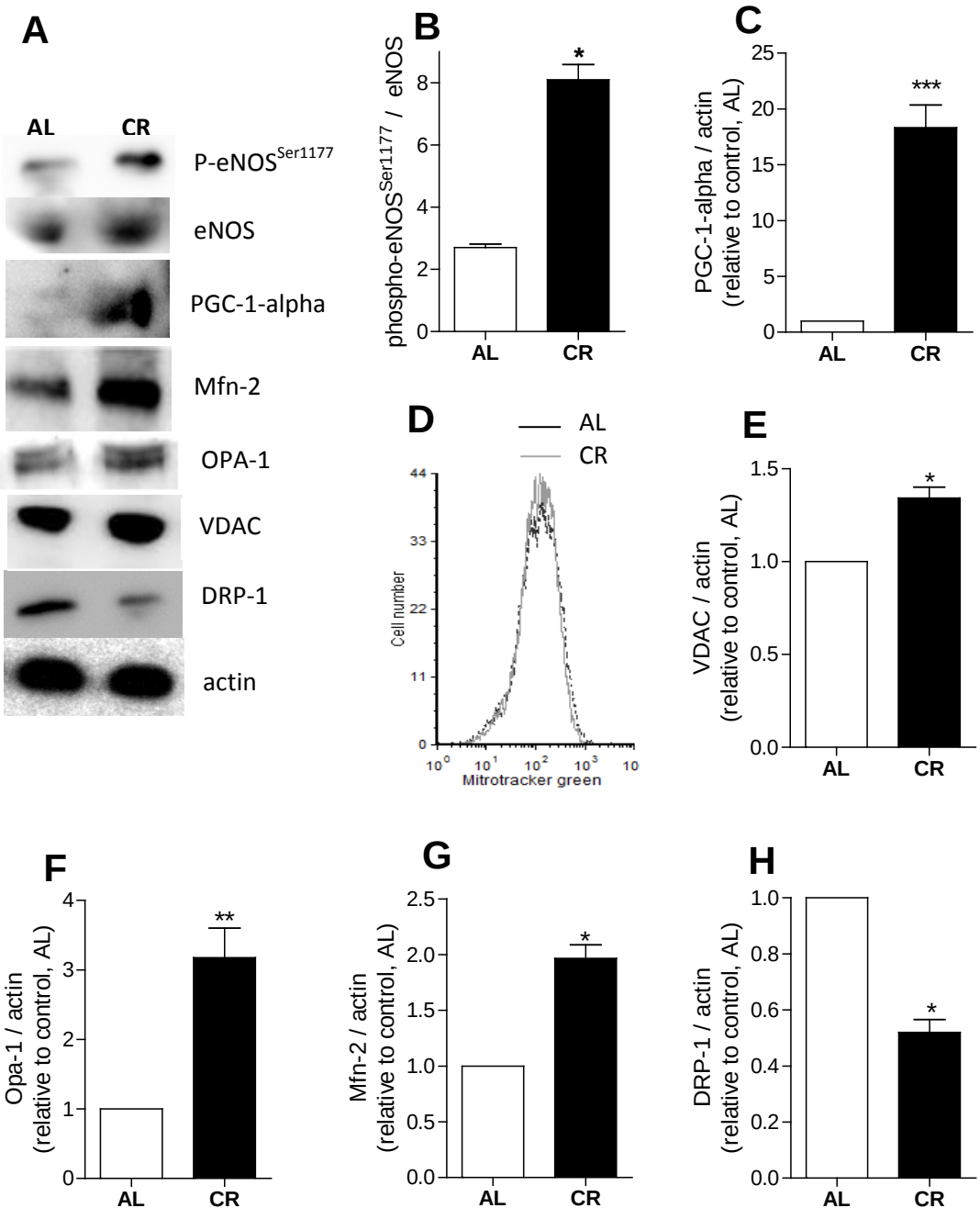

Cerqueira et al., 2014, Figure 3

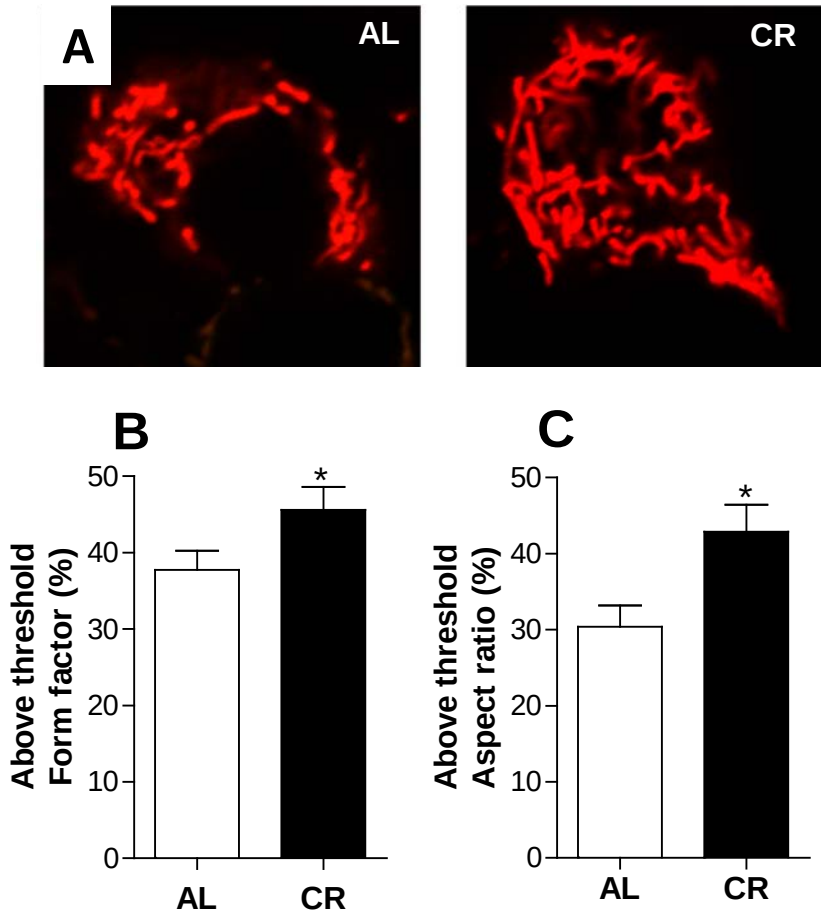

Cerqueira et al., 2014, Figure 4

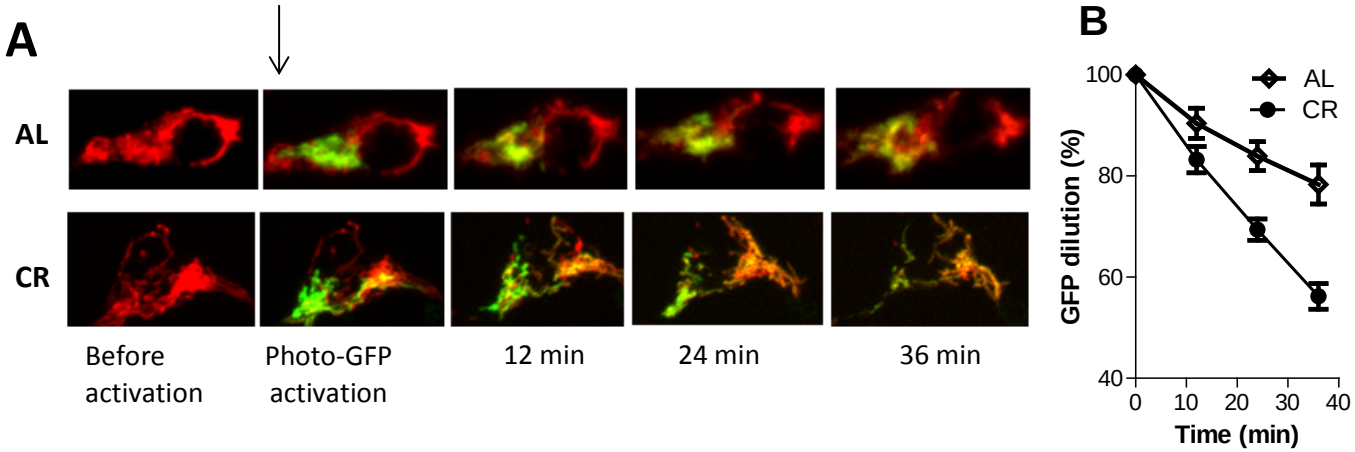

Cerqueira et al., 2014, Figure 5

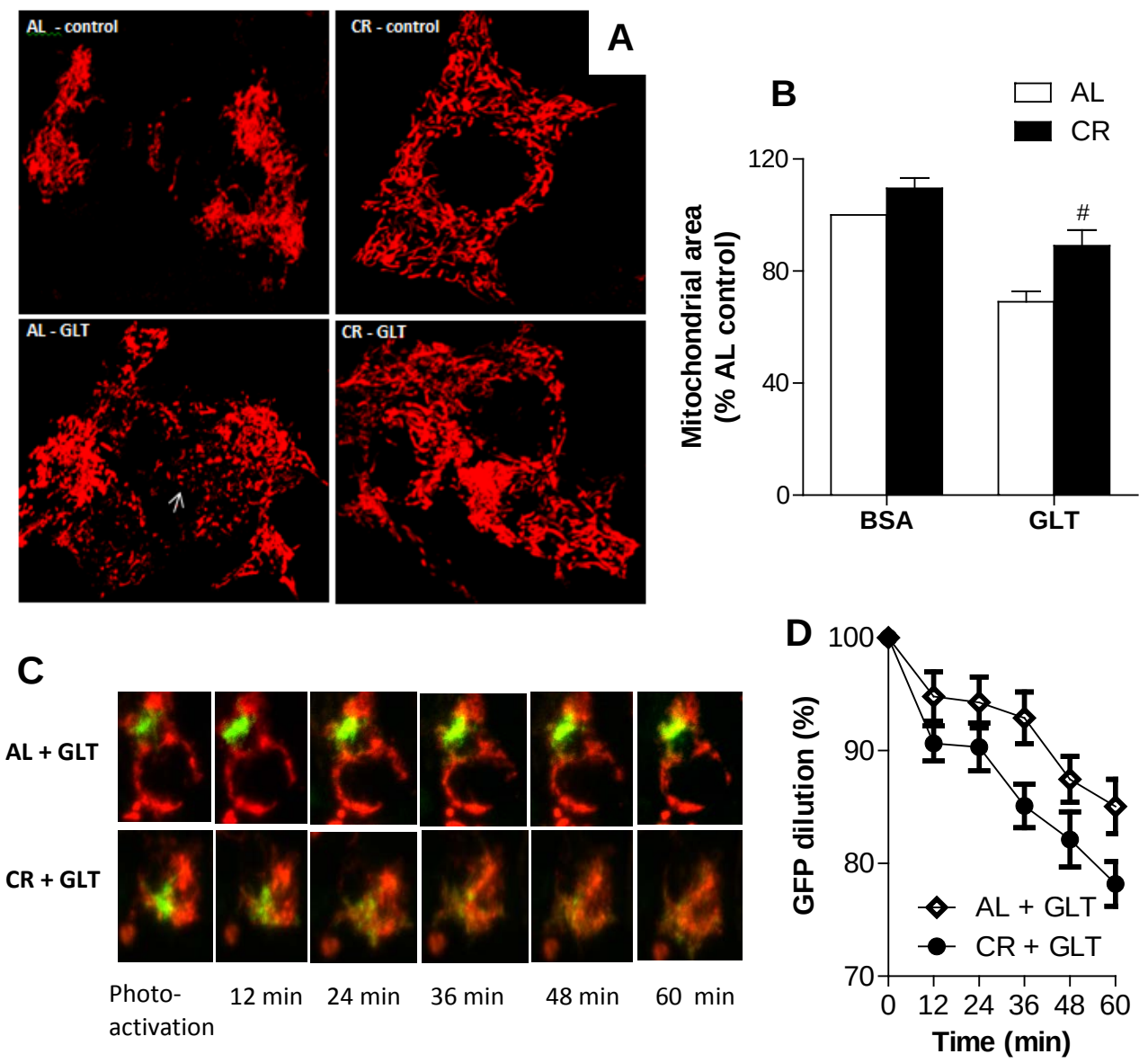

Cerqueira et al., 2014, Figure 6

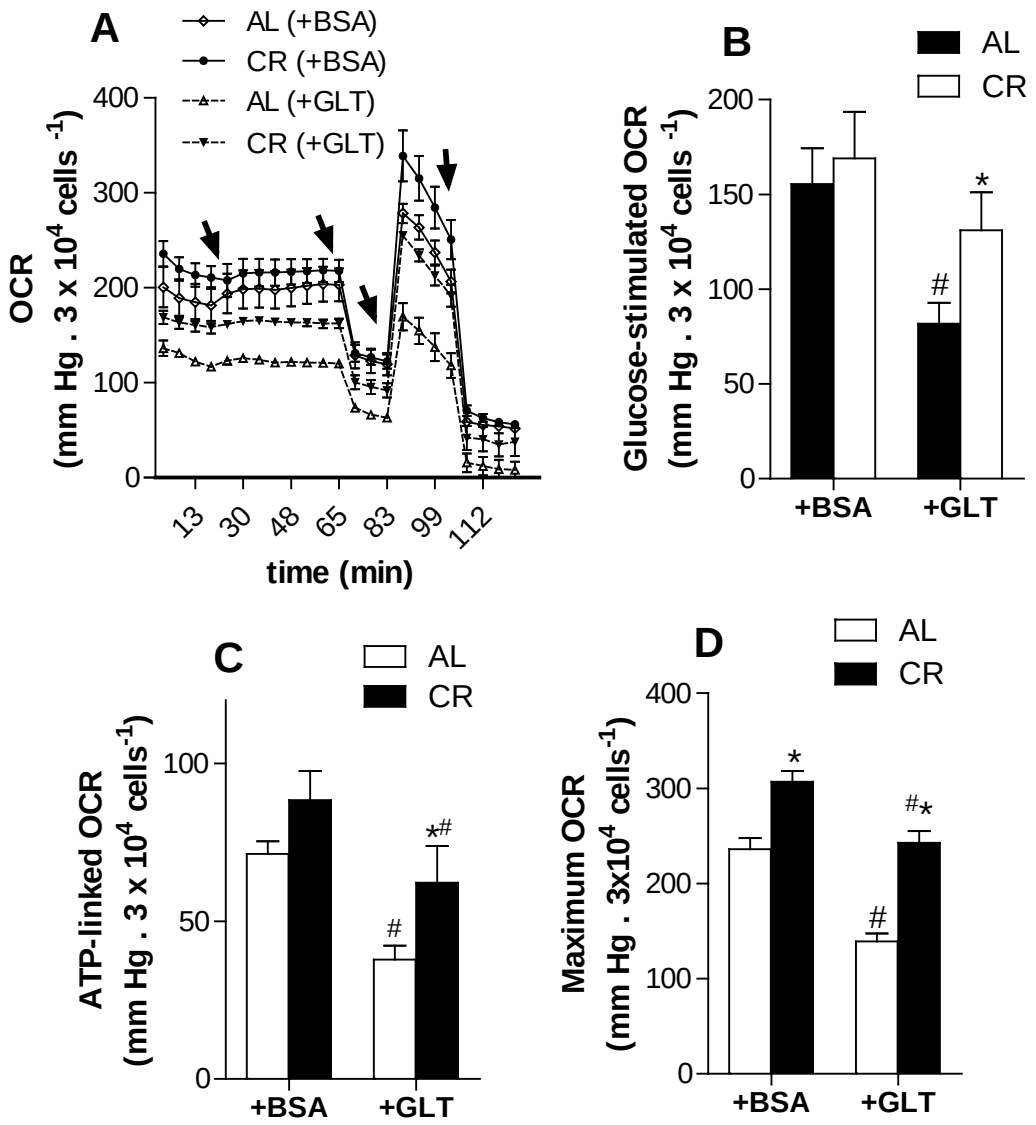

Cerqueira et al., 2014, Figure 7